

DIPLOMARBEIT

Design of gas cleaning processes for SNG- production from biogenic residues

ausgeführt zum Zwecke der Erlangung des akademischen Grades eines
Diplomingenieurs unter der Leitung von

Univ.Prof. Dipl.-Ing. Dr.techn. Hermann Hofbauer

am

Institut für Verfahrenstechnik, Umwelttechnik und Technische Biowissenschaften

betreut von

Dipl.-Ing. Dr.techn. Stefan Müller

Dipl.-Ing. Josef Fuchs

eingereicht an der Technischen Universität Wien
Fakultät für Maschinenwesen und Betriebswissenschaften

von

Michael Malicha

Matrikelnummer 0928730

Denisgasse 4/11

1200 Wien

Preface

First, I would like to thank Dipl.-Ing. Dr.techn. Stefan Müller for the chance to write my master thesis at the working group gasification and gas cleaning, as well as for the professional supervision, guidance and the patience in answering my questions throughout the process of my research. Additionally, I want to thank Dipl.-Ing. Josef Fuchs for his great assistance and his advices.

Furthermore, I want to thank all the people at the working group gasification and gas cleaning for their support and friendly integration.

Finally, I want to thank my family, friends and work colleagues for all the encouragement. Above all, I am grateful to Ines, who was very patient, supportive and helped me during the whole process of my master thesis.

Acknowledgement

The present work is part of the research project RenewableSteelGases in cooperation with voestalpine Stahl GmbH; voestalpine Stahl Donawitz GmbH; K1-MET GmbH; MU Leoben, Lehrstuhl für Verfahrenstechnik des industriellen Umweltschutzes; JKU Linz, Energieinstitut. RenewableSteelGases receives financial support from the research program “Energieforschung” funded by the “Austrian Climate and Energy Fund”.

Abstract

Nowadays many countries wish to use their domestic biomass resources for energy production in order to decrease carbon dioxide emissions and the import of energy. Efforts to cut carbon dioxide emissions have led to the development of renewable energy technologies such as wind turbines, photovoltaics and the use of biomass. The targets of the European Commission till 2030 are to cut greenhouse gas emissions by 40 % relative to 1990 levels and to increase renewable energy sources up to 27 %. However, the energy intensive industries and the transport sector remain largely dependent on fossil energy resources, mainly natural gas and oil products.

The aim of this work is the design of a cold and hot gas cleaning process for synthetic natural gas (SNG) production from biogenic residues. To gain a data basis, a gasification experiment with hazelnut shells as fuel was conducted at TU Wien's dual fluidized bed gasifier. With the obtained data first a scale up to an 8 MW_{th} gasifier was conducted. Further on mathematical models were created to design reactors which are able to meet the specified limits of the methanation catalyst.

The results obtained that at the exit of both gas cleaning processes several specified limits of impurities which are harmful for the methanation catalyst were not reached. Additional cleaning devices or optimization of the existing ones is necessary to further reduce these impurities. Furthermore, both gas cleaning processes were discussed in terms of energy demand and needed recourses per day to clean the gas.

The outcome of this master thesis was that, based on the used calculation models, an implementation of both cleaning sections in the biomass to SNG process is possible. However, to meet the requirements of the methanation catalyst the designed gas cleaning processes have to be adapted. Further research should be done to evaluating the designed gas cleaning processes experimentally and with the use of simulations. Additionally, the long-term behaviour of the methanation catalyst has to be investigated.

Kurzfassung

Heutzutage setzen viele Länder darauf Ihre inländischen Biomasseressourcen für die Energieproduktion zu nutzen um die CO₂-Emissionen zu reduzieren und unabhängig vom Import zu werden. Durch das Bestreben die CO₂-Emissionen zu senken setzen die Länder vermehrt auf die Entwicklung und Förderung von alternativen und nachhaltigen Energiesystemen wie zum Beispiel Windkraft, Fotovoltaik oder die Nutzung von Biomasse. Ziele der europäischen Kommission bis 2030 sind die Treibhausgasemissionen gegenüber 1990 um mindestens 40 % zu senken und eine Erhöhung des Anteils erneuerbarer Energiequellen auf mindestens 27 %. Trotz alledem sind große Kraftwerke und der Sektor Verkehr und Transport auf fossile Energieträger wie Öl und Gas angewiesen.

Das Ziel dieser Diplomarbeit ist es eine mögliche Kalt- bzw. Heißgasreinigungsanlage zu entwerfen um diese in ein Kraftwerk zu implementieren welches synthetisches Erdgas aus biogenen Reststoffen herstellt. Um Daten für die weitere Auslegung der Gasreinigungen zu generieren wurde ein Vergasungsexperiment an der TU Wien mit Haselnusschalen als Brennstoff durchgeführt. Mit den generierten Daten wurde zuerst ein 8 MW_{th} Vergaser hinsichtlich Menge an produzierendem Produktgas ausgelegt. Weiters wurden Berechnungsmethoden erarbeitet um die einzelnen Reaktoren der jeweiligen Gasreinigung zu berechnen. Ziel dieser Auslegung ist es ein Produktgas bereitzustellen welches den Anforderungen des Methanierungskatalysators genügt.

Die Berechnungsergebnisse zeigten, dass beide ausgelegten Gasreinigungen nicht in der Lage sind alle für den Katalysator schädlichen Stoffe so weit zu reduzieren das sie den Anforderungen genügen. Zusätzliche Gasreinigungsapparate müssten installiert oder die bestehenden optimiert werden. Weiters wurden beide Gasreinigungsprozesse hinsichtlich Energiebedarf diskutiert. Auch ein Vergleich der benötigten Ressourcen pro Tag um das Gas zu reinigen wurden durchgeführt.

Das Resultat dieser Arbeit ist, dass basierend auf den Berechnungsmethoden eine Implementierung beider Gasreinigungen in einen Prozess, der synthetisches Erdgas erzeugt, prinzipiell möglich ist. Jedoch werden die Anforderungen des Methanierungskatalysators hinsichtlich Gasqualität nicht vollständig erreicht und es müssen Adaptierungen am Gasreinigungsprozess vorgenommen werden. Weiter Forschung sollte in die experimentell untersucht und vermessen in die erarbeitete Prozesskette investiert werden. Darüber hinaus sollte das Langzeitverhalten des Methanierungskatalysators untersucht werden.

Table of contents

1	INTRODUCTION	1
2	STATE OF THE ART OF SNG-PRODUCTION FROM BIOMASS GASIFICATION	3
2.1	DUAL FLUIDIZED BED GASIFICATION	3
2.2	SORPTION ENHANCED REFORMING (SER).....	7
2.3	BASIC PRINCIPLES OF METHANATION	12
2.4	METHANATION REACTOR TYPES	17
2.5	GAS CLEANING	22
2.6	FUTURE OF R&D CHALLENGES.....	28
3	EXPERIMENTAL GASIFICATION OF BIOGENIC RESIDUES	29
3.1	DESCRIPTION OF THE TEST PLANT AND USED FUEL.....	29
3.2	EXPERIMENTAL PROCEDURE.....	31
3.3	RESULTS	32
4	MATHEMATICAL MODELS FOR THE CALCULATION OF GAS CLEANING PROCESSES ..	34
4.1	REFERENCE DATA FOR GASIFIER SCALE UP	35
4.2	MODELS FOR REACTOR DESIGN.....	37
5	DESIGN OF GAS CLEANING PROCESSES	44
5.1	CONCEPT FOR COLD GAS CLEANING	44
5.2	CONCEPT FOR HOT GAS CLEANING	47
6	CALCULATION RESULTS FOR GAS CLEANING PROCESSES	51
6.1	COLD GAS CLEANING REACTORS.....	51
6.2	HOT GAS CLEANING REACTORS.....	56
7	DISCUSSION OF RESULTS AND SUMMARY	61
8	CONCLUSION AND OUTLOOK	67
	ABBREVIATIONS & SYMBOLS	69
	REFERENCES	73
	ANNEX	78

1 Introduction

In the past the availability of fossil energy resources has been a major reason for the successful development of wealthy societies in some parts of our world. The excessive use of fossil energy resources leads to significant negative impacts on our environment and climate. In recent times pressures on the global environment have led to calls for an increased use of renewable energy sources. Europe has experienced a change in the way its energy is generated and consumed. Rising concerns over climate change and security of supply have led European countries to invest in renewable technologies. For the next years, the European Commission has defined a set of non-binding rules which builds upon previous legislation with the aim of ensuring a 40 % cut in greenhouse gas emission in 2030 relative to 1990 levels. Furthermore, an increase in renewable energy sources up to 27 % is targeted [1,7].

Biomass is, among renewable energy sources, a potential source of renewable energy. The conversion of biogenic materials into a suitable form of energy can be achieved using a number of different technologies. Usually electricity or liquid fuels for combustion engines are produced from biomass [2]. A promising technology to process biomass for industrial applications is dual fluidized bed gasification. The generated product gas from biomass gasification can be used to produce further synthetic products, such as synthetic natural gas (SNG), methanol or Fischer-Tropsch diesel and gasoline [5].

The aim of the present work is to find answers to the following research question: “can a process for the production of SNG from biogenic residues be designed that meets the requirements of the methanation catalyst?” The produced SNG can be injected into the grid for the utilization in households, gas turbines or industries which require natural gas for their production processes. The interest in this technology raised in the 1950s until the 1980s [5]. With the aim of the European Commission to replace up to 20% of European fuel consumption by biofuel, replacing natural gas partly with bio-methane becomes necessary [5].

To find out if a process for the production of SNG from biogenic residues can be designed the present work is structured as follows. First, the state of the art of SNG-production from biomass gasification is presented. This chapter includes a literature review on dual fluidized bed gasification, sorption enhanced reforming, methanation, the different reactor types for methanation, gas cleaning and finally further R&D challenges in this field. In **Chapter 3** a conducted gasification experiment with biogenic residues at the advanced 100 kW_{th} test plant at the TU Wien is described. Subsequently in **Chapter 4**, a scale up, based on the gathered data from the experiment, to an 8 MW_{th} gasifier was done. Further on mathematical models were created to design reactors which are able to meet the specified limits of the methanation catalyst. In **Chapter 5** a cold and hot gas cleaning process was designed and described

based on the mathematical models for the individual reactors. The results obtained from the calculation models are displayed in **Chapter 6**. Starting with the cold gas cleaning process each reactor is represented through a flow chart. Additionally, a short description of the working principle from the respective reactor is given. Furthermore, calculated key parameters are shown as well. **Chapter 7** discusses the calculation results. The cleaning performance of the gas cleaning processes was evaluated by using the specified limits of the methanation catalyst as a reference. Furthermore, the calculated key parameters of the respective gas cleaning process are given and discussed. Finally, **Chapter 8** concludes the work providing answers to the research question and gives suggestions for further research on the SNG production process from biogenic residues especially in terms of gas cleaning.

2 State of the art of SNG-production from biomass gasification

2.1 Dual fluidized bed gasification

In general gasification represents a thermochemical process where a fuel is converted into a gas under high temperatures and a lack of oxygen (O₂). Drying, devolatilization and gasification are the main steps from solid fuels to a gaseous product. For one particle, all process steps mentioned before are observed [10]. The major operating parameters for gasification are pressure and temperature. In addition to that various gasification agents such as air, steam, carbon dioxide or oxygen can be used [4]. **Table 1** shows the main reactions occurring during the gasification process including if the respective enthalpy of each reaction is endothermic or exothermic.

Table 1: Important reactions of gasification and combustion [10,11]

Name of reaction		Enthalpy	
Heterogeneous reactions (gas-solid)			
Oxidation of carbon	$C + O_2 \rightarrow CO_2$	Highly exothermic	Eq. 2.1
Partial oxidation of carbon	$C + \frac{1}{2} O_2 \rightarrow CO$	Exothermic	Eq. 2.2
Heterogeneous water-gas reaction	$C + H_2O \rightarrow CO + H_2$	Endothermic	Eq. 2.3
Boudouard reaction	$C + CO_2 \rightarrow 2 CO$	Endothermic	Eq. 2.4
Hydrogenation of carbon	$C + 2 H_2 \rightarrow CH_4$	Slightly exothermic	Eq. 2.5
Generalised steam gasification of solid fuel (bulk reaction)	$C_x H_y O_z + (x - z) H_2 O \rightarrow x CO + \left(x - z + \frac{y}{2}\right) H_2$	Endothermic	Eq. 2.6
Homogeneous reactions (gas-gas)			
Oxidation of hydrogen	$2 H_2 + O_2 \rightarrow 2 H_2 O$	Highly exothermic	Eq. 2.7
Water-gas shift	$CO + H_2 O \leftrightarrow CO_2 + H_2$	Slightly exothermic	Eq. 2.8
Methanation	$CO + 3 H_2 \leftrightarrow CH_4 + H_2 O$	Exothermic	Eq. 2.9
Generalised steam reforming of hydrocarbons	$C_x H_y + x H_2 O \rightarrow x CO + \left(x + \frac{y}{2}\right) H_2$	Endothermic	Eq. 2.10
Generalised dry reforming of hydrocarbons	$C_x H_y + x CO_2 \rightarrow 2x CO + \frac{y}{2} H_2$	Endothermic	Eq. 2.11

The most commonly used gasification agent in biomass gasification is still air [10]. This means the product gas has a high content on nitrogen and cannot be used for further methanation. In the framework of synthetic natural gas (SNG) production steam is used as a gasification agent frequently. With regard to the following methanation step, the generated product gas has a favourable ratio between hydrogen and carbon monoxide and contains no nitrogen [5]. To increase the hydrogen content in the product gas carbon dioxide removal is an important part of the SNG-production process (**Eq. 2.8**). To realize the product gas requirements mentioned above a dual fluidized bed gasifier is a suitable and well-developed

technology, also at commercial scale [5,6]. Furthermore, fluidized bed systems can handle a wide range of fuels and do not need an air separation unit compared to entrained flow systems [6]. **Figure 1** shows the basic principle of a dual fluidized bed gasifier. The system consists of two reactors, a gasification reactor and a combustion reactor. The solid fuel and steam as gasification and fluidization agent is fed to the gasification section. The combustion section is fed with the circulating bed material including remaining wood char and fluidized with air which leads to a combustion and heats up the bed material to higher temperatures. Additionally, fuel can be added to increase the temperature.

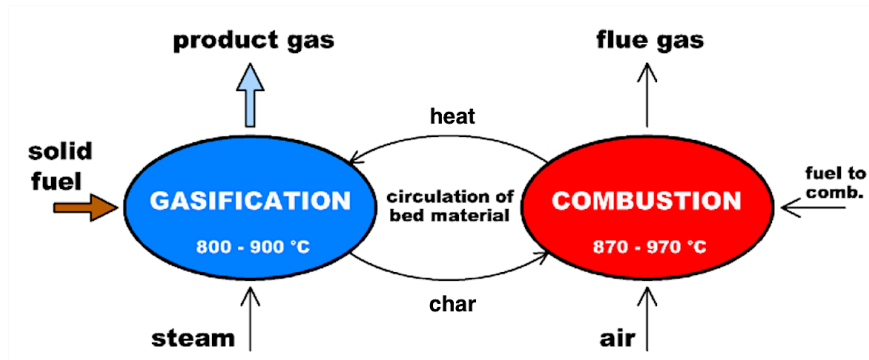


Figure 1: Basic principle of a dual fluidized bed gasifier [6]

The produced hot flue gas is separated from the bed material via a cyclone and leaves the system whereas the hot bed material returns to the gasification section and provides the heat for the endothermic gasification reactions. Steam as gasification agent enables water-gas reactions and steam reforming of hydrocarbons in the gasification reactor. This allows to produce a product gas rich of hydrogen [3,7]. Low tar content in the product gas can be achieved by catalytic active bed materials or special reactor designs [8]. **Table 2** shows the gasification parameter and product gas composition for dual fluidized bed steam gasification.

Table 2: Product gas composition of dual fluid gasification from internal data

		advanced 100 kW _{th} , TU Wien	advanced 100 kW _{th} , TU Wien	Unit
Gasification parameters	Fuel	Wood pellets	Wood pellets	-
	T _{Bubbling Bed}	800	650	°C
	T _{Column}	810	711	°C
	Steam to fuel ratio	0.6	0.7	kg/kg
	Fuel input	20.3	20.3	kg/h
	Product gas yield	0.8	0.8	Nm ³ _{db} /kg _{fuel,daf}
	Product gas power	87	87	kW
	Gasification agent	Steam	Steam	-
	Bed material	Olivine + 10 % limestone	Limestone	-
	Operation mode	Conventional gasification	Sorption enhanced reforming	-
Main components	Hydrogen (H ₂)	35 – 45	50 – 75	vol.-% _{db}
	Carbon monoxide (CO)	20 – 30	4 – 12	vol.-% _{db}
	Carbon dioxide (CO ₂)	15 – 25	5 – 20	vol.-% _{db}
	Methane (CH ₄)	8 – 15	8 – 15	vol.-% _{db}

Gas components and Impurities	Acetylene (C ₂ H ₂)	N/A	N/A	vol.-% _{db}	
	Ethylene (C ₂ H ₄)	1 – 4	1.5 – 2	vol.-% _{db}	
	Ethane (C ₂ H ₆)	0.3 – 1	0.5 – 1	vol.-% _{db}	
	Propene (C ₃ H ₆)	N/A	N/A	vol.-% _{db}	
	Propane (C ₃ H ₈)	0.2 – 0.5	0.05 – 0.2	vol.-% _{db}	
	Ammonia (NH ₃)	0.02 – 0.4	0.02 – 0.4	vol.-% _{db}	
	Hydrogen sulphide (H ₂ S)	0 – 0.04	0 – 0.04	vol.-% _{db}	
	Carbonyl sulphide (COS)	0 – 0.001	0 – 0.001	vol.-% _{db}	
	Hydrochloric acid (HCl)	0.0005 – 0.03	0.0005 – 0.03	vol.-% _{db}	
	Hydrogen cyanide (HCN)	0.01 – 0.04	0.01 – 0.04	vol.-% _{db}	
	Nitrogen (N ₂)	0 – 0.5	0 – 0.5	vol.-% _{db}	
	Water (H ₂ O)	25 – 45	45 – 65	vol.-%	
	Dust and char	30 – 80	20 – 50	g/Nm ³ _{db}	
	Gravimetric tar	1 – 6	0.7 – 2.2	g/Nm ³ _{db}	
	GCMS tar	2 – 15	1 – 7	g/Nm ³ _{db}	
	GCMS tar composition				
	Naphthalene	800 – 4700	N/A	mg/Nm ³ _{db}	
	Benzene (B)	6000 – 6400	N/A	mg/Nm ³ _{db}	
	Toluene (T)	0 – 400	N/A	mg/Nm ³ _{db}	
	Ethylbenzene (E)	0 – 5	N/A	mg/Nm ³ _{db}	
Xylene (X)	0 – 5	N/A	mg/Nm ³ _{db}		
Critical components in ash					
Arsenic (As)	0	0	mg/g _{Ash,db}		
Natrium (Na)	~ 10	~ 20	mg/g _{Ash,db}		

The species acetylene, ethylene, propene, ammonia, hydrogen sulphide, carbonyl sulphide, hydrochloric acid, hydrogen cyanide, nitrogen, water, dust, char, tar, arsenic and natrium are considered as **impurities** in this master thesis. **Figure 2** shows the classic (1) and advanced (2) design of the 100 kW_{th} dual fluidized bed pilot plant developed at TU Wien. The classic design is typically used at the existing industrial plants, which consists of a bubbling-fluidized bed as gasification reactor and a fast-fluidized bed as combustion reactor. The two reactors are connected via a loop seal or chute on the lower and a loop seal on the upper part of the reactor. The bed material, which leaves the combustion reactor, is separated from the flue gas via a cyclone and then introduced into the gasification reactor again. Whereas the advanced gasification reactor consists of two main parts to improve the gas-solid contact within the reactor. The lower part where the fuel is introduced, is operated as bubbling fluidized bed. The upper part is designed as a counter-current column with turbulent fluidized zones. The hot bed material, which is separated from the flue gas stream, is introduced into the column. Further, the column is equipped with constrictions, which leads to an increased bed material hold-up over the height of the column. As a result, the interaction of bed material and product gas in the upper part of the gasification reactor is increased significantly. In addition, the advanced design enhances abrasion resistance for pure calcite (CaCO₃) as bed material due to two gravity separators on top of the reactors. Compared to the use of cyclones, the gas and particle velocities are lower, which leads to smooth separation of the calcite from the gas streams [3,6,9].

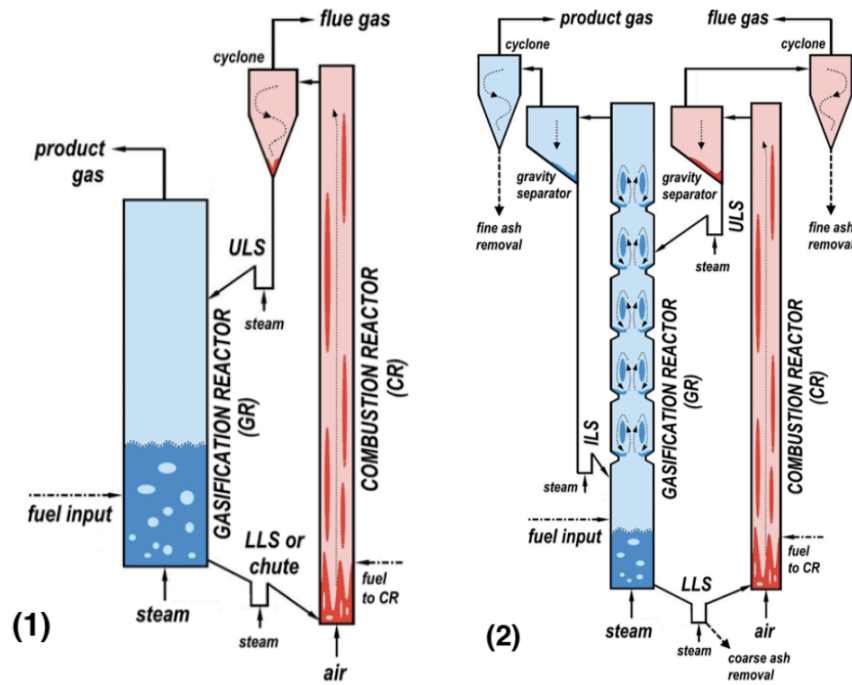


Figure 2: Classic (1) and advanced (2) design of the 100 kW_{th} dual fluidized bed pilot plant at TU Wien [6]

Two other concepts in the context of SNG – production from biomass will be briefly mentioned now. Both technologies are not yet available at commercial scale but could have promising future as the complexity of the whole SNG production process is reduced. Hydrothermal gasification is a technology to convert wet biomass directly into hydrogen and/or methane. To reach a nearly complete thermochemical reaction of the organic compounds supercritical water, at 400 °C – 700 °C and 200 – 300 bar, is used. At such high pressure the methane formation is favoured. In contrast to methane, hydrogen and carbon monoxide formation increase with temperature. Another possibility is the hydrogasification. Hydrogen is used as gasification agent. This lead to a higher methane content in the product gas [3,5,10].

In the upcoming chapter the gasification technology sorption enhanced reforming (SER) is discussed in more detail. With SER the hydrogen to carbon monoxide ratio can be controlled by adjusting the gasification temperature. Limestone, which is used as bed material, can captures carbon dioxide and reduce impurities such as tar. A product gas composition can be achieved with good preconditions for the methanation step.

2.2 Sorption enhanced reforming (SER)

Based on the dual fluidized bed gasification principle a beneficial product gas composition, with regard to the methanation step, can be achieved by using limestone as bed material for the fluidized beds. Limestone offers the possibility to remove carbon dioxide from the gasification reactor and transport it in the combustion reactor. A product gas with hydrogen contents up to 70 vol.-%_{db} can be achieved. Furthermore, an adjustment of the hydrogen to carbon monoxide ratio in a wide range can be gained with sorption enhanced reforming (SER). At the same time the tar content is reduced through catalytic activity of limestone [7]. **Figure 3** shows the basic principle of the SER process.

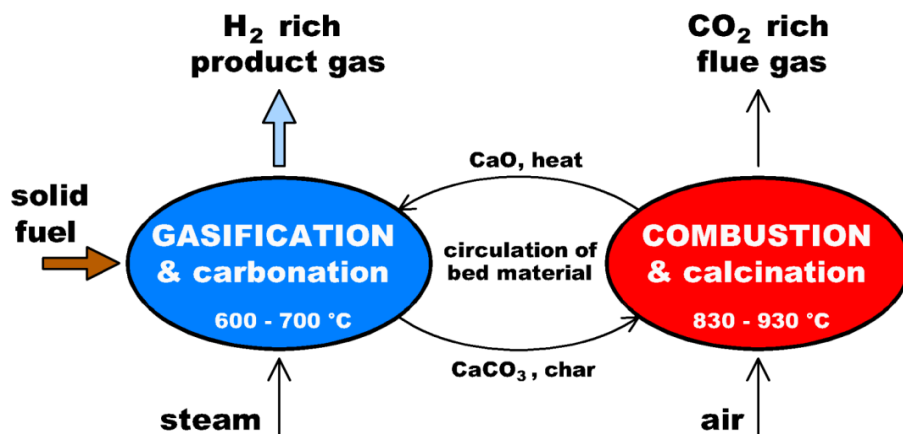
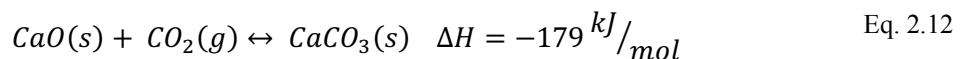
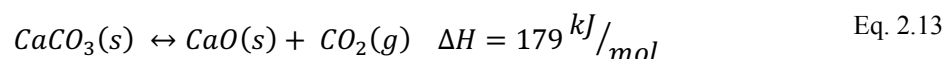


Figure 3: Basic principle of sorption enhanced reforming (SER) [28]

The basic idea of SER is to carbonize the calcium oxide (CaO) in the gasification reactor by a capture of carbon dioxide from the product gas according to the following reaction:



The resulting calcium carbonate (CaCO₃) is transported to the combustion reactor where a calcination takes place:



Carbon dioxide is formed and released into the hot flue gas. For this purpose, the temperature in the gasification reactor has to be decreased down to around 650 °C and the combustion reactor must be operated at temperatures above 800 °C (**Figure 4**) [12]. The removal of carbon dioxide from the product gas pushes the water gas shift reaction (**Eq. 2.8**) to the product side, leading to an increased hydrogen content of around 70 vol.-%_{db} and a lower carbon monoxide and carbon dioxide content of around 10 vol.-%_{db} each [5].

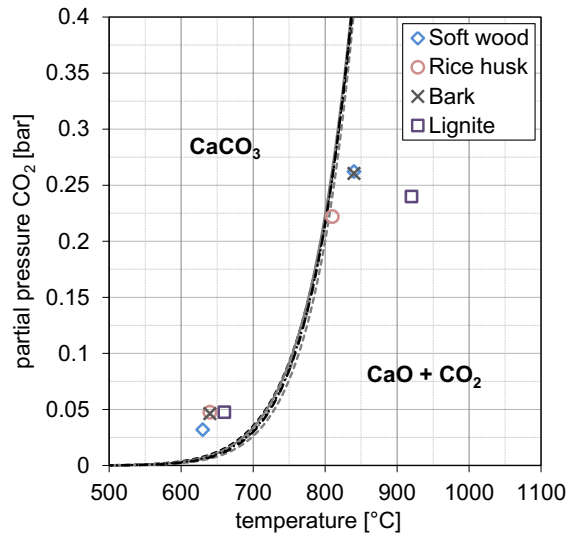


Figure 4: Equilibrium partial pressure of CO₂ dependent on reaction temperature [28]

The product gas composition is highly dependent from the temperature for SER-operation. Parameters like fuel type, water content of fuel, calcium oxide cycling rate etc. can have an influence on the product gas composition as well [6,8]. **Figure 5** shows the hydrogen to carbon monoxide ratio (1) and the content of main components in the product gas (2) over the gasification temperature. The hydrogen to carbon monoxide ratio and the methane content are mostly decisive in regard to further methanation of the product gas. As it can be seen in (1) the SER-process offers the possibility to adjust the hydrogen to carbon monoxide ratio by adapting the gasification temperature. From around 620 °C to 680 °C a ratio between 8 to 10 can be reached which is suitable for further methanation. From 700 °C upwards the ratio drops down to 2 at about 800 °C. Graph (2) additionally shows the temperature range for SER-operation from around 620 °C to 680 °C and for conventional gasification from up to 800 °C. It can be seen that the stoichiometric ratio of hydrogen to carbon monoxide to carbon dioxide is around 7:1:1 inside the temperature range for SER-operation. This ratio is ideal for further methanation.

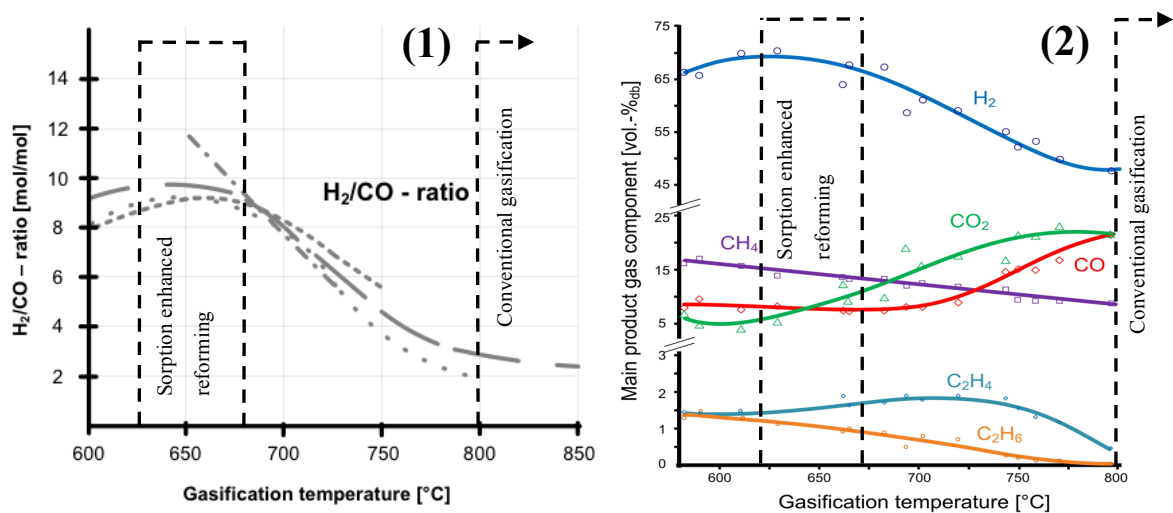


Figure 5: Hydrogen to carbon monoxide ratio (1) and main components in the product gas (2) over gasification temperature (from internal sources)

To keep up a continuously good SER operation a stable and reactive carbon dioxide sorbent is needed. In addition, the sorbent should be capable to maintain a low attrition rate and a high carbon dioxide load during long time operation. Also, a catalytic activity with respect to tar removal is desirable. Therefore, the properties **attrition**, **carbon dioxide sorption capacity**, **catalytic activity** and the **influence of impurities on limestone** will be discussed in more detail.

Attrition is the result of mechanical, thermal and chemical stress. During fluidization, particles are subjected to mechanical stress arise from collisions and surface wear. Under the typical operating conditions of SER, bed material particles will experience thermal stress due to the temperature difference between gasification and combustion reactor and chemical stress due to **Eq. 2.12** and **Eq. 2.13** as well. Especially for limestone higher calcination temperature and higher impact velocity results in higher attrition [12,13]. Material properties, e.g. surface quality, relative hardness of the particle or particle shape, influence the type and extent of attrition. Softer or porous materials like limestone abrade much more than harder or compact ones. Attrition is occurring at a higher rate in the combustion reactor (**Eq. 2.12**) than in the gasification reactor (**Eq. 2.13**) [14]. This is owed to the fact that calcined particles are lighter and more fragile than carbonated ones which are denser and more compact. Different approaches on improving the attrition resistance of limestone were investigated. Pelletisation and an addition of various binders were tested in a pilot fluidized bed system. It was found out that pelletisation is an inadequate approach for reducing the attrition. Further the addition of cement as a binder just marginal improves the mechanical strength of the resultant pellets [13].

A **carbon dioxide sorption capacity** of 0.785 kg_{CO2} per kg_{CaO} is achieved at complete carbonation according to the ratio of 1 mol carbon dioxide to 1 mol calcium oxide (**Eq. 2.12**). Several mechanisms, e.g. sintering or changes in pore structure, lead to a loss of carbon dioxide capture capacity. Especially after many cycles of carbonation and calcination the capacity decreases significantly [15]. Several authors investigated calcination and carbonation of different limestones regarded to their carbon dioxide uptake [16,17]. It is reported that the sorption of carbon dioxide by calcium oxide particles leads to a loss of pore volume and to the development of a layer of calcium carbonate which reduces the carbon dioxide diffusion rate. In addition to that, the carbon dioxide capture capacity behaviour during a number of cycles was investigated. It was observed that the uptake highly decreases in the first cycles and tends to stabilize with increasing cycle number. **Figure 6** illustrates the reduction of porosity of a calcium oxide particle after one cycle (1) and after 22 h in a dual fluidized bed gasifier with alternating carbonation and calcination cycles (2). On the left picture, it is visible that the pore structure is in a suitable shape after one cycle. After 22 h of operation in a gasifier with alternating cycles the loss of pore volume is visible and the surface becomes smooth at some areas.

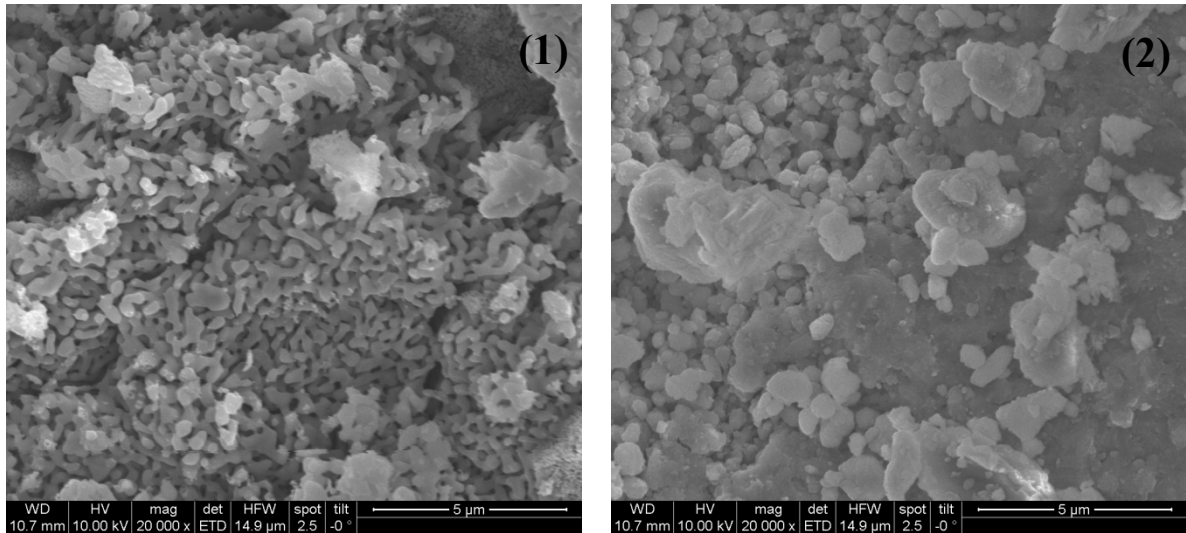


Figure 6: Scanning electron microscope (SEM) pictures illustrate the decay of porosity of calcium oxide. After one calcination cycle (1) and after 22 h (2) in a dual fluidized bed gasifier with alternating carbonation and calcination cycles. (recorded at TU Wien)

Limestone is **catalytically active** regarding tar reforming. Tar causes problems for the methanation catalysts and is also a well-known by-product from steam gasification of biomass. In case of relatively low temperatures during SER compared to conventional gasification higher tar contents in the product gas would be expected. However, due to the **catalytical activity** of limestone regarding tar reforming, lower tar values can be reached within the SER-process [11]. Tar formation is influenced by the gasification temperature, fuel type, catalytic activity of the bed material, steam to fuel ratio and fuel water content. **Table 3** gives an overview about typical tar ranges for different types of gasifier with limestone as bed material.

Table 3: Gravimetric and GCMS tar ranges for different gasifier with limestone as bed material

	Unit	20 kW _{th} , IFK Stuttgart [18]	200 kW _{th} , IFK Stuttgart [19]	Classical 100 kW _{th} , TU Wien [20]	advanced 100 kW _{th} , TU Wien [21]	SER 8 MW _{th} , CHP Güssing [22]
Gasification temperature	°C	655	~ 650	600 – 700	600 – 700	676
Gravimetric tar	g/Nm ³ _{db}	29	6 – 31	0.3 – 3.0	0.7 – 2.2	1
Gas chromatography mass spectrometry (GCMS) tar	g/Nm ³ _{db}	n.a.	n.a.	2 – 9	2.5 – 8.3	n.a.

Impurities such as ammonia, sulphur or chlorine influence the reactivity of limestone as well. Sulphur and chlorine and their chemical combinations will now be discussed in more detail. Sulphur dioxide (SO₂) for example has a deactivating effect on the carbon dioxide sorption capacity due to the formation of calcium sulphate (CaSO₄) [23,24]. Experiments with calcium oxide and hydrogen sulphide revealed that high hydrogen sulphide concentrations of around 0.22 vol.-%_{db} have a deactivating and irreversible effect on the bed material [25]. In case of chlorine as impurity calcium chloride (CaCl₂) is a possible

product that can be formed and can have a deactivating effect on carbon dioxide sorption capacity. In case of a further methanation of the product gas from SER the knowledge about the formation of impurities during the gasification step is essential. Upcoming the basic principles of methanation as well as different methanation reactor types are discussed. Additionally, discussions about usability and performance of several catalytic materials, which initiate the heterogeneously catalysed methanation process, are done.

2.3 Basic principles of Methanation

Methanation, in association with SNG-production from biomass gasification, is a heterogeneously catalysed process where gaseous species react in the presence of a solid material. The aim of this synthesis step is to produce a gas which can be injected into the natural gas grid. This means the SNG must have more than 96 % methane and can contain ethane to a lower extent. Also, species with low or even no volumetric heating values, such as hydrogen, nitrogen or carbon dioxide, are allowed at the range of a few percent. Due to its toxicity carbon monoxide has to be under 0.5 % [4,5]. The complex product gas composition from gasification (**Table 2**) leads to a number of reactions beside the actual methanation. The main reactions occurring in a methanation reactor are shown in **Table 4**.

Table 4: Important reactions of methanation [5]

Name of reaction		Enthalpy	
Homogeneous reactions (gas-gas)			
Carbon monoxide methanation	$3 H_2 + CO \leftrightarrow CH_4 + H_2O$	Exothermic	Eq. 2.14
Carbon dioxide methanation	$4 H_2 + CO_2 \leftrightarrow CH_4 + 2 H_2O$	Exothermic	Eq. 2.15
Homogeneous water-gas shift	$CO + H_2O \leftrightarrow CO_2 + H_2$	Slightly exothermic	Eq. 2.16
Hydrogenation to methane	$C_2H_2 + H_2 \rightarrow C_2H_4$	Exothermic	Eq. 2.17
	$C_2H_4 + H_2 \rightarrow C_2H_6$	Exothermic	Eq. 2.18
	$C_2H_x + \left(4 - \frac{x}{2}\right) H_2 \rightarrow 2 CH_4$	Exothermic	Eq. 2.19
Heterogeneous reactions (gas-catalyst surface)			
Boudouard reaction	$2 CO \leftrightarrow C + CO_2$	Exothermic	Eq. 2.20
Carbon methanation	$2 H_2 + C \leftrightarrow CH_4$	Slightly exothermic	Eq. 2.21
Heterogeneous water-gas shift	$C + H_2O \rightarrow CO + H_2$	Endothermic	Eq. 2.22

To which extent the reactions from **Table 4** occur depends on several parameters like product gas composition of gasification, chosen catalyst, reactor type and design as well as the applied operation conditions. Therefore, the methanation catalysts as well as a thermodynamic view on the main reactions (**Eq. 2.14** and **Eq. 2.15**) will be mentioned in this chapter. Since 1902 several authors do have investigated metals which promote the methanation reaction, based on a catalytic reaction. These metals are: Ruthenium, nickel, copper, cobalt, iron, and molybdenum. **Figure 7** shows a nickel-based catalyst (1) as it is used in fixed bed methanation reactors and a scanning electron microscope picture of a catalyst surface (2). Nickel-based catalysts are by far the most applied one for methanation. The metal is relatively cheap and it is very active. Further nickel has the highest selectivity to methane in comparison to the other metals listed before [29]. Due to various process conditions for methanation different materials can be added to the catalyst material. For isothermal operation for example, highly porous γ -

alumina can be used as support. Under adiabatic methanation conditions, where high temperature occurs, α -alumina is often used as support, eventually with of a small percentage of magnesia and lanthanum for stabilization and to resist carbon deposition [44].

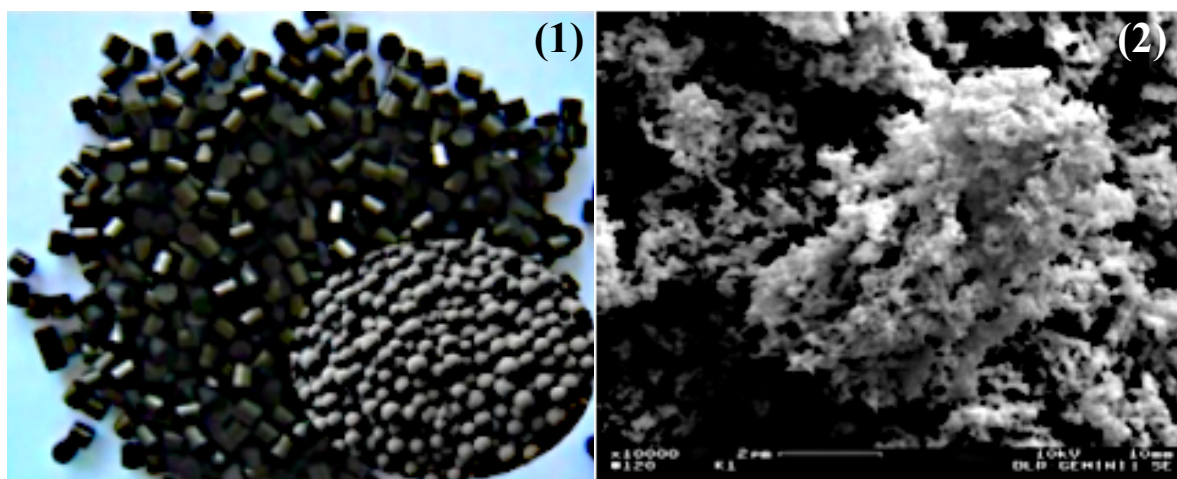


Figure 7: Nickel-based catalyst (1), scanning electron microscope recording of a catalyst surface (2) [47,69].

An essential problem at catalytic reactions is catalyst deactivation. The loss of catalytic activity and/or selectivity over time is a major problem of industrial catalytic processes. **Table 5** and **Table 6** represent an overview of the different mechanisms of catalyst deactivation and a comparison between different catalyst materials respectively. As some biogenic fuels contain a number of harmful elements for the methanation catalyst, e.g. sulphur and nitrogen the mechanism poisoning will be discussed in more detail.

Table 5: Mechanisms of catalyst deactivation [30]

Mechanism	Type	Description
Poisoning	Chemical	Strong chemisorption of species or impurities (e.g. sulphur compounds) on catalytic sites, thereby blocking sites for catalytic reaction
Fouling	Mechanical	Physical deposition of species from fluid phase onto the catalytic surface and in catalyst pores (e.g. carbon deposition)
Thermal degradation	Thermal	Thermally induced loss of catalytic surface area and support area (e.g. sintering due to pore collapse); chemical transformations of catalytic phases to non-catalytic phases
Vapor formation	Chemical	Reaction of gas with catalyst phase to produce an inactive bulk or volatile compounds, which exit the reactor.
Vapor – solid and solid – solid reactions	Chemical	Reaction of fluid, support, or promoter with catalytic phase to produce inactive phase
Attrition/crushing	Mechanical	Loss of catalytic material due to abrasion Loss of internal surface area due to mechanical-induced crushing of the catalyst particle, attrition, size reduction of catalyst particles or break up of catalyst granules

Table 6: Comparison of different catalyst materials [29,30,44]

Catalyst material	advantages	disadvantages
Ruthenium (Ru)	<ul style="list-style-type: none"> - six times more active than nickel and three times more active than iron - long term catalytic activity - at temperatures above 100 °C methane was produced at a total pressure of less than 0.13 bar 	<ul style="list-style-type: none"> - much more expensive than nickel - produces higher hydrocarbons under methanation conditions - traces of sulphur compounds rapidly deactivate the catalyst
Nickel (Ni)	<ul style="list-style-type: none"> - very active for methanation when present in a form having high surface area - most selective to methane of all materials - cheap and therefore mostly used. Lots of combinations with supported materials have been investigated - nearly complete carbon monoxide conversion possible at 280 °C 	<ul style="list-style-type: none"> - easily poisoned by sulphur compounds (a fault common to all of the more active methanation catalysts) - can react with carbon monoxide to form a carbonyl, Ni(CO)₄, a carbide, Ni₃C, or even free carbon
Cobalt (Co)	<ul style="list-style-type: none"> - similar activity for methanation to that of nickel - nearly complete carbon monoxide conversion possible at 340 °C 	<ul style="list-style-type: none"> - Tends to deposit carbon more than nickel catalysts under the same operating conditions - produces higher hydrocarbons under methanation conditions
Iron (Fe)	<ul style="list-style-type: none"> - similar activity for methanation to that of nickel 	<ul style="list-style-type: none"> - The conversion of CO only reached 20 % even at 340 °C - rapid carbon deposition - produces higher hydrocarbons under methanation conditions
Molybdenum (Mo)	<ul style="list-style-type: none"> - Sulphur resistant and, in fact, are commonly sulphided before used - selectivity to methane up to 94 % 	<ul style="list-style-type: none"> - relatively high temperatures needed for conversion - selectivity and activity declines with rising hydrogen sulphide contents - moderate activity

Nitrogen is mostly present as ammonia in the product gas. Sulphur can form hydrogen sulphide, carbonyl sulphide, carbon disulphide, mercaptans and a high number of thiophenic species [5]. The tolerable level of sulphur for nickel-based catalysts depends on the hydrogen content, the sulphur partial pressure and the temperature. Continuously present sulphur traces in the feed gas lead to a highly stable and nearly irreversible coating on the nickel surface. Furthermore, sulphur blocks the carbon monoxide and hydrogen adsorption on the nickel surface. Once sulphur is adsorbed on the catalyst surface it is very challenging to remove it again. A possibility to desorb the sulphur is by a complex redox cycle procedure using low oxygen partial pressure and subsequent reduction [30,44]. The only methanation catalyst unaffected by sulphur impurities consists of molybdenum sulphide [29].

Another important issue, related to catalyst deactivation, for the operation of catalysts in methanation is carbon deposition (fouling). This mechanism can be caused by carbon monoxide and hydrocarbons. **Figure 8** illustrates possible effects on the functioning of a supported metal catalyst due to fouling. Carbon may chemisorb as a monolayer or physically adsorb in multilayers and in either case block access of reactants to metal surface sites. Furthermore, micro- and mesopores can be plugged such that access of reactants is denied to many crystallites inside these pores. The formation of the different carbon deposits mainly depends on temperature, on the partial pressures of steam, hydrogen, carbon monoxide, and hydrocarbons, on the nickel crystallite size and on the different materials added to support the catalyst [44].

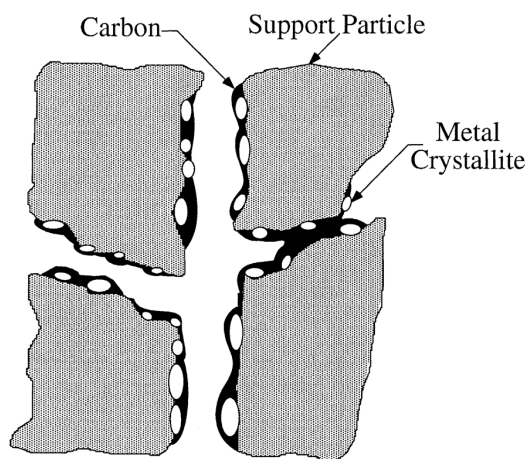


Figure 8: Conceptual model of fouling, crystallite encapsulation and pore plugging of a supported metal catalyst due to carbon deposition [30].

The reaction mechanism occurring on the catalyst surface to form methane is under investigation for a long time. However, there is still a variety of proposed reaction mechanisms, surface intermediates and rate-determining steps. This can be explained by the wide range of catalysts, operating conditions and the different kinetic approaches to describe the mechanisms. One approach, which is accepted by several authors, assumes the methanation to proceed via molecular adsorption and subsequent dissociation of carbon monoxide. This leads to an adsorbed carbon as intermediate on the catalyst surface, which is stepwise hydrogenated to methane [5,29]. Further the effects of temperature, pressure, hydrogen to carbon monoxide and carbon dioxide ratio were investigated on the methanation reactions. This happens in terms of their effects on the conversion of carbon monoxide and carbon dioxide, methane selectivity and yield, as well as on the deposition of carbon [29,31]. **Figure 9** shows how the carbon is distributed within the different molecules as predicted by the thermodynamic equilibrium in the range from 200 °C to 500 °C and different pressures. Picture (1) compares the situation for stoichiometric mixtures of hydrogen and carbon monoxide with a ratio of $H_2/CO = 3$ and picture (2) for hydrogen and carbon dioxide with a ratio of $H_2/CO_2 = 4$. In general, the equilibrium of **Eq. 2.14** and **Eq. 2.15** is influenced by temperature as well as pressure. A high methane yield over 99 % can be obtained at temperatures around 200 °C to 300 °C, a pressure of up to 30 bar and a hydrogen to carbon monoxide ratio over 3

without significant carbon deposition. On the other hand, an increase in temperature leads to a methane decrease, whereas the unreacted carbon monoxide, hydrogen, carbon dioxide, and deposited carbon increase simultaneously. The carbon deposition occurs when the temperature is higher than 450 °C [31]. Carbon formation can be remarkably suppressed if the feed gas contains steam. Impurities such as higher hydrocarbons (e.g. ethylene) are known to be harmful because they lead to carbon deposition on the catalyst. Therefore, these compounds should be completely removed in the feed gas to maximize the methane yield and minimize carbon formation [5].

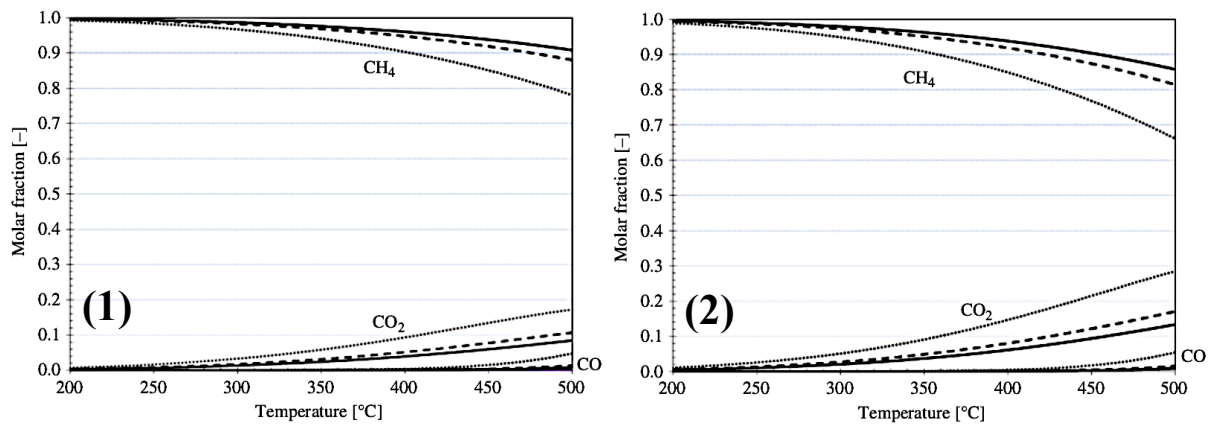


Figure 9: Distribution of carbon atoms within the different molecules as predicted by the thermodynamic equilibrium for stoichiometric mixtures of: hydrogen to carbon monoxide with a ratio of 3 (1) and hydrogen to carbon dioxide with a ratio of 4 (2) in the range from 200 °C to 500 °C and different pressures (1bar = dotted lines, 5bar = dashed lines and 10bar = full line) [5]

These thermodynamic outcomes correspond with a laboratory experiment in which the selective methanation of carbon monoxide in presence of carbon dioxide was investigated using several nickel and ruthenium catalysts [32]. Within this experiment a gas mixture, consisting of 0.3 % carbon monoxide, 80 % hydrogen and 20 % carbon dioxide, was fed to each catalyst at atmospheric pressure and temperatures between 125 °C and 300 °C. The conclusion of the experimental campaign was that each catalyst showed a maximum conversion between 200 °C and 250 °C. With further increase of temperature, a reverse shift reaction occurred which lead to a faster production of carbon monoxide from carbon dioxide than it was consumed to form methane. When nickel was used as a catalyst material the amount of carbon monoxide in the produced gas exceeded the amount originally present in the feed at 300 °C. Furthermore, it was figured out that selective methanation of carbon monoxide in the presence of carbon dioxide is practicable at atmospheric pressure but that very low space velocities and moderate temperatures, probably below 225 °C for ruthenium, would be required to achieve low ppm values of carbon monoxide in the produced gas.

2.4 Methanation reactor types

The initial industrial application of the methanation has been the removal of traces of carbon oxide from hydrogen-rich feed gases in ammonia plants. During the 1950s and 1970s the methanation process management changed from being a gas cleaning step to a main synthesis process. The main difference in converting synthesis gas with high carbon monoxide concentrations to methane compared to the originally intended gas cleaning step is the higher amount of the exothermic heat of the reaction. There are two major objectives in the development of catalysed methanation reactor concepts. The first one is to control the temperature inside the reactor because the methanation reaction is strongly exothermic and equilibrium limitation occur at higher temperatures [33]. For stoichiometric mixtures of hydrogen and carbon monoxide, temperatures significantly above 700 °C can be reached [5]. The second one is to minimize catalyst deactivation due to thermal stress. The different methanation reactor types developed up to now can be differentiated according to the heat removal concept applied. Besides a few special reactor concepts, fixed bed and fluidized bed reactors have been proven suitable to meet these requirements [33].

Fixed bed reactors

To produce SNG by using a fixed bed design a series of reactors are needed to reach a desired methane yield. The gas has to be cooled in between the fixed bed reactors due to the strongly exothermic methanation reaction and the consequently occurring equilibrium limitation. With this process management (**Figure 11**) full conversion can be reached with a series of adiabatic reactors with intermittent and recirculation cooling [32]. **Figure 10** shows the temperature profile in a series of adiabatic fixed bed methanation reactors.

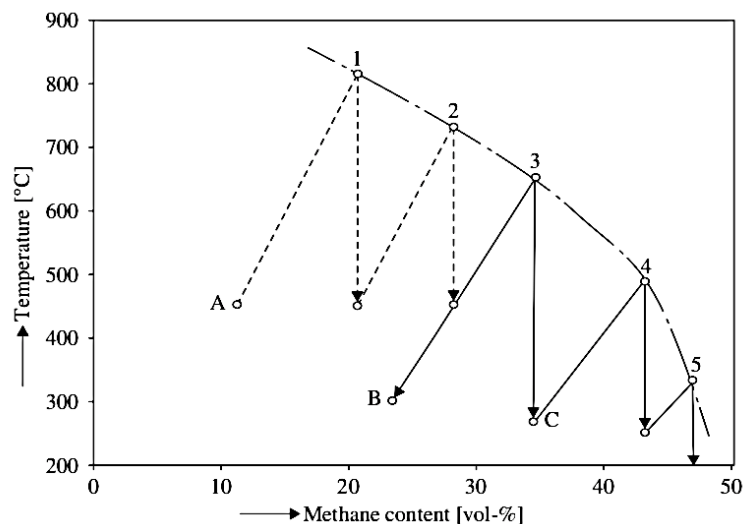


Figure 10: Temperature profile in a series of adiabatic fixed bed methanation reactors. Dash-dotted line: equilibrium limitation. Dashed lines: without product gas recycle. Full lines: with product gas recycle. [5]

In the 1960s and 1970s Lurgi developed a methanation unit including two adiabatic fixed bed reactors with internal recycle. Two pilot plants, based on the reactor concept developed in the 1960s and 1970s, were erected by Lurgi in cooperation with SASOL in Sasolburg (South Africa) and EL Paso Natural Gas Corporation in Schwechat (Austria) respectively. The two plants were operating for 1.5 years with the aim to test the performance of a commercial catalyst with 20 wt.-% Ni/Al₂O₃ and a catalyst with high nickel content. The used feed gas has a similar composition to that from **Table 2** for conventional gasification. The commercial catalyst showed a fast deactivation. The catalyst with high nickel content showed a good stability over 4000 operating hours. The adiabatic equilibrium temperature of 450 °C was reached after 20 % of the catalyst bed for fresh catalyst and after 32 % of the catalyst bed at around 4000 h. This slight deactivation is owed to increasing nickel crystallite size and to decreasing hydrogen chemisorption by approximately 50 % [33,35].

Another process called TREMP-process (Topsoes recycle energy efficient methanation process) was developed by Haldor Topsoe A/S. The process is similar to the Lurgi process with the difference that the TREMP-process decreases the recirculation rate by means of a more temperature stable catalyst. **Figure 11** shows an exemplary fixed bed methanation with intermediate cooling and gas recycle based on the TREMP-process. Haldor Topsoe A/S developed a new nickel based methanation catalyst, named MCR-2X, with significantly higher temperature stability to around 700 °C. The catalyst is alumina supported with a stabilized micro-pore system to decrease nickel crystallite sintering. The surface is high on nickel and free of alkaline [36]. The developed catalyst is way more active at lower temperatures of around 300 °C than standard nickel-based catalysts and can keep that activity at lower temperatures in case the catalyst has experienced high temperatures of around 700 °C before. This characteristic is useful when the temperature profile goes down due to catalyst deactivation [35,36].

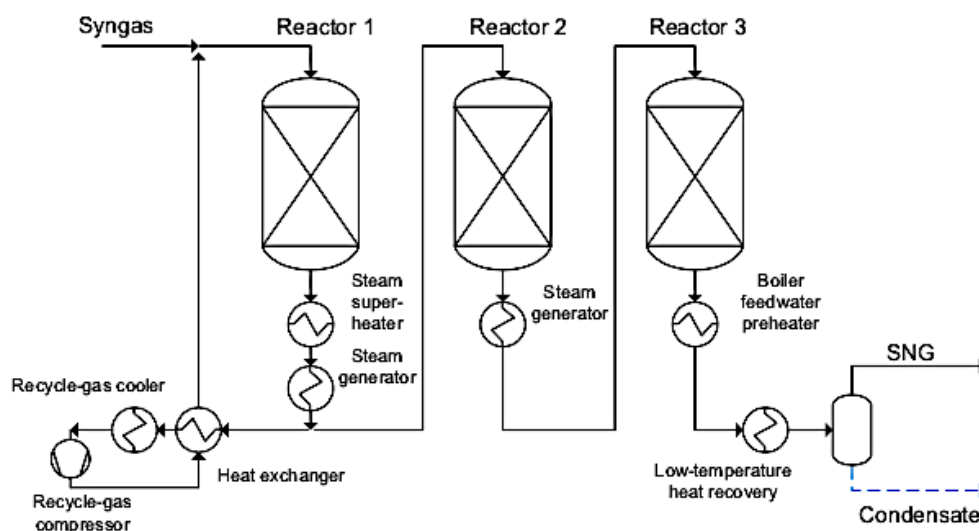


Figure 11: Exemplary fixed-bed methanation with intermediate cooling and gas recycle [45]

Fluidized bed reactors

Large-scale plants which proceed heterogeneously catalysed reactions with high exothermicity prefer fluidized bed reactors because a nearly isothermal operation is possible [33]. The nearly isothermal operation mode in a fluidized bed methanation reactor is reached by a heat dispersion over a large reactor volume, such that a significantly increased heat transfer area can be used. Through the movement of the particles in a fluid the heat transfer to cooling surfaces increases. Technically two modes of operation for fluidized bed methanation have been developed [5]. One operation mode is a bubbling fluidized bed. Here the catalyst particles are suspended in the up-flowing reaction gas. The other one is called bubbling column. In this system three phases are present. An inert liquid phase, the reaction gas and the catalytic particles. The gas and solid particles are both suspended in the inert liquid phase. With this concept, the heat transport and the thermal inertia can be improved [37]. In comparison with the fixed bed version fluidized bed reactors show some advantages. Heat as well as mass transfer are higher, it is possible to remove, add and recycle the catalyst particles continuously during operations. Further catalyst deactivation by carbon deposition and the formation of carbon fibres does not appear and carbon deposition is avoided due to the high particle movement [33,38].

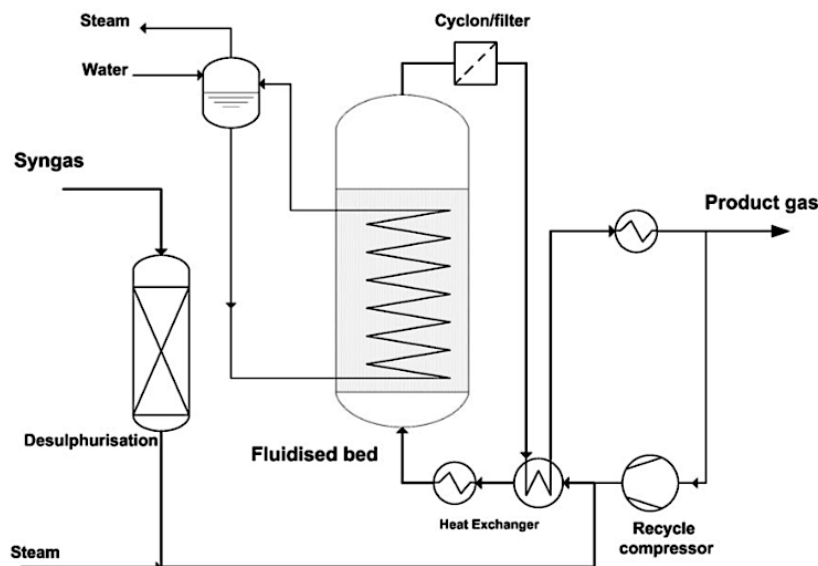


Figure 12: Thyssengas flow diagram of a bubbling fluidized bed with recycle cooling and immersed vertical heat exchanger tubes [33]

The biggest fluidized bed reactor to date was erected and operated within the Comflux project in Germany from 1975 to 1986 by the Thyssengas GmbH (Figure 12). At the development stage of this project research was done e.g. on catalyst deactivation, attrition resistance and the influence of sulphur on the methanation [39]. In terms of sulphur poisoning for the catalyst two different catalysts were investigated in the presence of up to 140 ppm hydrogen sulphide. Both catalysts, nickel molybdenum (NiMo) and nickel tungsten (NiW) both in metallic and sulfidic form, could handle the presence of

hydrogen sulphide. However, a high temperature of around 600 °C to 700 °C and a certain amount of pressure are necessary to reach equilibrium conversion.

Bubbling column

This type of methanation reactor was developed in the terms of introducing a liquid phase to the fluidized bed (**Figure 13**). One advantage is that the liquid phase acts as a buffer for the emerging heat of reaction. This behaviour is favourable to keep the reactor above “ignition” temperature when frequent start-up and shut-down are necessary, for example, in power to gas applications. The used liquid should have a very low vapor pressure, a high thermal stability and solubility for the reaction gases. Further it should not react with other species or deactivate the catalyst. To reach a high mass transfer the viscosity and surface tension should be low [33,37]. The company Chem. System Inc. (United States) conducted pilot scale tests on bubbling columns with the purpose to produce SNG. After 300 h of operation the results showed low conversion and high catalyst loss from the bubbling column [5].

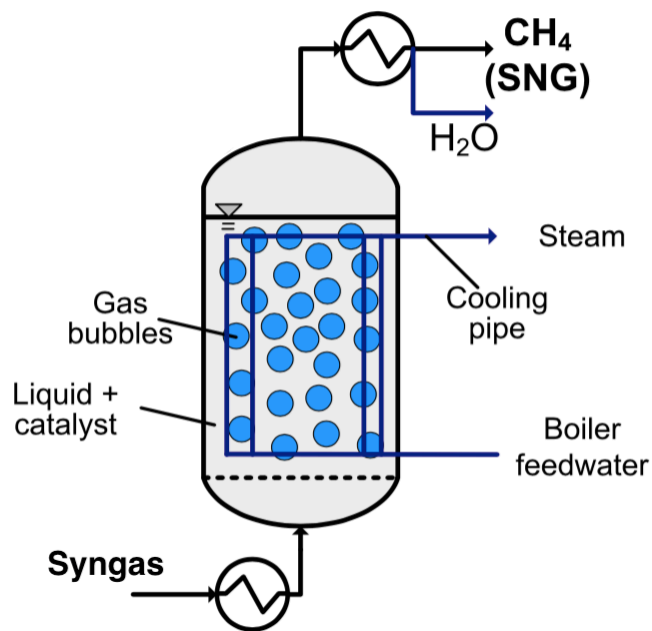


Figure 13: Schematic of a three-phase methanation reactor [46]

Finally, a comparison of the three different reactor types for methanation was done. **Table 7** summarizes the positive and negative characteristics of each reactor type.

Table 7: Comparison of different reactor types for methanation [37]

	Adiabatic fixed bed	Fluidized bed	Bubbling column
Advantages	<ul style="list-style-type: none"> - High reaction rate - Low mechanical load on catalyst - Wide range of operation - Simple catalyst handling - Simple dimensioning and scale up 	<ul style="list-style-type: none"> - Effective heat removal - Small temperature gradients - Good mass transfer - Only one reactor necessary 	<ul style="list-style-type: none"> - Very effective heat removal - Isothermal conditions - Less sensitive to fluctuating feed streams - Replacement of the catalysts during operation
Drawbacks	<ul style="list-style-type: none"> - High thermal load on catalyst - Removal of heat challenging - Temperature gradients - Multiple reactors in series - Several compressors and/or heat exchangers necessary 	<ul style="list-style-type: none"> - High mechanical load on catalyst (attrition) - Entrainment of catalyst - Reduction of conversion due to bubbling 	<ul style="list-style-type: none"> - Liquid-side mass transfer limitations - Backmixing possible - Evaporation and decomposition of heat transfer liquid

2.5 Gas cleaning

The generated product gas from biomass gasification contains mainly gas components such as hydrogen, carbon monoxide and dioxide and methane. Additionally, impurities are also present. Especially sulphur compounds are harmful for methanation catalysts. Also tar, nitrogen-containing compounds, particle matter and higher hydrocarbons influence the methanation process in a negative way and have to be removed.

Gas cleaning technologies can be divided into three different categories according to the operating temperature. In general, the range is between -60 °C and 1000 °C. **Cold gas cleaning** is operating at ambient temperature and below. Due to product gas temperatures of up to 850 °C at the exit of the gasifier of a dual fluidized bed system low temperature gas cleaning requires cooling in order to suit the temperature limits of the downstream filtration system and cleaning reactors [5,40]. **Warm gas cleaning** facilities operate at a temperature range of 100 °C to 400 °C. Cooling and/or reheating of the product gas has to be done depending on the used cleaning facilities [5,40]. **Hot gas cleaning** units operate above 400 °C. It is a promising technology that can offer significant efficiency gains in the conversion process from biomass to e.g. SNG. In the whole process chain of hot gas cleaning no cooling or reheating of the product gas should be needed [5,40,41]. **Table 8** summarizes some advantages and disadvantages of cold, warm and hot gas cleaning.

Table 8: Advantages and disadvantages of cold, warm and hot gas cleaning [5]

	Cold gas cleaning	Warm gas cleaning	Hot gas cleaning
Advantages	- Well-developed and widely used	- In operation at small pilot scale - Hot gas filtration possible	- No heating or cooling should be necessary
Drawbacks	- Cooling units necessary - Spent washing liquids need to be regenerated	- Heating and/or cooling units necessary - No commercial use till now	- Temperature resistance of the materials is a problem - No commercial use till now

In the following different cleaning technologies for **nitrogen**, **sulphur** and **chloride** containing compounds as well as **particulate matter** and **tar** will be described. Based on this cleaning technologies the temperature profile of a potential cold and hot gas cleaning process is given. Furthermore, gas cleaning roots of industrial methane production plants are presented.

Nitrogen and chloride containing compounds:

Ammonia and hydrogen chloride are the main nitrogen and chloride containing compounds in the product gas. Water scrubber are used at low temperatures to remove both compounds because they are polar molecules and have a high affinity with water. At high temperatures sorption materials can remove

hydrogen chloride. The material trona for example is capable of reducing down to 40 ppb at 600 °C from initially 20 ppm [5]. In terms of ammonia catalytic decomposition to nitrogen and hydrogen or selective oxidation to NO_x is possible at high temperatures [49]. Catalytic materials based on noble materials like ruthenium or tungsten (W) show good activities for decomposition of ammonia [5].

Sulphur

In the generated product gas sulphur is mainly present in the form of hydrogen sulphide, carbonyl sulphide, carbon disulphide (CS₂) and sulphur containing hydrocarbons [5]. Different cleaning methods exist to remove these corrosive compounds. Within wet sulphur scrubber liquid solvents are used to remove sulphur compounds by physical or chemical sorption. Depending on the used solvent hydrogen sulphide, carbonyl sulphide and sulphur containing hydrocarbons can be absorbed. Wet scrubber operate in a temperature range of -60 °C to 20 °C [40]. Additionally, regeneration units can be implemented to recover elemental sulphur. Commonly used solvents are amines such as monoethanolamine (MEA), diethanolamine (DEA) and methyldiethanolamine (MDEA). Physical absorption is preferred due to minimal solvent loss and high loadings which can be achieved compared to chemical solvents [5]. Furthermore, sorption materials like zinc-based materials and activated carbon are used to capture mainly hydrogen sulphide. **Figure 14** shows zinc oxide (ZnO) pellets on the left picture and activated carbon pellets on the right one. These two materials are mostly used in terms of hydrogen sulphide removal [49,50]. Sorption capacities for zinc oxide and activated carbon are in the range of 0.06 to 0.3 g_{H₂S} per g_{ZnO} and 0.3 to 0.7 g_{H₂S} per g_{Activated Carbon} respectively [51,65].

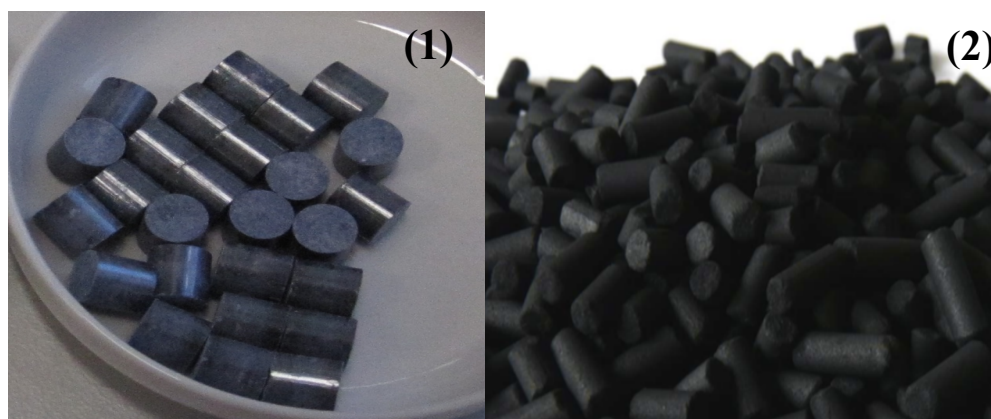


Figure 14: Zinc oxide (1) and activated carbon (2) as sorption materials for the removal of hydrogen sulphide [51,52]

State of the art wet scrubber and sorption materials are not able to capture sulphur species, beside hydrogen sulphide, efficiently enough to protect the methanation catalyst [5,40]. Due to this, these species e.g. carbonyl sulphide have to be transformed to hydrogen sulphide. Via hydrogenation for example carbonyl sulphide is catalytically converted to hydrogen sulphide with hydrogen.

Particulate matter:

A simple, robust and inexpensive technology to remove large amounts of particles is a cyclone. They are also an integral part of most dual fluidized bed gasifier to remove bed material from the product gas [6]. The operation temperature can go up to 1000 °C. Electrostatic precipitators, bed filters, bag filters, rigid filters and wet scrubber for particle removal can be used as well to reduce the particle load of the product gas. **Table 9** shows the characteristics of these particle removal technologies. A disadvantage of wet scrubber is that a complete removal of impurities needs big and therefore cost intensive columns [5,39]. In case of hot gas filtration, the sulphur and alkali content in the product gas can be reduced inside the filter by adding high temperature sorption materials [41]. Up to now, most conventional high temperature filtration units cannot ensure long-term stable operation for temperatures above 450 °C [5].

Table 9: Characteristics of particle removal technologies [5]

	Unit	Cyclones	Electrostatic precipitators	bed filters	bag filters	rigid filters	wet scrubber
Operating temperature	°C	< 1000	< 500	< 870	< 370	< 1150	< 100
Pressure drop	Pa	500-3000	30-400	1000-6000	600-2300	1000-10000	100-1000
Dust concentration raw gas	g m ⁻³	< 1000	< 50	< 100	< 100	< 100	< 10
Dust concentration clean gas	mg m ⁻³	> 100	> 25	< 10	1-10	< 1	> 10
Filtration grade	µm	~ 5	~ 5	~ 3	~ 1	~ 0.5	~ 1

Tar:

Tar consists of condensable organic compounds. They vary from primary oxygenated products to heavier deoxygenated hydrocarbons and polycyclic aromatic hydrocarbons. An intergovernmental effort has defined tar as all hydrocarbons with molecular weights greater than that of benzene [53]. Tar can condensate during the cleaning process if the temperature drops under their dew point. This lead to operational problems like plugging of piping and fouling of equipment as shown in **Figure 15**. In contrast to this, tar separated from the product gas stream contain a considerable amount of energy. Therefore, tar can be combusted as an additional fuel compound. Furthermore, they can be converted to lower molecular hydrocarbons like methane. This can be done via catalytic, thermal or plasma assisted cracking of the tar molecules. Thermal cracking decomposes tar into lighter hydrocarbons at temperatures from 900 °C to 1300 °C and residence times from 0.5 s to 5 s respectively [42].

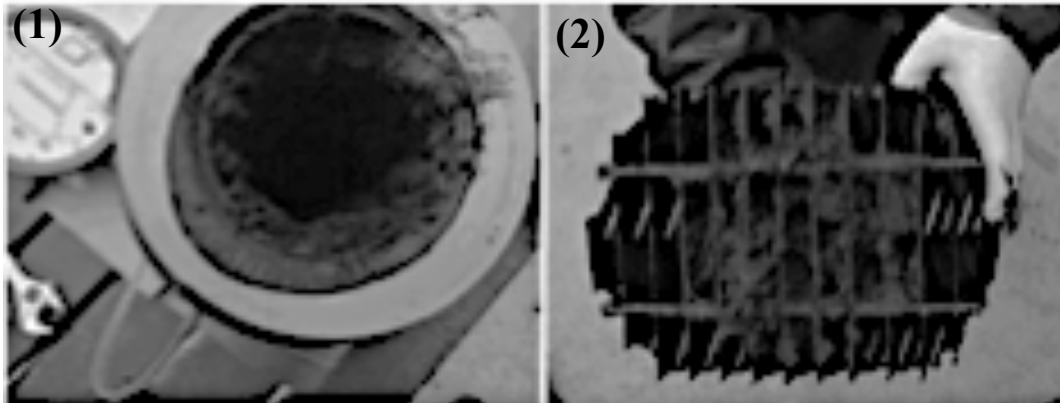


Figure 15: Plugging of piping (1) and fouling of equipment (2) [48]

Since the outlet temperature of the gasifier is not high enough for thermal cracking, the product gas needs to be heated up. Catalytic cracking of tar molecules operates at temperatures from 600 °C to 900 °C and hence can be operated without heating up the product gas. As catalysts natural compounds, e.g. dolomites, olivine or ferrous metal oxides as well as synthetic compounds, e.g. char, alkali metal carbonates or activated alumina are in use [5]. Plasma assisted cracking is very effective for removal of tar from biomass gasification gas at higher temperatures but suffers from a number of disadvantages such as limited lifetime of the pulsed power devices, their high costs, and high energy demand of the overall process [49].

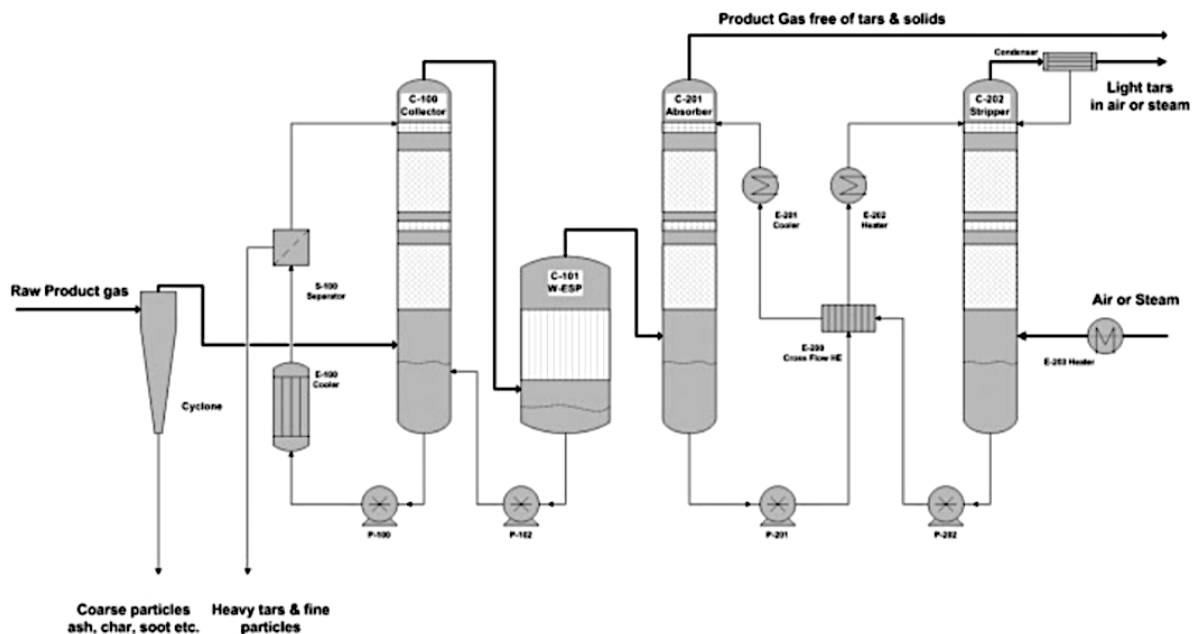


Figure 16: Simplified process flow diagram of OLGA [48]

Beside the high temperature conversion methods tar can be removed physically. At temperatures below 450 °C tar start to condensate and the resulting tar aerosols can be removed from the product gas with e.g. wet scrubber [39]. Wet scrubber, however, dissolve the tar in the wash liquid. The lower the operating temperature of the scrubber, the more tar compounds condensate. The efficiency of wet

scrubber can be improved when oil is used as solvent. **Figure 16** shows a simplified process flow diagram of a multi stage tar removal concept called OLGA developed by the Energy Research Centre of the Netherlands (ECN). Experimental procedures tested the system downstream a 500 kW_{th} air blown circulating fluidized bed gasifier. The tar load of the generated product gas is around 15 g/Nm³. The results showed that heavy tars are removed completely, light and hetero cyclic tars were reduced down to 0.01 % respectively [48]. OLGA is based on a multiple stage scrubber in which the gas is cleaned by special scrubbing oil. In the first section (the collector), the gas is cooled down by the scrubbing oil. Heavy tars are removed at this stage. In the second stage (the absorber/stripper), lighter gaseous tars are absorbed by the scrubbing oil resulting in a product gas practically free from tar and solids. In the absorber column, the scrubbing oil is saturated by these lighter tars. This saturated oil is regenerated in a stripper. Hot air is used to strip the tars of the scrubbing oil. All heavy and light tars can be recycled to the gasifier where they are destructed and contribute to the energy efficiency. Between the collector and the absorber, a wet electrostatic precipitator (w-ESP) is installed to remove fine solid aerosols from the product gas. Besides OLGA single packed columns are commonly used to physically remove tar from the product gas stream with the use of rapeseed methyl ester (RME) as solvent.

Industrial methane production plants and their gas cleaning solutions [5,33]:

Figure 17 shows a block flow diagram of the 1 MW_{SNG} demonstration plant in Güssing (Austria). A FICFB gasifier is used to produce the product gas. This gasification process is operated in Güssing since 2002 for a combined heat and power (CHP) plant and has reached more than 40000 h of operation. The conversion of product gas to SNG consist of gas conditioning, fluidized bed SNG synthesis and gas upgrading. The entire process chain has the potential for lower investment and lower operating cost than conventional fixed bed SNG synthesis [70].

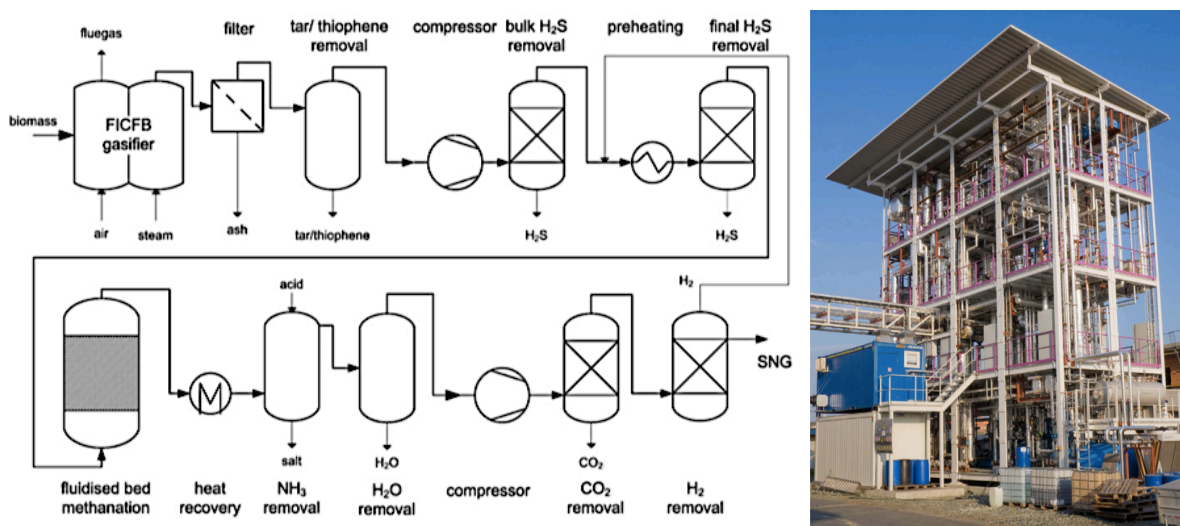


Figure 17: Block flow diagram of the 1 MW_{SNG} demonstration plant in Güssing (Austria) converting wood derived producer gas to SNG [33]

The SNG-production plant from in Gothenburg is the largest SNG-product plant from biomass till now. A SNG-output of up to 20 MW_{SNG} can be reached. **Figure 18** show the simplified principal layout of the plant. First, a dual fluidized bed gasifier generates the product gas. After cooling and filtering the product gas enters the RME-scrubber. Here a near complete tar removal is executed. Spent RME including tar is recycled to the combustion reactor acting as fuel. Next a series of fixed bed reactors, filled with activated carbon, are installed to capture the remaining tar. The four beds are operated alternately and when saturated they are regenerated by steam. Afterwards the product gas is pressurized to 16 bar in a six-stage intercooled compressor. After the pressurization the unsaturated hydrocarbons are hydrogenated in the olefin hydrogenator and the carbonyl sulphide is hydrolysed in the COS hydrolyser. The product gas now enters an amine scrubber to remove hydrogen sulphide and approximately 50 % of carbon dioxide. The remaining sulphur is removed down to 0.1 ppm in a subsequent sulphur guard reactor equipped with zinc oxide pellets. A part of the product gas is then shifted in the shift converter to adjust the hydrogen to carbon monoxide ratio and undergoes a pre-methanation step before the remaining carbon dioxide is removed down to 0.1 % again in an amine scrubber. Finally, the methanation takes place in four consecutive fixed bed methanation reactors.

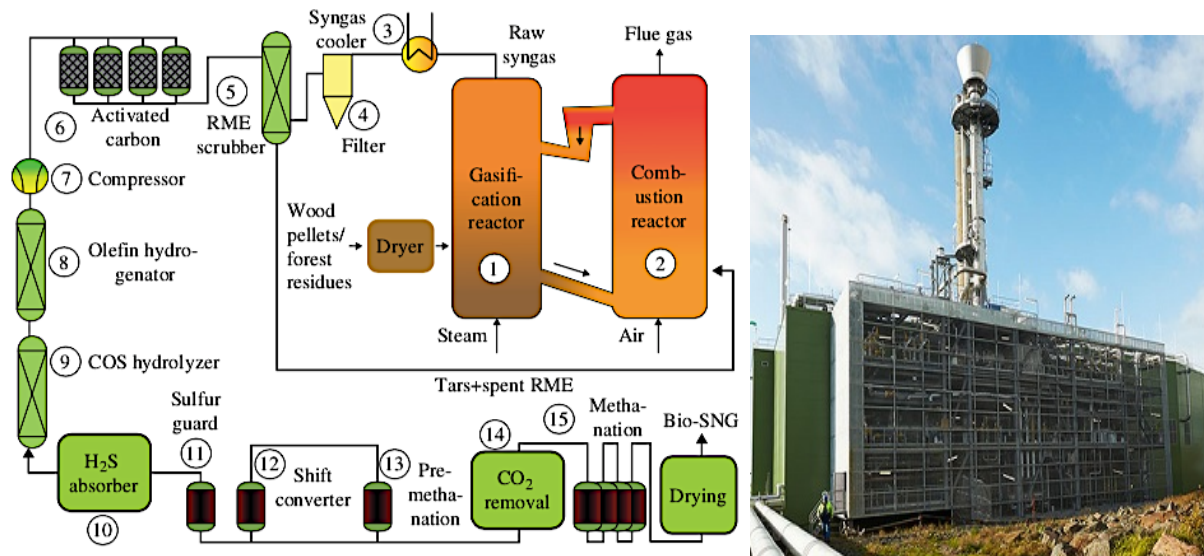


Figure 18: Simplified principal layout of the GoBiGas plant in Gothenburg (Sweden) [5]

Table 10 gives some key parameters of the installed gasifiers in Güssing (Austria) and in Gothenburg (Sweden).

Table 10: Key parameters of the used gasifiers in Güssing in Gothenburg [5,7]

Key parameter	Güssing (Austria)	Gothenburg (Sweden)	Unit
Thermal power gasifier (lhv)	8	32	MW _{th}
Cold gas efficiency	70	76	%
Steam to fuel ratio	0.6	N/A	kg _{H2O} /kg _{fuel,waf}
Abso. water conversion rate	0.2	N/A	kg _{H2O} /kg _{H2O}

2.6 Future of R&D challenges

To break down the complexity of the whole SNG – production process from biomass gasification research and development is going on for several years. Since to date there are still areas which needs to be improved. The improvement of methanation catalysts is one topic where intense research is done [29]. The aim of this research is to find catalyst supporting materials which increase the resistance against catalyst poisons like sulphur on the one hand and on the other hand withstand higher temperatures without sintering and loss of activity. In addition to that investigations are made to design catalytic reactor systems capable of removing heat without costly equipment or high gas recycle rates, e.g. fluidized bed methanation.

In terms of gas cleaning research activities are investigating cold and hot gas cleaning processes with the aim to further improve the efficiency of the whole process chain and provide a feasible gas for further methanation [5]. Especially under investigation, in terms of hot gas cleaning, are the reactive hot gas filter and integrated desulfurization with methanation to shorten the gas cleaning chain. Of course, an integrated desulfurization with methanation requires catalytic materials which can handle sulphur compounds or can be regenerated. Mo-based catalysts are investigated in this context since they are active in the presence of sulphur species and become even more active when the hydrogen sulphide concentration is increased [5,29,31,44]. **Figure 19** shows a possible flow chart of an integrated high temperature process for the conversion of biomass to SNG with a combined desulfurization and methanation without the need for scrubbing. The process would start with gasification of biomass followed by high temperature filtration to remove particulate matter. After this a high temperature reforming unit converts tar at temperature above 700 °C. The following unit removes most of the inorganic sulphur compounds by using a high temperature sorbent like zinc oxide. Afterwards the methanation unit should include a catalyst which is either tolerant towards sulphur species that are not removed by the previous sorbent or can be regenerated multiple times.

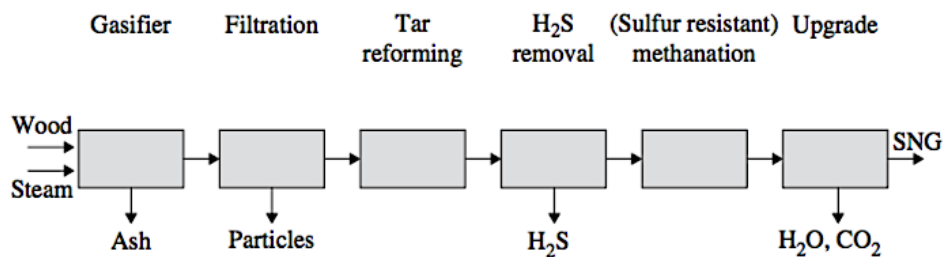


Figure 19: Flow chart of an integrated high temperature process for the conversion of biomass to SNG with a combined desulfurization and methanation [5]

3 Experimental gasification of biogenic residues

Within the present work the design of gas cleaning facilities for a SNG process from biomass gasification is executed. Therefore, first of all a gasification experiment with biogenic residues has been performed. Two stable operation points are targeted, one at around 650 °C and at around 800 °C. Hazelnut shells were chosen as fuel for the experiment. The generated product gas composition is then used to further design the gas cleaning processes. On the following pages a description of the test plant and the experimental procedure is given. Furthermore, the results of the gasification experiment are summarized.

3.1 Description of the test plant and used fuel

The experimental procedure was executed at the 100 kW_{th} dual fluidized bed pilot plant designed by TU Wien. This dual fluidized bed concept shown in **Figure 20** covers two reactor units which are interconnected with two loop seals.

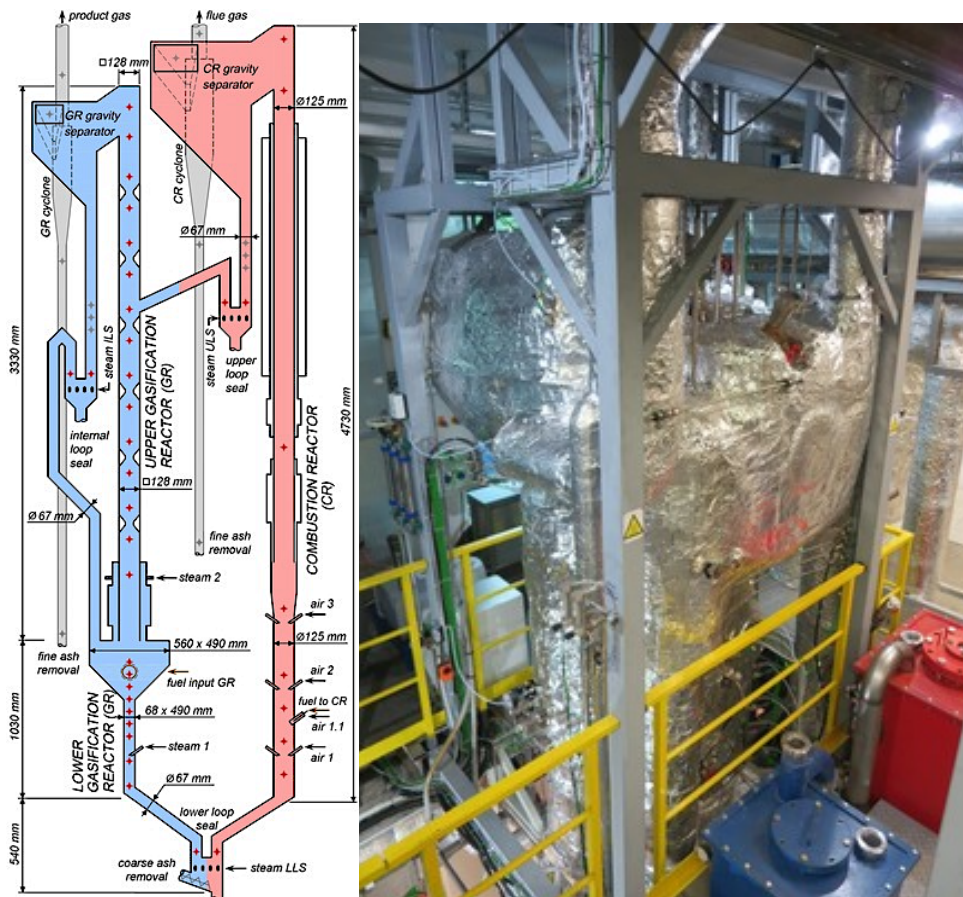


Figure 20: 100 kW_{th} dual fluidized bed pilot plant designed by TU Wien [9].

The gasification reactor (GR) consists of two parts, a lower and an upper one. The lower part is operated as a bubbling bed and the upper one is a counter current column. The combustion reactor (CR) is operated as a fast fluidized bed. To compensate heat losses of the plant and effectively control the temperature oil can be injected into the CR. Depending on the operation of the pilot plant temperature differences of around 100-300 °C are needed between CR and GR. To reach these differences the upper loop seal can be cooled. Furthermore, the whole plant is equipped with several online temperature and pressure measurement devices. Additionally, an online product gas composition measurement system is installed. **Table 11** summarizes the key parameters of the test plant.

Table 11: Key parameters of the 100 kW_{th} pilot plant designed by TU Wien [6]

Key parameter	Value	Unit
Thermal power gasifier (lhv)	100	kW _{th}
Cold gas efficiency	84	%
Steam to fuel ratio	0.7	kg _{H2O} /kg _{fuel,waf}
Abso. water conversion rate	0.31	kg _{H2O} /kg _{H2O}

Hazelnut shells acted as fuel for the gasification experiment. **Table 12** shows the fuel analysis for hazelnut shells in comparison with wood pellets. Limestone was used as bed material because of its capability to capture carbon dioxide during SER operation. **Figure 21** represents limestone (1) and hazelnut shells (2) in the shape as both materials were used during operation.

Table 12: fuel analysis of wood pellets and hazelnut shells [54]

		Wood pellets	Hazelnut shells	Value
Fuel properties	Water	< 7	< 10	wt.-%
	Ash content 550 °C	0.2	1.5	wt.-% _{odb}
	Volatiles	86	75	wt.-%
	Lower heating value	19	19	MJ/kg _{db}
Elementary composition	Carbon (C)	51	52	wt.-% _{odb}
	Hydrogen (H)	6	6	wt.-% _{odb}
	Nitrogen (N)	0.2	0.4	wt.-% _{odb}
	Sulphur (S)	-	0.03	wt.-% _{odb}
RFA-analysis	Chlorine (Cl)	-	0.03	wt.-% _{odb}
	Arsenic (As)	-	-	mg/g _{Ash,db}
	Natrium (Na)	10	16	mg/g _{Ash,db}



Figure 21: Limestone (1) and Hazelnut shells (2) which were used as bed material and fuel respectively.

3.2 Experimental procedure

Start-up of the pilot plant:

Heating up the plant to around 400 °C was done via electrical heating devices. From 400 °C wood and oil were added to the reactors and burned with air. A negative oxygen trend in the product gas is an indicator that the oxidation takes place. At a temperature of around 800 °C the bed material was calcined (**Eq. 2.13**). The calcination of limestone was completed when the carbon dioxide content in the product gas was declining. **Figure 22** shows the bed material flow through the upper loop seal.

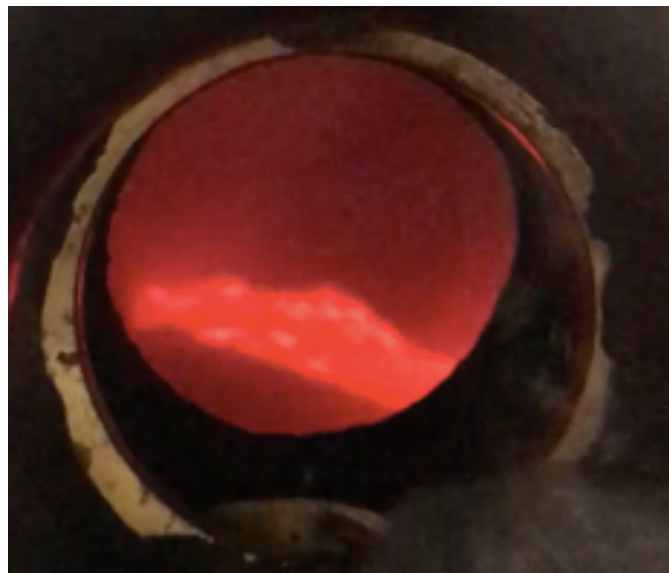


Figure 22: Bed material flow through the upper loop seal during heating up the pilot plant

Operation mode:

First of all, a switch from air to steam as gasification agent had to be done. Then a steady-state operation at around 650 °C and around 800 °C in the GR was targeted and further reached. **Figure 23** shows the concentration profile of the main product gas components (1) and the temperature profile over the height of both reactors (2) at a steady operation using hazelnut shells as fuel.

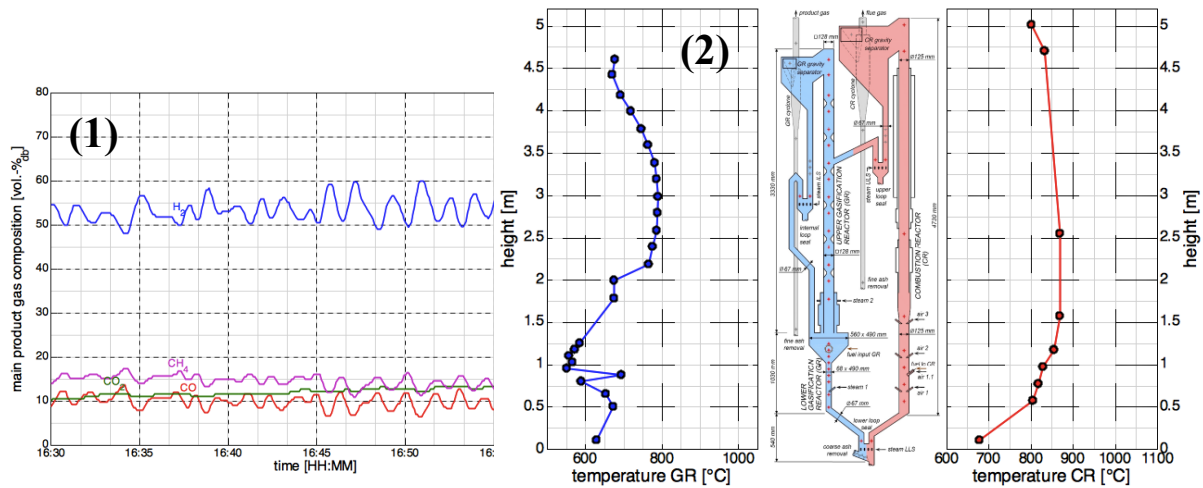


Figure 23: Main components of the generated product gas from hazelnut shells gasification received from an online measurement (1) and the temperature profile over the height of both reactors (2)

3.3 Results

Theoretically the ideal molar ratio of the product gas components hydrogen, carbon monoxide and carbon dioxide is 7:1:1 for further methanation. This ratio can be reached at a gasification temperature of around 650 °C with limestone as bed material (**Figure 5**). Therefore, the collected data from gasification at around 650 °C are used to evaluate the product gas composition. To create a reference product gas composition another test run with wood pellets as fuel was executed at the same gasification temperature of around 650 °C. The evaluation of the respective product gas composition was conducted by an IPSE simulation.

Table 13 shows the product gas composition from the gasification of hazelnut shells and wood pellets evaluated by IPSE as well as reference data. This reference product gas composition was finally used to design the gas cleaning facilities. The reference values for not measured species were received from other gasification experiments which were executed at similar conditions. Furthermore, the reference values for ammonia, hydrogen sulphide, carbonyl sulphide, hydrochloric acid and hydrogen cyanate were calculated by using the fuel analysis given in **Table 12** and the literature [10]. The aim of this calculation was to determinate the highest possible concentrations of these species in the product gas.

Table 13: Received product gas compositions from the gasification experiment.

	advanced 100 kW _{th} , TU Wien	advanced 100 kW _{th} , TU Wien	Reference data for calculation	Unit	
Gasification parameters	Fuel	wood pellets	Hazelnut shells	Hazelnut shells	-
	T _{Bubbling Bed}	654	642	650	°C
	T _{Column}	711	817	817	°C
	Steam to fuel ratio	0.7	1.1	1.1	kg/kg
	Fuel input	20	17	17	kg/h
	Product gas yield	0.8	0.7	0.7	Nm ³ _{db} /kg _{fuel,daf}
	Product gas power	87	81	81	kW
	Gasification agent	steam	steam	steam	-
	Bed material	limestone	limestone	limestone	-
	Operation mode	SER	SER	SER	-
Main components	Hydrogen (H ₂)	65	57	57	vol.-% _{db}
	Carbon monoxide (CO)	8	10	10	vol.-% _{db}
	Carbon dioxide (CO ₂)	8	16	16	vol.-% _{db}
	Methane (CH ₄)	14	14	14	vol.-% _{db}
Gas components and impurities	Acetylene (C ₂ H ₂)	n.m.	n.m.	0	vol.-% _{db}
	Ethylene (C ₂ H ₄)	1.6	1.7	1.7	vol.-% _{db}
	Ethane (C ₂ H ₆)	1	0.5	0.5	vol.-% _{db}
	Propene (C ₃ H ₆)	n.m.	n.m.	0	vol.-% _{db}
	Propane (C ₃ H ₈)	0.2	0.05	0.05	vol.-% _{db}
	Ammonia (NH ₃)	0.1	0.2	0.7	vol.-% _{db}
	Hydrogen sulphide (H ₂ S)	0	0.03	0.02	vol.-% _{db}
	Carbonyl sulphide (COS)	n.m.	n.m.	0.005	vol.-% _{db}
	Hydrochloric acid (HCl)	0	0.03	0.005	vol.-% _{db}
	Hydrogen cyanide (HCN)	n.m.	n.m.	0.02	vol.-% _{db}
	Nitrogen (N ₂)	0	0	0	vol.-% _{db}
	Water (H ₂ O)	47	64	64	vol.-%
	Dust and char	n.m.	n.m.	2.5	g/Nm ³ _{db}
	Gravimetric tar	n.m.	n.m.	0.4	g/Nm ³ _{db}
	GCMS tar	n.m.	n.m.	7.4	g/Nm ³ _{db}
	GCMS tar composition				
	Naphthalene	n.m.	n.m.	0.9	g/Nm ³ _{db}
	Benzene (B)	n.m.	n.m.	6	g/Nm ³ _{db}
	Toluene (T)	n.m.	n.m.	0	g/Nm ³ _{db}
	Ethylbenzene (E)	n.m.	n.m.	0	g/Nm ³ _{db}
	Xylene (X)	n.m.	n.m.	0	g/Nm ³ _{db}
	Critical components in ash				
Arsenic (As)	-	-	0	mg/g _{Ash,db}	
Sodium (Na)	10	16	16	mg/g _{Ash,db}	

4 Mathematical models for the calculation of gas cleaning processes

Based on the experimental data first a scale up to an 8 MW_{th} gasifier was done to represent potential gas cleaning processes which could be used for industrial scaled SNG-production plants from biomass gasification. Further on mathematical models were created to design reactors which are able to efficiently remove the product gas impurities given in **Table 13**. The major indicator was to provide a gas which suits the specified limits of the upcoming methanation catalyst. **Table 14** shows specified limits of impurities which are harmful for a nickel based methanation catalyst and reference values which are used to evaluate the efficiency of the designed gas cleaning processes. Furthermore, each reactor will be characterized in terms of:

- reactor surface,
- required liquid or solid cleaning agent to reach the specified limits,
- height of the substance-exchanging layer
- required catalysator volume for catalytic reactions

Table 14: Specified limits of a nickel based methanation catalyst from internal research

Product gas components	Value	Reference data	Unit
Acetylene (C ₂ H ₂)	N/A	N/A	vol.-% _{db}
Ethylene (C ₂ H ₄)	0.1 – 0.3	0.2	vol.-% _{db}
Propene (C ₃ H ₆)	0 – 0.8	0.4	vol.-% _{db}
Ammonia (NH ₃)	1 – 10	5	ppm
Hydrogen sulphide (H ₂ S)	0.3 – 30	10	ppm
Carbonyl sulphide (COS)	< 1	0.8	ppm
Hydrochloric acid (HCl)	0.1 - 5	2	ppm
Hydrogen cyanide (HCN)	< 1	0.8	ppm
Nitrogen (N ₂)	< 1	0.8	vol.-% _{db}
Water (H ₂ O)	0 – 30	10	vol.-%
Dust and char	N/A	N/A	g/Nm ³ _{db}
Gravimetric tar	< 0.01	0.005	g/Nm ³ _{db}
GCMS tar	0.2 – 11	3	g/Nm ³ _{db}
GCMS tar composition			
Naphthalene	< 1	0.8	g/Nm ³ _{db}
Benzene (B)	0.4 – 10	3	g/Nm ³ _{db}
Toluene (T)	N/A	N/A	g/Nm ³ _{db}
Ethylbenzene (E)	N/A	N/A	g/Nm ³ _{db}
Xylene (X)	N/A	N/A	g/Nm ³ _{db}
Critical components in ash			
Arsenic (As)	< 2000	100	mg/Nm ³ _{db}
Sodium (Na)	< 1	0.8	mg/Nm ³ _{db}

4.1 Reference data for gasifier scale up

To scale up the gasifier from 100 kW_{th} to 8 MW_{th} the product gas yield (y_{HS}) and the lower heating value (H_u) were used. **Table 15** summarizes the values for these two parameters.

Table 15: Used parameters for the gasifier scale up

Parameter	Unit	Value
y_{HS}	$Nm^3_{db}/kg_{HS,daf}$	0.7
H_u	$MJ/kg_{HS,db}$	19

First the mass flow rate of the fuel (\dot{m}_{HS}) is calculated (**Eq. 4.1**). Then the volumetric flow rate of the product gas (\dot{V}_{PG}) is received by multiplying the mass flow rate of the fuel (\dot{m}_{HS}) with the product gas yield (y_{HS}) (**Eq. 4.2**).

$$\dot{m}_{HS} = \frac{E_{Gasifier}}{H_u} = \frac{8 MW_{th}}{H_u} * 3.6 = 1.5 \frac{t_{db}}{h} \quad \text{Eq. 4.1}$$

$$\dot{V}_{PG} = \dot{m}_{HS} * y_{HS} * 1000 = 1050 \frac{Nm^3_{db}}{h} \quad \text{Eq. 4.2}$$

According to the literature the volumetric product gas flow rate of an 8 MW_{th} gasifier using wood pellets as fuel is 1800 Nm³/h [7]. Therefore, an efficiency reference (η) of 1.6 is introduced to compensate the difference as shown in **Eq. 4.3**.

$$\dot{V}_{PG,\eta} = \dot{V}_{PG} * \eta = 1680 \frac{Nm^3_{db}}{h} \quad \text{Eq. 4.3}$$

The calculated volumetric flow rate ($\dot{V}_{PG,\eta}$) in **Eq. 4.3** is water free. The amount of water is 64 vol.-% according to the evaluated reference product gas composition given in **Table 13**. The calculated volumetric flow of water (\dot{V}_{H_2O}) is given in **Eq. 4.4**. To receive the mass flow out of the volumetric water flow, the specific volume of water (v) at 1 bar and 650 °C is used. **Eq. 4.5** shows the calculated water mass flow.

$$\dot{V}_{H_2O} = 0.64 * \frac{\dot{V}_{PG,\eta}}{1 - 0.64} = 2986 \frac{Nm^3}{h} \quad \text{Eq. 4.4}$$

$$\dot{m}_{H_2O} = \frac{1}{v_{1 bar, 650 \text{ } ^\circ\text{C}}} * \dot{V}_{H_2O} * \frac{1}{1000} = 1.5 \frac{t}{h} \quad \text{Eq. 4.5}$$

With further knowledge of the parameters cp_{PG} , \bar{M}_{PG} , $\bar{\rho}_{PG}$ the product gas is fully defined to design the gas cleaning reactors. The average molar mass of the product gas \bar{M}_{PG} is calculated by dividing the sum of the product gas species masses $m_{x,PG}$ through the sum of their respective molar amount $n_{x,PG}$ as given in **Eq. 4.6**. By further dividing \bar{M}_{PG} through the molar volume $V_{m,N}$ at norm conditions, which is at 0°C and 1 bar, the average density $\bar{\rho}_{PG}$ is calculated (**Eq. 4.7**). The specific heat capacity cp_{PG} is received from the literature [55].

$$\bar{M}_{PG} = \frac{\sum_{x=1}^{17} m_{x,PG}}{\sum_{x=1}^{17} n_{x,PG}} = 14 \frac{kg_{ab,daf}}{kmol} \quad \text{Eq. 4.6}$$

$$\bar{\rho}_{PG} = \frac{\bar{M}_{PG}}{V_{m,N}} = \frac{\bar{M}_{PG}}{22.4 \frac{m^3}{kmol}} = 0.6 \frac{kg_{ab,daf}}{m^3} \quad \text{Eq. 4.7}$$

Table 16 summarizes the defined product gas parameters which are needed, apart from the product gas composition, to design the gas cleaning reactors. According to internal research the dust and char content in the product gas is assumed to be $< 5 \text{ mg/Nm}^3$ at the exit of the filter.

Table 16: Defined parameters of the product gas

Variable	Unit	Value
T_{PG}	°C	650
$\dot{V}_{PG,\eta}$	Nm^3_{ab}/h	1680
\dot{m}_{H_2O}	t/h	1.5
cp_{PG}	$kJ/kmol * K$	33
\bar{M}_{PG}	$kg_{ab,daf}/kmol$	14
$\bar{\rho}_{PG}$	$kg_{ab,daf}/m^3$	0.6

4.2 Models for reactor design

On the following pages the individual reactors were designed in order to create two types of gas cleaning processes, a cold and a hot one. Based on following mechanisms, mathematical models for the reactors of both gas cleaning processes were created:

- **Absorption [56]**
- **Adsorption [56]**
- **Hydrogenation [57]**
- **Steam reforming [58]**
- **Decomposition [5,49]**

Additionally, **thermal calculations** are done.

First of all, the reactor surface is calculated as shown in **Eq. 4.8**. The reactor surface depends on the existing temperature at the respective stage of the gas cleaning processes. The admissible gas velocity w_g is assumed to be constantly 1.19 m/s [55].

$$A_c = \frac{\dot{V}_X * \frac{273.15 + T_X}{273.15}}{w_g} \quad \text{Eq. 4.8}$$

Absorption:

The term absorption describes the process of gas or vapor solution in a liquid medium. Starting point for the calculation is defining an appropriate solvent to remove harmful impurities from the product gas. Water, rapeseed methyl ester (RME) and amine are chosen for the cold gas cleaning process. Next the related molar fractions in the gas ($Y_{X,\alpha}$, $Y_{X,\omega}$) and liquid ($X_{X,\alpha}$, $X_{X,\omega}$) phase are calculated for the respective impurity X. $Y_{X,\alpha}$ calculated in **Eq. 4.9** describes the molar fraction of species X in the gas phase at the entry of the respective column.

$$Y_{X,\alpha} = \frac{\sum_{X=1}^n \dot{m}_{PG,X}}{G_T} = \frac{\sum_{X=1}^n \dot{m}_{PG,X}}{\dot{m}_{PG} - \sum_{X=1}^n \dot{m}_{PG,X}} \quad \text{Eq. 4.9}$$

By choosing a desired separation efficiency (β) the molar fraction of the impurity X in the gas phase at the exit of the scrubber ($Y_{X,\omega}$) is calculated (**Eq. 4.10**).

$$Y_{X,\omega} = \frac{\left(1 - \frac{\beta}{100}\right) * \sum_{X=1}^n \dot{m}_{PG,X}}{G_T} = \frac{\left(1 - \frac{\beta}{100}\right) * \sum_{X=1}^n \dot{m}_{PG,X}}{\dot{m}_{PG,X} - \sum_{X=1}^n \dot{m}_{PG,X}} \quad \text{Eq. 4.10}$$

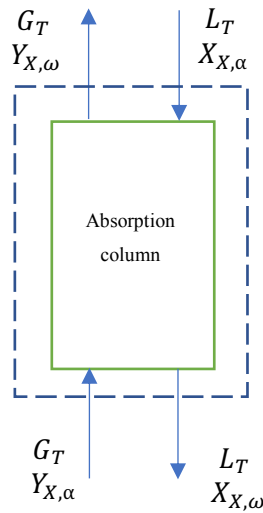
With the choice of the separation efficiency (β), the amount of absorptive can be calculated as well (**Eq. 4.11**).

$$\dot{m}_{Abs} = \frac{\beta}{100} * \sum_{X=1}^n \dot{m}_{PG,X} \quad \text{Eq. 4.11}$$

In this calculation, the assumption was made that the absorbent enters the column without contamination. This means that the molar fraction of the impurity X in the liquid phase at the entry of the reactor ($X_{X,\alpha}$) is equal to zero (**Eq. 4.12**).

$$X_{X,\alpha} = 0 \quad \text{Eq. 4.12}$$

The knowledge of the solvent stream (L_T) is necessary to calculate the molar fraction of the impurity X in the liquid phase at the exit of the reactor ($X_{X,\omega}$). For this reason, a species balance around the reactor is done (**Eq. 4.13**).



$$L_{T,min} * X_{X,\alpha} + G_T * Y_{X,\alpha} = L_{T,min} * X_{X,\omega,max} + G_T * Y_{X,\omega} \quad \text{Eq. 4.13}$$

$$L_{T,min} = \frac{G_T * (Y_{X,\alpha} - Y_{X,\omega})}{X_{X,\omega,max} - X_{X,\alpha}} = \frac{\dot{m}_{Abs}}{X_{X,\omega,max} - X_{X,\alpha}}$$

The missing variable $X_{X,\omega,max}$ in **Eq. 4.13**, which describes the maximal molar fraction of the impurity X in the liquid phase at the exit of the reactor, is calculated by using the equilibrium equation (**Eq. 4.14**). $X_{X,\omega,max}$ is in equilibrium with $Y_{X,\alpha}$.

$$\frac{Y_X}{1 + Y_X} = \frac{H_{X,Y}}{p} * \frac{X_X}{1 + X_X} \quad \text{Eq. 4.14}$$

Now the minimum solvent stream ($L_{T,min}$) in **Eq. 4.13** can be calculated. The effective solvent stream (L_T) is obtained with **Eq. 4.15**. The minimum solvent ratio (v_{min}) in this equation states that the incoming gas phase with the loading $Y_{X,\alpha}$ is just in equilibrium with the liquid phase which leaves the reactor. In practice the solvent ratio (v) or the solvent stream (L_T) is 1.3 to 1.6 times higher than the minimum ones.

$$v = \frac{L_T}{G_T} = (1.3 - 1.6) * v_{min} = (1.3 - 1.6) * \frac{L_{T,min}}{G_T} \quad \text{Eq. 4.15}$$

$$L_T = (1.3 - 1.6) * L_{T,min}$$

Alternatively to **Eq. 4.15**, the respective solvent streams (L_T) can be received using a solubility diagram. In case of tar and ammonia + hydrochloric acid absorption in RME and water respectively such diagrams could be evaluated (**Figure 24**) [55,59]. For hydrogen sulphide and carbon dioxide absorption in methyldiethanolamine no values could be evaluated and therefore just **Eq. 4.15** was used to describe the solvent streams (L_T).

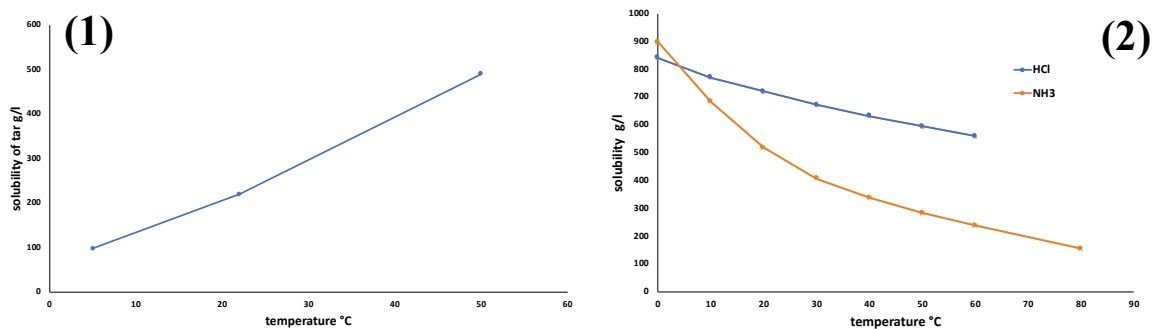


Figure 24: Solubility diagram for tar in RME (1) and ammonia + hydrochloric acid in water (2) [55,59]

Eq. 4.16 shows how to calculate the solvent stream (L_T) by using the solubility diagram.

$$L_T = \frac{\dot{m}_{Abs}}{c_{X,Y}} \quad \text{Eq. 4.16}$$

With L_T the molar fraction (loading) of the impurity X in the liquid phase at the exit of the reactor ($X_{X,\omega}$) can be calculated (**Eq. 4.17**).

$$X_{X,\omega} = \frac{\dot{m}_{Abs}}{L_T} \quad \text{Eq. 4.17}$$

The height of the substance-exchanging layer (z_{Abs}) is calculated with the HTU/NTU-concept (**Eq. 4.18** to **Eq. 4.21**).

$$z_{Abs} = HTU * NTU \quad \text{Eq. 4.18}$$

The HTU/NTU-concept is commonly used in absorption technology. **Eq. 4.19** shows the equation to calculate the number of transfer units (NTU). In this equation dY_X corresponds to the achievable concentration change of the gas phase in the height element dz of the bed. This concentration change takes place because of the driving force $Y_X - Y_X^*$.

$$NTU = \int_{Y_w}^{Y_\alpha} \frac{dY_X}{Y_X - Y_X^*} = \frac{Y_{X,\alpha} - Y_{X,w}}{(Y_X - Y_X^*)_{ln,m}} \quad \text{Eq. 4.19}$$

$$(Y_X - Y_X^*)_{ln,m} = \frac{(Y_X - Y_X^*)_\alpha - (Y_X - Y_X^*)_w}{\ln \left(\frac{(Y_X - Y_X^*)_\alpha}{(Y_X - Y_X^*)_w} \right)} \quad \text{Eq. 4.20}$$

$$HTU = \frac{G_T}{k_{Gy} * \varphi * \alpha * A_c} \quad \text{Eq. 4.21}$$

The height of the transfer unit (HTU) is calculated with **Eq. 4.21**.

HTU decreases with:

- sinking volume flow rate of the product gas (G_T)
- increasing material transition coefficient (k_{Gy})
- increasing specific surface of the bulk material (α)

Adsorption:

Adsorption describes the deposition of a component out of the gas phase onto the surface of a solid. In the framework of adsorptive gas cleaning for further methanation solids like zinc oxide (ZnO) or activated carbon can be used. The related mass fractions in the gas phase ($Y_{X,\alpha}$, $Y_{X,\omega}$) and on the solid surface ($X_{X,\alpha}$, $X_{X,\omega}$) are defined first, similar to the calculation procedure of absorption.

Instead of molar fractions (absorption) mass fractions are used for the calculation (**Eq. 4.22**). The reason for this is that the sorbent manufacturers provide the sorption capacity for their products in g/kg.

$$Y_{X,\alpha} = \frac{\sum_{X=1}^n \dot{m}_{PG,X}}{G_T} = \frac{\sum_{X=1}^n \dot{m}_{PG,X}}{\dot{m}_{PG} - \sum_{X=1}^n \dot{m}_{PG,X}} \quad \text{Eq. 4.22}$$

By selecting a desired separation efficiency (β) the calculation of the mass fraction $Y_{X,\omega}$ and the adsorbed mass flow \dot{m}_{Ads} can be done (**Eq. 4.23** and **Eq. 4.24**).

$$Y_{X,\omega} = \frac{\left(1 - \frac{\beta}{100}\right) * \sum_{X=1}^n \dot{m}_{PG,X}}{G_T} = \frac{\left(1 - \frac{\beta}{100}\right) * \sum_{X=1}^n \dot{m}_{PG,X}}{\dot{m}_{PG} - \sum_{X=1}^n \dot{m}_{PG,X}} \quad \text{Eq. 4.23}$$

$$\dot{m}_{Ads} = \frac{\beta}{100} * \sum_{X=1}^n \dot{m}_{PG,X} \quad \text{Eq. 4.24}$$

As for absorption the assumption was made that the provided adsorbent is without contamination (**Eq. 4.25**).

$$X_{X,\alpha} = 0 \quad \text{Eq. 4.25}$$

The mass fraction $X_{X,\omega}$ indicates the equilibrium loading of the respective adsorbents. ε is a correction factor as operational conditions decrease the adsorption capacity ($B_{Y,X}$) (**Eq. 4.26**).

$$X_{X,\omega} = B_{Y,X} * \varepsilon \quad \text{Eq. 4.26}$$

The bulk density ρ_Y in **Eq. 4.27** is provided by the manufacturer for the respective sorption material. With the knowledge of ρ_Y and the assumption that the bulk height of the sorption material (z_{Ads}) is 1 m the regeneration cycle (t_y) can be calculated (**Eq. 4.27**).

$$z_{Ads} = \frac{G_T * (Y_{X,\alpha} - Y_{X,\omega}) * t_y}{(X_{X,\omega} - X_{X,\alpha}) * \rho_Y * A_c} = \frac{S_Y}{\rho_Y * A_c} \quad \text{Eq. 4.27}$$

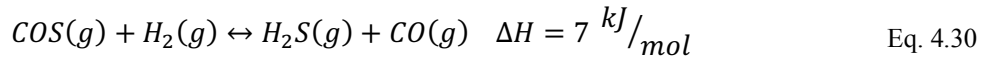
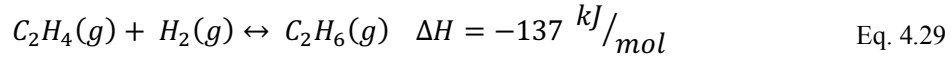
Catalysator volume [68]:

The required catalysator volume (V_{cat}) to proceed the reactions for hydrogenation, steam reforming and decomposition is calculated by using the product gas volume flow (\dot{V}_{PG}) and the residence time (τ) (**Eq. 4.28**).

$$\frac{1}{\tau} = \frac{\dot{V}_{PG}}{V_{cat}} \quad \text{Eq. 4.28}$$

Hydrogenation:

To fully define the hydrogenator the knowledge of the catalysator volume (V_{cat}) (Eq. 4.28) and the molar amount of resulting C_2H_6 (Eq. 4.29) and COS (Eq. 4.30) molecules is necessary. Additionally, the hydrogen (H_2) amount for the hydrogenation reaction (Eq. 4.29) has to be calculated.

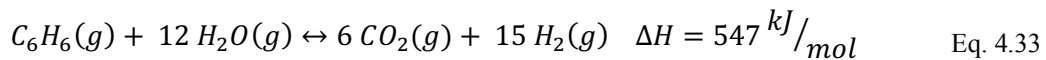
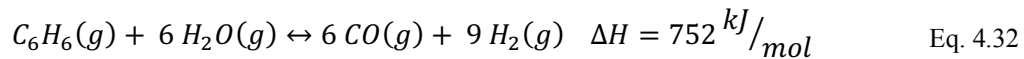


$$\dot{n}_Y = \frac{\dot{n}_X * M_Y}{M_X} \quad \text{Eq. 4.31}$$

With the stoichiometric relation shown in Eq. 4.31 the hydrogen amount as well as the molar amount of resulting C_2H_6 and COS molecules can be calculated.

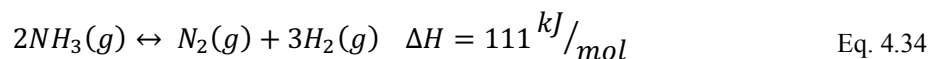
Steam reforming:

The steam reforming reaction is a catalytic reaction as well. The catalysator volume (V_{cat}) is calculated with Eq. 4.28. The assumption was made that benzene represent tars and that only the steam reforming reactions (Eq. 4.32 and Eq. 4.33) take place. To calculate the molar amount of the products and educts Eq. 4.31 was used.



Decomposition:

To calculate the catalytic decomposition of ammonia Eq. 4.34 was used. Again, the catalysator volume (V_{cat}) and the molar amount of the occurring products was calculated with Eq. 4.28 and Eq. 4.31 respectively.



Heat balance:

To cool down and remove the water content from the product gas the following approach was chosen (Eq. 4.35 to Eq. 4.37):

$$\dot{Q}_{cool} = \dot{Q}_{PG} + \dot{Q}_{H_2O} \quad \text{Eq. 4.35}$$

$$\dot{Q}_{PG} = \dot{m}_{PG} * cp_{PG} * (T_{PG,in} - T_{PG,out}) \quad \text{Eq. 4.36}$$

$$\dot{Q}_{H_2O} = \dot{m}_{H_2O} * \Delta h_{H_2O,condense} \quad \text{Eq. 4.37}$$

The condensation enthalpy of water $\Delta h_{H_2O,condense}$ is received from the steam table.

To balance the heat during the respective cleaning process the heat of reaction and/or the condensation heat of the involved species was considered (**Eq. 4.38**). In case of tar adsorption, the condensation heat of benzol ($\Delta h_{c,Benzol} = 31 \frac{kJ}{mol}$) was used to describe the occurring thermal amount (**Eq. 4.39**). To describe the thermal situation of hydrogen sulphide adsorption during hot gas cleaning also the condensation heat of hydrogen sulphide was used ($\Delta h_{c,H_2S} = -21 \frac{kJ}{mol}$) (**Eq. 4.40**). For the absorption processes, except tar adsorption in the RME-scrubber, the assumption was made that no heat is released or needed. **Table 17** summarizes the heat of reaction for the different chemical reactions occurring at the respective temperature during the cold and hot gas cleaning process.

$$\dot{Q}_{Reaction} = \dot{n}_X * \Delta H \quad \text{Eq. 4.38}$$

$$\dot{Q}_{Reaction} = \dot{n}_{Tar} * \Delta h_{c,Benzol} \quad \text{Eq. 4.39}$$

$$\dot{Q}_{Reaction} = \dot{n}_{H_2S} * \Delta h_{c,H_2S} \quad \text{Eq. 4.40}$$

Table 17: Heat of reaction for the different chemical reactions occurring at the respective temperature during the cold and hot gas cleaning process received from HSC 6

Principal	Cold gas cleaning	$\Delta H \frac{kJ}{mol}$	Hot gas cleaning	$\Delta H \frac{kJ}{mol}$
Adsorption	$ZnO + H_2S \leftrightarrow ZnS + H_2O$	333	$Na_2CO_3 + 2HCl \leftrightarrow 2NaCl + CO_2 + H_2O$	-142
	$2NaOH + H_2S \leftrightarrow Na_2S + 2H_2O$	22		
Steam reforming	-		$C_6H_6 + 6 H_2O \leftrightarrow 6 CO + 9 H_2$	752
	-		$C_6H_6 + 12 H_2O \leftrightarrow 6 CO_2 + 15 H_2$	547
Hydrogenation	$C_2H_4 + H_2 \leftrightarrow C_2H_6$	-137	$C_2H_4 + H_2 \leftrightarrow C_2H_6$	-137
	$COS + H_2 \leftrightarrow H_2S + CO$	7	$COS + H_2 \leftrightarrow H_2S + CO$	7
Decomposition	-		$2NH_3 \leftrightarrow N_2 + 3H_2$	111

5 Design of gas cleaning processes

A potential design of a cold and hot gas cleaning process is described in this chapter. The design is based on the mathematical models for the individual reactors shown in **Chapter 4**.

5.1 Concept for cold gas cleaning

Figure 25 shows the flow chart of the calculated cold gas cleaning process. The basic idea of this reactor arrangement is from [57]. **Figure 25** is slightly modified.

Hot product gas leaves the gasifier, dust is separated via a cyclone and the gas is cooled successively by two heat exchangers, down to 180 °C. Next, a filter removes most of the solid particles from the gas stream. These solids, mainly composed of char, can be returned to the combustor as additional fuel.

The gas stream is then directed to a scrubber where rapeseed methyl ester (RME) absorbs tar molecules. Additionally, the solid particle concentration can further be reduced. The liquid solvent (RME) also cools down the product gas to approximately 40 °C. Thus, the water content can be reduced down to approximately 6 vol.-%. This amount of water is within the specified limit of 10 vol.-% for the methanation catalyst. The condensed water leaves the absorber together with the organic solvent and the absorbed tar. Spent RME can be regenerated and fed back to the scrubber or sent to the combustor for final disposal. The water can be used to produce steam to serve as a gasification agent.

The product gas now almost free of tar and water is fed to a reactor equipped with an activated carbon filter. The activated carbon can adsorb traces of tar and sulphur components. Chemical and physical adsorption processes occur. Hydrogen sulphide is chemically adsorbed by either adding oxygen to the product gas or by impregnating the activated carbon with sodium hydroxide (NaOH). Adding oxygen to this type of product gas can lead to oxidation reactions which is very dangerous. Therefore, impregnated activated carbon is chosen as sorbent for adsorbing hydrogen sulphide. Tar adsorption occurs as physical adsorption where the molecules stick on the activated carbon surface. The condensation heat is used to describe and calculate this physical tar adsorption process. At the exit of the activated carbon filter the tar content has to be reduced to under 3 g/Nm³_{db} to meet the specified limit of the methanation catalyst.

Next the product gas reaches a water scrubber. Ammonia and hydrochloric acid are polar molecules and have a high affinity to water. This leads to high separation efficiencies. The spent water can be regenerated and fed back to the absorber. The specified limit of the methanation catalyst for ammonia and hydrochloric acid is 5 ppm and 2 ppm respectively. Then the gas is compressed and cooled to increase the pressure for the methanation without heating up the product gas. As mentioned in the first

chapter, the methanation reactions favour high pressure and low temperature. Therefore, a pressure of around 10 bar is set.

The pressurized product gas then reaches a hydrogenator. Here the hydrogenation of alkenes to alkanes take place. Furthermore, carbonyl sulphides are transformed into hydrogen sulphide at this stage. The hydrogen demand for the reactions can be consumed directly from the product gas. For further methanation the specified limits for alkenes and carbonyl sulphides are 0.2 vol.-%_{db} and 0.8 ppm respectively. A zinc-based catalyst is supporting the hydrogenation.

In case of hydrogen sulphide brakes through the activated carbon bed or results from carbonyl sulphides transformation an amine scrubber is installed. Different amine-based solvents exist. The solvent methyldiethanolamine can absorb hydrogen sulphide and carbon dioxide. The additional carbon dioxide removal can be beneficial because a simultaneously carbon monoxide and carbon dioxide methanation is difficult to execute. Furthermore, the ratio between hydrogen and carbon dioxide can be adjusted to the ideal of 4:1. At the exit of the amine scrubber the hydrogen sulphide content has to be under 10 ppm to meet the specified limit of the methanation catalyst.

Before entering the methanation reactor the product gas can enter guard reactors if necessary. These reactors can be equipped with different adsorbent materials e.g. zinc oxide, depending on the remaining harmful compounds to be removed from the product gas. Special attention is payed to sulphur compounds as these compounds are harmful for the sensitive methanation catalyst. Thus, a fixed bed reactor equipped with zinc oxide is installed at the end of the cold gas cleaning section.

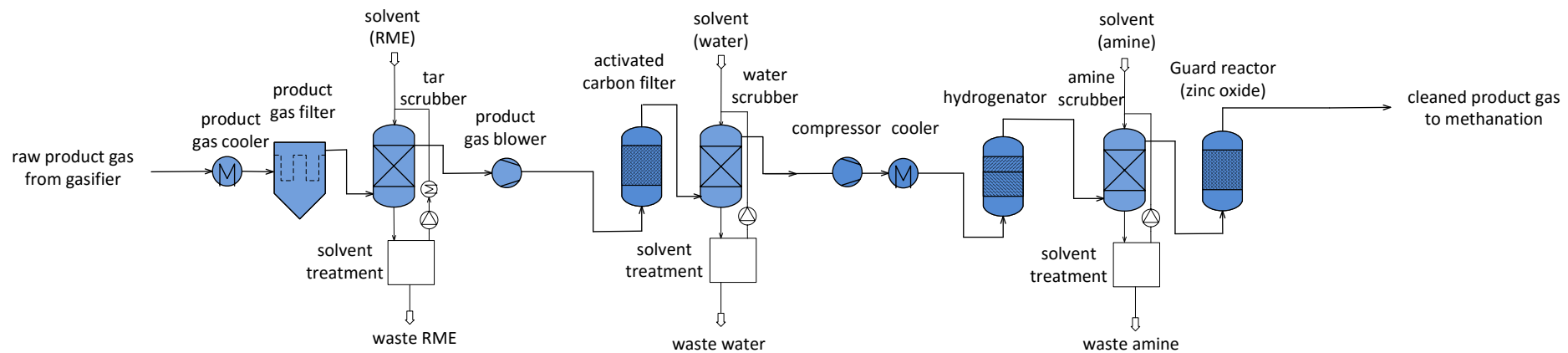


Figure 25: Flow chart cold gas cleaning

5.2 Concept for hot gas cleaning

In recent years growing research and attention has been paid to hot gas cleaning systems because the process should have a lower energy demand than conventional wet scrubbing processes. Furthermore, the waste water disposal problem can be greatly reduced because of mostly catalytic reactions [60]. **Figure 26** shows a flow chart of the calculated hot gas cleaning section were the product gas can be used for further methanation. It should be noted that in comparison with hot gas cleaning, cold gas cleaning systems are well developed and commonly used today [5,60].

Directly after the gasifier and cyclone the product gas enters a hot gas filter where solid particles are removed from the gas stream. This type of hot gas filter is usually equipped with porous ceramic filter candles at the inside. The separated solids can be returned to the combustor for supporting the oxidation as it is done at the cold gas cleaning section.

Next, the nearly solid-free product gas reaches a fixed bed reactor filled with trona ($\text{Na}_2\text{CO}_3 \cdot \text{NaHCO}_3 \cdot 2\text{H}_2\text{O}$) and zinc titanium oxide (ZnTiO_3) in the ratio 2:1. Trona is a mineral which adsorbs hydrogen chloride and zinc titanium oxide is an inorganic compound which adsorbs hydrogen sulphide. After this cleaning process the hydrogen chloride content has to be under 2 ppm to meet the specified limit of the methanation catalyst.

The product gas is then directed to a steam reformer. Since steam reforming reactions are strongly endothermic, heat is required to process the product gas. The required heat can be provided e.g. via an electrical or jacket heating at the outside of the reactor. As steam reforming catalyst a precious metal with low methane activity, like platinum or nickel supported with copper, is used. The methane activity can be further lowered by decreasing the reforming temperature. High tar conversion, with precious metals, can be obtained already at around 850 °C, whereas temperatures above 900 °C are required to have a high methane conversion. Additionally, precious metal catalysts are highly active in converting organic sulphur compounds and have a low affinity to coke formation but their price is high.

After the steam reformer the product gas enters a reactor where ammonia is catalytically decomposed to nitrogen and hydrogen. Iron catalysts are used for the decomposition. Temperatures above 800 °C are typically needed when the reaction takes place in the presence of other gas components such as hydrogen, carbon monoxide, carbon dioxide or synthetic mixtures of these gases. According to the specified limit of the methanation catalyst the ammonia content has to be lower than 5 ppm at the exit this reactor. Furthermore, the amount of resulting nitrogen has to be lower than 0.8 vol.-%_{db}.

Next, the product gas is directed into a drier where the water content can be reduced to 6 vol.-%. The water content is in the range of the specified limit of the methanation catalyst. The gas temperature after the drier is at around 40 °C.

To protect the upcoming compressor against any remaining tar molecules a fixed bed reactor equipped with activated carbon is installed. As for the cold gas cleaning a mixture of impregnated and standard activated carbon is chosen to remove remaining tar as well as hydrogen sulphide molecules. According to the specified limit of the methanation catalyst the tar and hydrogen sulphide content have to be lower than 3 g/Nm³_{db} and 10 ppm respectively.

Then the product gas is compressed and cooled to set the conditions for the methanation. Similar to the cold gas cleaning section the dried, compressed and cooled product gas enters a hydrogenator equipped with a zinc-based catalyst to hydrogenate alkenes to alkanes and carbonyl sulphides to hydrogen sulphide. For further methanation the specified limits for alkenes and carbonyl sulphides are 0.2 vol.-%_{db} and 0.8 ppm respectively.

As for the cold gas cleaning process a guard reactor equipped with e.g. zinc oxide is installed to further reduce harmful species like hydrogen sulphide

Finally, **Figure 27** shows a flow chart of the whole SNG-production process from hazelnut shells gasification including the hot (1) and cold (2) gas cleaning process.

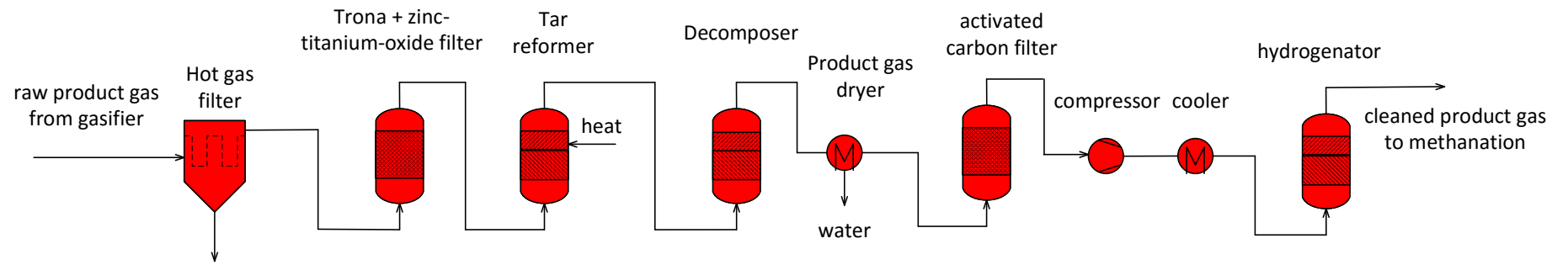


Figure 26: Flow chart hot gas cleaning

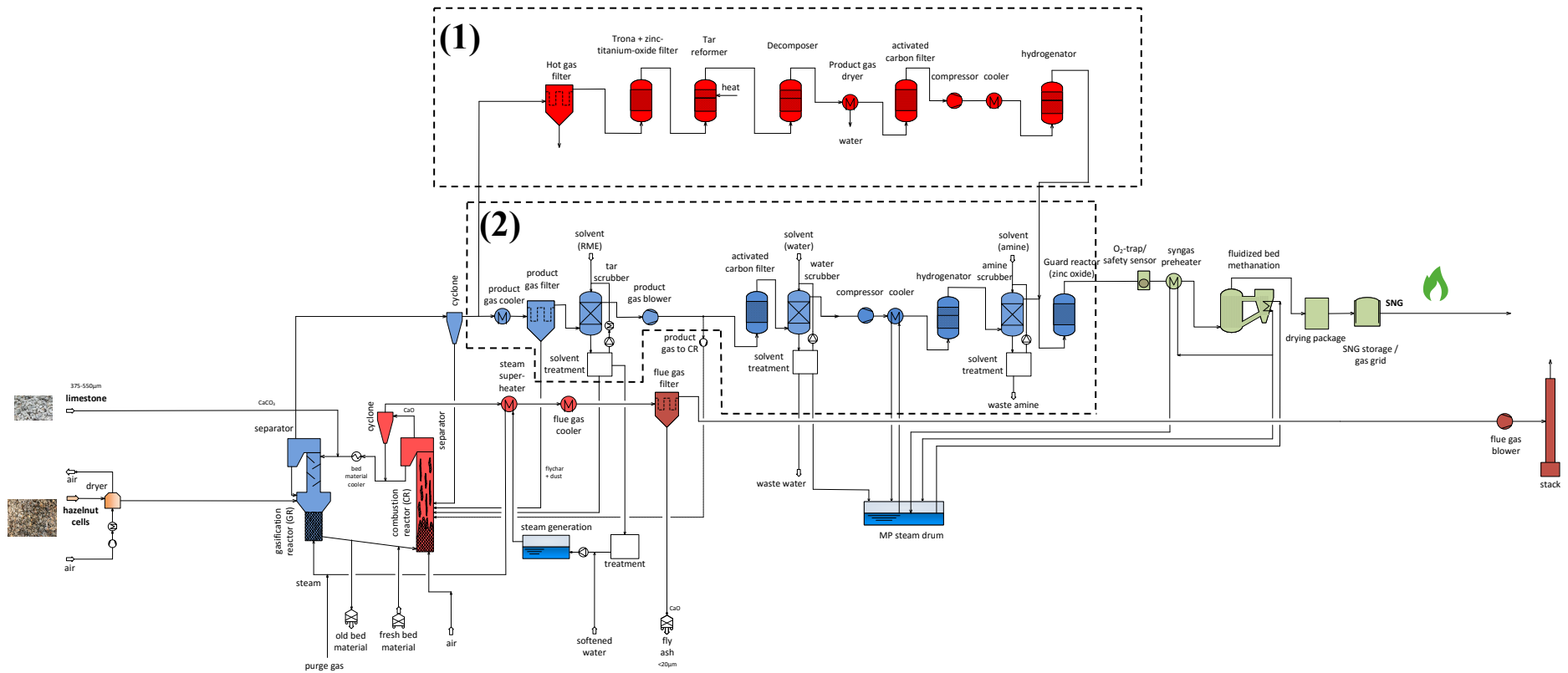


Figure 27: flow chart of the SNG-production process from hazelnut shells gasification including the hot (1) and cold (2) gas cleaning process

6 Calculation results for gas cleaning processes

Based on the mathematical models shown in **Chapter 4** the calculation results of each reactor from both gas cleaning processes given in **Chapter 5** is represented. Furthermore, a flow chart of the respective reactor is displayed which includes all significant parameters. The characterisation of each reactor, the made assumptions and the complete set of calculated parameters (**Eq. 4.8** to **Eq. 4.40**) can be found in the appendix (**Table 36** to **Table 56**).

6.1 Cold gas cleaning reactors

RME-scrubber

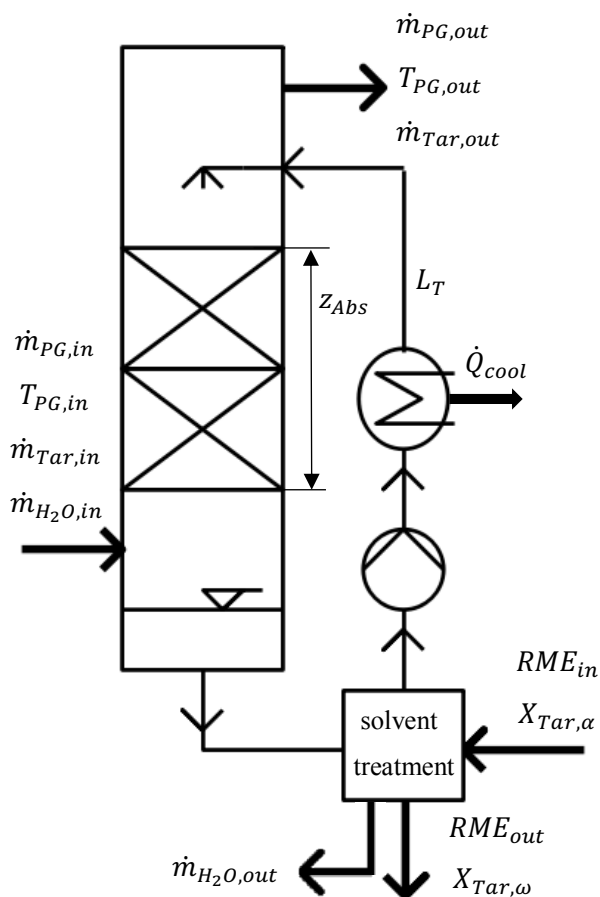


Figure 28: Flow chart of the RME-scrubber

The incoming product gas mass flow ($\dot{m}_{PG,in}$) into the RME-scrubber (**Figure 28**) is $1063 \frac{kg}{h}$ with a tar content ($\dot{m}_{Tar,in}$) of $13 \frac{kg}{h}$. Additionally, $1500 \frac{kg}{h}$ of water ($\dot{m}_{H_2O,in}$) enters the RME-scrubber as well. The inlet temperature of the gas is $180 \text{ }^\circ\text{C}$. After the absorption process the tar content ($\dot{m}_{Tar,out}$) is $0.1 \frac{kg}{h}$. The mass flow of water ($\dot{m}_{H_2O,out}$) is reduced to $90 \frac{kg}{h}$. **Table 18** summarizes some key parameters of the RME-scrubber.

Table 18: Parameters of the RME-scrubber

Parameter	Value	Unit
L_T (Eq. 4.13)	298	kg/h
L_T (Eq. 4.16)	30	kg/h
z_{Abs}	9	m
A_{Column}	1.8	m^2
$T_{PG,out}$	40	$^\circ\text{C}$
\dot{Q}_{cool}	1.2	MW

Activated carbon filter

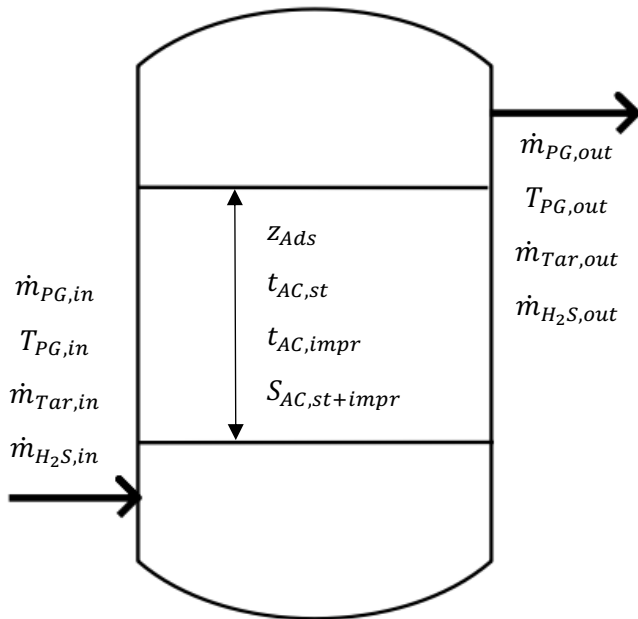


Figure 29: Flow chart of the activated carbon filter

After the RME-scrubber a product gas mass flow ($\dot{m}_{PG,in}$) of $1050 \frac{kg}{h}$ enters the activated carbon filter shown in **Figure 29**. The tar ($\dot{m}_{Tar,in}$) and hydrogen sulphide ($\dot{m}_{H2S,in}$) content is $0.13 \frac{kg}{h}$ and $0.5 \frac{kg}{h}$ respectively. After the adsorption process the tar ($\dot{m}_{Tar,out}$) and hydrogen sulphide ($\dot{m}_{H2S,out}$) content is reduced to $1 \frac{g}{h}$ and $25 \frac{g}{h}$ respectively. **Table 19** summarizes some key parameters of the activated carbon filter. The standard activated carbon (AC,st) adsorbs tar and the impregnated activated carbon (AC,impr) adsorbs hydrogen sulphide.

Table 19: Parameters of the activated carbon filter

Parameter	Value	Unit
z_{Ads}	1	<i>m</i>
A_{Column}	0.45	m^2
$t_{AC,st}$	39	<i>days</i>
$t_{AC,impr}$	10	<i>days</i>
$S_{AC,st+impr}$	540	<i>kg</i>
$T_{PG,out}$	40	$^{\circ}C$
$\dot{Q}_{Reaction}$	74	<i>W</i>

Water-scrubber

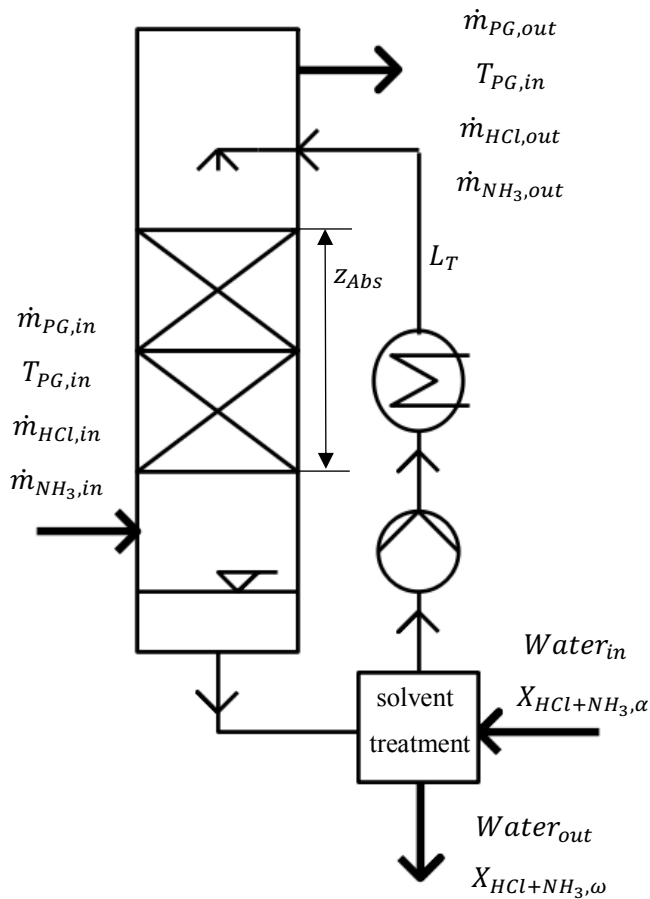


Figure 30: Flow chart of the water-scrubber

A product gas mass flow ($\dot{m}_{PG,in}$) of $1049 \frac{kg}{h}$ enters the water scrubber shown in **Figure 30**. The incoming amount of hydrogen chloride ($\dot{m}_{HCl,in}$) and ammonia ($\dot{m}_{NH_3,in}$) is $0.14 \frac{kg}{h}$ and $9 \frac{kg}{h}$ respectively. After the absorption process $1.3 \frac{g}{h}$ of hydrogen chloride ($\dot{m}_{HCl,out}$) and $89 \frac{g}{h}$ of ammonia ($\dot{m}_{NH_3,out}$) are left in the product gas. **Table 20** summarizes some key parameters of the water-scrubber.

Table 20: Parameters of the water-scrubber

Parameter	Value	Unit
L_T (Eq. 4.13)	4060	kg/h
L_T (Eq. 4.16)	15	kg/h
z_{Abs}	34	m
A_{Column}	0.45	m^2
$T_{PG,out}$	40	$^{\circ}C$

Hydrogenator

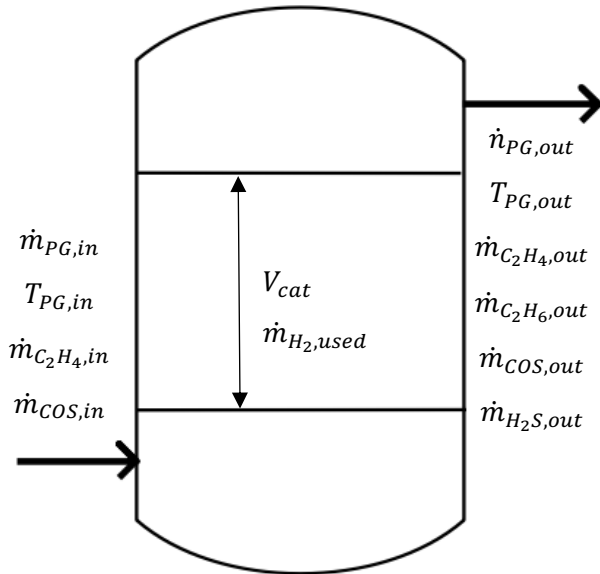


Figure 31: Flow chart of the hydrogenator

After increasing the pressure to around 16 bar without heating up the product gas a total mass flow of $1040 \frac{kg}{h}$ enters the hydrogenator shown in **Figure 31**. The incoming amount of olefin ($\dot{m}_{C_2H_4,in}$) and carbonyl sulphide ($\dot{m}_{COS,in}$) is $36 \frac{kg}{h}$ and $0.2 \frac{kg}{h}$ respectively. The olefin content ($\dot{m}_{C_2H_4,out}$) is reduced to $0.36 \frac{kg}{h}$ and the amount of resulting C_2H_6 ($\dot{m}_{C_2H_6,out}$) is $38 \frac{kg}{h}$. Carbonyl sulphide ($\dot{m}_{COS,out}$) is reduced to $2 \frac{g}{h}$ whereas the hydrogen sulphide ($\dot{m}_{H_2S,out}$) content increases to $0.15 \frac{kg}{h}$. **Table 21** summarizes some key parameter of the hydrogenator.

Table 21: Parameters of the hydrogenator

Parameter	Value	Unit
V_{cat}	0.3	m^3
$\dot{m}_{H_2,used}$	2.6	kg/h
A_{column}	0.55	m^2
$T_{PG,out}$	111	$^{\circ}C$
$\dot{Q}_{Reaction}$	- 46	kW

Amine-scrubber

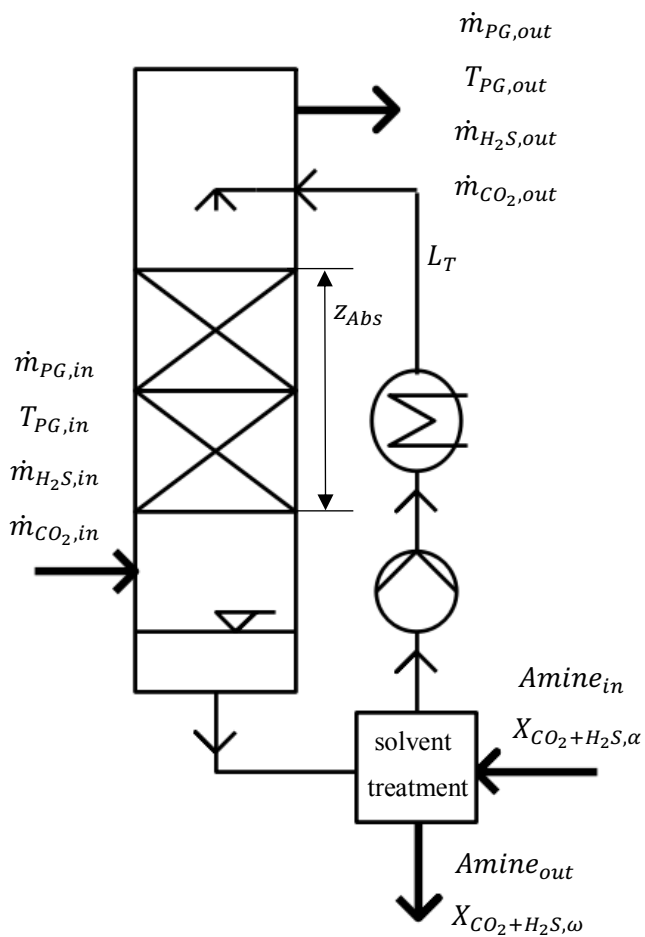


Figure 32: Flow chart of the amine-scrubber

Finally, a mass flow ($\dot{m}_{PG,in}$) of $1040 \frac{kg}{h}$ enters the amine scrubber shown in **Figure 32**. The incoming amount of carbon dioxide ($\dot{m}_{CO_2,in}$) and hydrogen sulphide ($\dot{m}_{H_2S,in}$) is $528 \frac{kg}{h}$ and $0.15 \frac{kg}{h}$ respectively. After the absorption process hydrogen sulphide ($\dot{m}_{H_2S,out}$) and carbon dioxide ($\dot{m}_{CO_2,out}$) are reduced down to $1.5 \frac{g}{h}$ and $264 \frac{kg}{h}$ respectively. The total product gas mass flow leaving the amine scrubber ($\dot{m}_{PG,out}$) is $825 \frac{kg}{h}$. **Table 22** summarizes some key parameters of the amine-scrubber.

Table 22: Parameters of the amine-scrubber

Parameter	Value	Unit
L_T (Eq. 4.13)	1155	kg/h
L_T (Eq. 4.16)	N/A	kg/h
z_{Abs}	1.5	m
A_{Column}	0.55	m^2
$T_{PG,out}$	66	$^{\circ}C$

6.2 Hot gas cleaning reactors

Trona and zinc-titanium-oxide filter

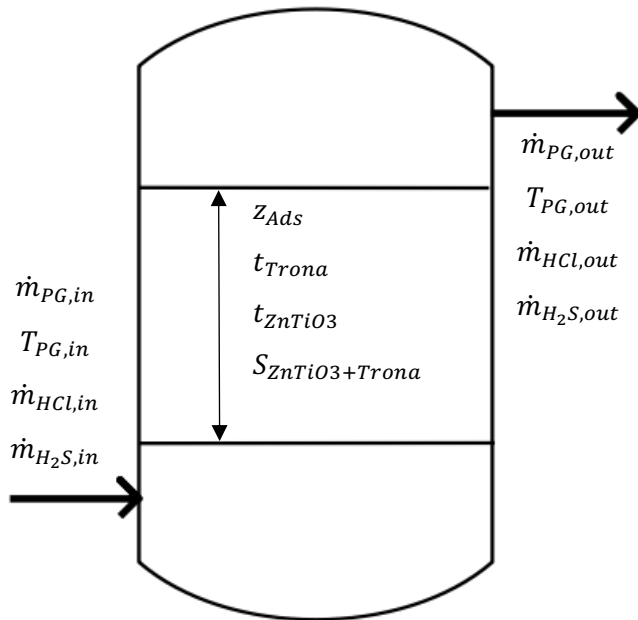


Figure 33: Flow chart of a reactor filled with trona and zinc-titanium-oxide

The incoming product gas mass flow ($\dot{m}_{PG,in}$) into the adsorption reactor (**Figure 33**) is $1063 \frac{kg}{h}$ with a temperature of $T_{PG,in} = 650 \text{ }^\circ\text{C}$. The hydrogen sulphide ($\dot{m}_{H_2S,in}$) and hydrochloric acid ($\dot{m}_{HCl,in}$) content is $0.5 \frac{kg}{h}$ and $0.14 \frac{kg}{h}$ respectively. After the adsorption process the product gas mass flow ($\dot{m}_{PG,out}$) is $1062 \frac{kg}{h}$ with a hydrogen sulphide content ($\dot{m}_{H_2S,out}$) of $26 \frac{g}{h}$. The hydrochloric acid content ($\dot{m}_{HCl,out}$) belongs to $7 \frac{g}{h}$. **Table 23** summarizes some key parameters of the trona + zinc-titanium-oxide filter. Trona adsorbs hydrochloric acid and zinc-titanium oxide adsorbs hydrogen sulphide.

Table 23: Parameters of the trona + zinc-titanium-oxide filter

Parameter	Value	Unit
z_{Ads}	1	<i>m</i>
A_{Column}	3.7	m^2
t_{Trona}	227	<i>days</i>
t_{ZnTiO_3}	15	<i>days</i>
$S_{ZnTiO_3+Trona}$	4417	<i>kg</i>
$T_{PG,out}$	650	$^\circ\text{C}$
$\dot{Q}_{Reaction}$	-0.2	<i>kW</i>

Steam reformer

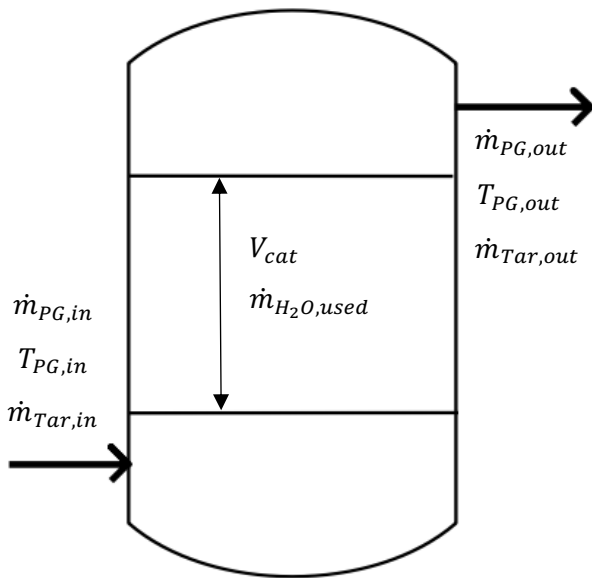


Figure 34: Flow chart of the steam reformer

A product gas mass flow ($\dot{m}_{PG,in}$) of $1062 \frac{kg}{h}$ enters the steam reformer shown in **Figure 34**. The incoming amount of tar ($\dot{m}_{Tar,in}$) is $13 \frac{kg}{h}$. To initiate the steam reforming reactions the temperature has to be increased to around $850 \text{ }^\circ\text{C}$. After the steam reformer the tar content ($\dot{m}_{Tar,out}$) is reduced down to $0.13 \frac{kg}{h}$. **Table 24** summarizes some key parameters of the steam reformer. \dot{Q}_{in} is the amount of energy which has to be provided to heat up the product gas from $650 \text{ }^\circ\text{C}$ to $850 \text{ }^\circ\text{C}$.

Table 24: Parameters of the steam reformer

Parameter	Value	Unit
V_{Cat}	0.65	m^3
$\dot{m}_{H_2O,used}$	27	kg/h
A_{column}	4.5	m^2
$T_{PG,out}$	850	$^\circ\text{C}$
\dot{Q}_{in}	280	kW
$\dot{Q}_{Reaction}$	30	kW

Decomposer

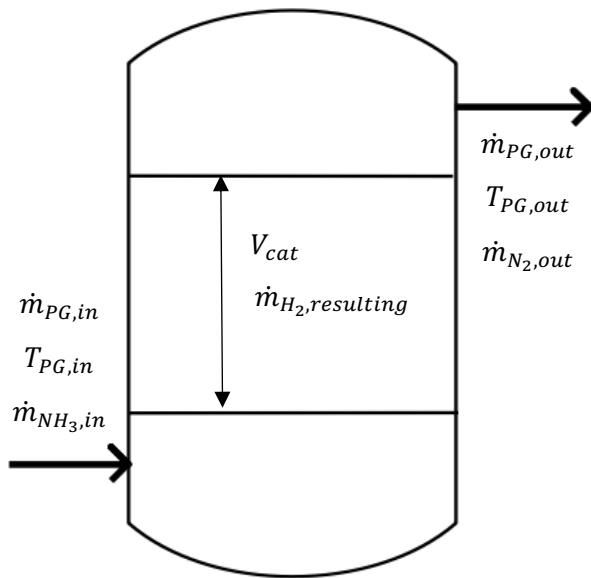


Figure 35: Flow chart of the decomposer

The product gas mass flow ($\dot{m}_{PG,in}$) into the decomposer, shown in **Figure 35**, is $1089 \frac{kg}{h}$. The input amount of ammonia ($\dot{m}_{NH_3,in} = 9 \frac{kg}{h}$) is decomposed into $7 \frac{kg}{h}$ nitrogen ($\dot{m}_{N_2,out}$) and $1.6 \frac{kg}{h}$ hydrogen ($\dot{m}_{H_2,resulting}$). **Table 25** summarizes some key parameters of the decomposer.

Table 25: Parameters of the decomposer

Parameter	Value	Unit
V_{cat}	0.65	m^3
A_{column}	4.2	m^2
$T_{PG,out}$	785	$^{\circ}C$
$\dot{Q}_{Reaction}$	16	kW

Product gas dryer

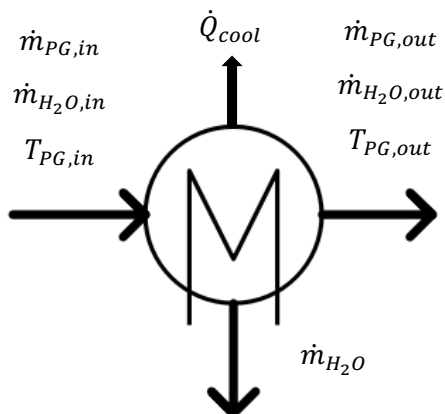


Figure 36: Flow chart of the product gas dryer

At this stage of the process the incoming mass flow of water ($\dot{m}_{H_2O,in}$) is reduced from $1500 \frac{kg}{h}$ down to $88 \frac{kg}{h}$ ($\dot{m}_{H_2O,out}$) with a product gas dryer shown in **Figure 36**. The product gas mass flow remains constant at $1089 \frac{kg}{h}$. **Table 26** summarizes some key parameters of the product gas dryer

Table 26: Parameters of the product gas dryer

Parameter	Value	Unit
$T_{PG,out}$	40	$^{\circ}C$
\dot{Q}_{cool}	1.4	MW

Activated carbon filter

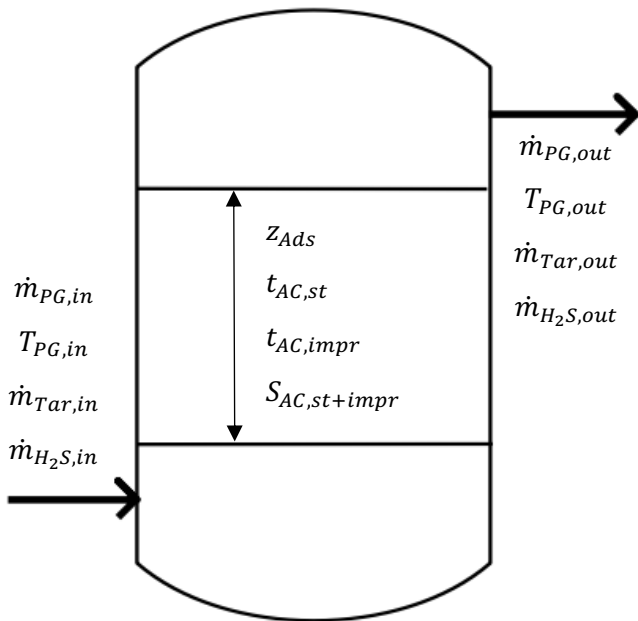


Figure 37: Flow chart of the activated carbon filter

Figure 37 shows the flow chart of the activated carbon filter. At the entry the tar ($\dot{m}_{Tar,in}$) and hydrogen sulphide ($\dot{m}_{H_2S,in}$) content is $0.13 \frac{kg}{h}$ and $26 \frac{g}{h}$ respectively. After the adsorption process the tar ($\dot{m}_{Tar,out}$) and hydrogen sulphide ($\dot{m}_{H_2S,out}$) content is reduced to $1.3 \frac{g}{h}$ and $0.3 \frac{g}{h}$ respectively.

Table 27 summarizes some key parameters of the activated carbon filter. The standard activated carbon (AC,st) adsorbs tar and the impregnated activated carbon (AC,impr) adsorbs hydrogen sulphide.

Table 27: Parameters of the activated carbon filter

Parameter	Value	Unit
z_{Ads}	1	<i>m</i>
A_{Column}	0.45	<i>m</i> ²
$t_{AC,st}$	39	<i>days</i>
$t_{AC,impr}$	200	<i>days</i>
$S_{AC,st+impr}$	540	<i>kg</i>
$T_{PG,out}$	40	<i>°C</i>
$\dot{Q}_{Reaction}$	- 10	<i>W</i>

Hydrogenator

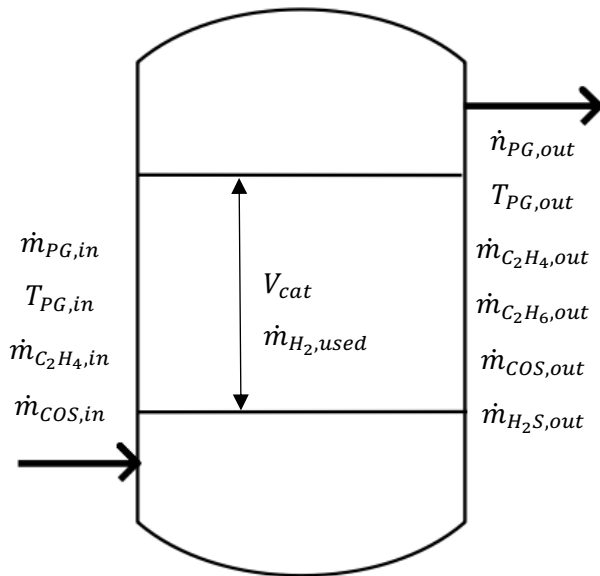


Figure 38: Flow chart of the hydrogenator

After increasing the pressure to around 16 bar without heating up the product gas a total mass flow of $1089 \frac{kg}{h}$ enters the hydrogenator shown in **Figure 38**. The incoming amount of olefin ($\dot{m}_{C_2H_4,in}$) and carbonyl sulphide ($\dot{m}_{COS,in}$) is $36 \frac{kg}{h}$ and $0.2 \frac{kg}{h}$ respectively. The olefin content ($\dot{m}_{C_2H_4,out}$) is reduced to $0.36 \frac{kg}{h}$ and the amount of resulting C_2H_6 ($\dot{m}_{C_2H_6,out}$) is $38 \frac{kg}{h}$. Carbonyl sulphide ($\dot{m}_{COS,out}$) is reduced to $2 \frac{g}{h}$ whereas the hydrogen sulphide ($\dot{m}_{H_2S,out}$) content increases to $0.15 \frac{kg}{h}$. **Table 28** summarizes some key parameters of the hydrogenator.

Table 28: Parameters of the hydrogenator

Parameter	Value	Unit
V_{cat}	0.3	m^3
$\dot{m}_{H_2,used}$	2.6	kg/h
A_{column}	0.53	m^2
$T_{PG,out}$	94	$^{\circ}C$
$\dot{Q}_{Reaction}$	- 46	kW

7 Discussion of results and summary

Based on the calculation models shown in **Chapter 4** a potential cold and hot gas cleaning process was designed and calculated in **Chapter 5** and **Chapter 6** respectively. On the following pages the calculation results of both gas cleaning processes are discussed. First the cleaning performance of the gas cleaning processes is evaluated by using the specified limits of the methanation catalyst as a reference. Furthermore, the calculated key parameters of the respective gas cleaning process are given and discussed.

Cleaning performance of the cold and hot gas cleaning process

Table 29 compares the product gas impurities which are harmful for the methanation catalyst at the exit of the cold and hot gas cleaning process with the specified limits of the methanation catalyst. Values coloured green are within the specified limit. Red and orange coloured values are outside the specified limit whereby the orange ones are just outside the specified limit.

Table 29: cleaning performance of both gas cleaning processes

Product gas components	Reference data for catalyst	Exit cold gas cleaning	Exit hot gas cleaning	Unit
Acetylene (C ₂ H ₂)	N/A	0	0	vol.-% _{db}
Ethylene (C ₂ H ₄)	0.2	0.02	0.02	vol.-% _{db}
Propene (C ₃ H ₆)	0.4	0	0	vol.-% _{db}
Ammonia (NH ₃)	5	70	70	ppm
Hydrogen sulphide (H ₂ S)	10	0.6	50	ppm
Carbonyl sulphide (COS)	0.8	0.5	0.5	ppm
Hydrochloric acid (HCl)	2	0.5	2.5	ppm
Hydrogen cyanide (HCN)	0.8	200	200	ppm
Nitrogen (N ₂)	0.8	0	0.5	vol.-% _{db}
Water (H ₂ O)	10	6	6	vol.-%
Dust and char	N/A	4	4	mg/Nm ³ _{db}
Gravimetric tar	0.005	0.0007	0.0007	g/Nm ³ _{db}
GCMS tar	3	0.0007	0.0007	g/Nm ³ _{db}
GCMS tar composition				
Naphthalene	0.8	-	-	g/Nm ³ _{db}
Benzene (B)	3	-	-	g/Nm ³ _{db}
Toluene (T)	N/A	-	-	g/Nm ³ _{db}
Ethylbenzene (E)	N/A	-	-	g/Nm ³ _{db}
Xylene (X)	N/A	-	-	g/Nm ³ _{db}
Critical components in ash				
Arsenic (As)	100	0	0	mg/Nm ³ _{db}
Natrium (Na)	0.8	0.1	0.1	mg/Nm ³ _{db}

At the exit of the cold gas cleaning process the ammonia and hydrogen cyanide concentrations are too high. To further reduce the amount of ammonia with the chosen cleaning technology several options exist. Installing a second water-scrubber or increasing the height of the substance-exchanging layer are possible. Using a further water-scrubber means under an environmental point of view more waste water, which has to be handled. On the other hand, enhancing the separation efficiency over 99.9 % leads to a drastically increasing height of the substance-exchanging layer as can be seen in **Figure 39**. Another possibility could be increasing the column diameter. This reduces the gas velocity which leads to an increasing contact time between the solvent and the gas stream. The removal of hydrogen cyanide was not considered in the design of the cold gas cleaning process. An additional reactor, capable of reducing the hydrogen cyanide content, has to be designed since the concentration is far too high according to the specified limit of the methanation catalyst.

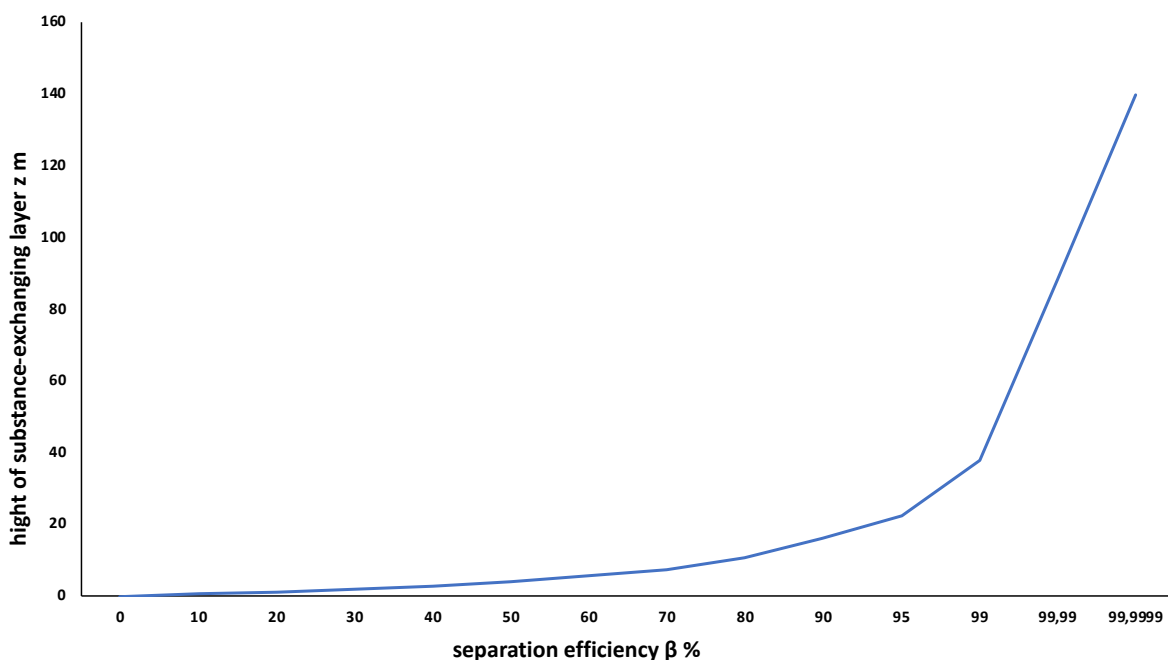


Figure 39: Change of height of substance-exchanging layer z over separation efficiency β at the example of the water-scrubber

In terms of the hot gas cleaning process the product gas content of ammonia, hydrogen sulphide, hydrochloric acid and hydrogen cyanide is above the specified limit of the methanation catalyst. As for the cold gas cleaning process the hydrogen cyanide removal was not considered during hot gas cleaning and has to be further investigated. The hydrochloric acid and hydrogen sulphide concentration could be further reduced by increasing the amount of the respective sorption material or by investigating other materials with a higher sorption capacity. Furthermore, the optimization of process parameters like residence time, temperature or pressure could favour the adsorption process. To meet the specified limit of the methanation catalyst for ammonia the decomposer has to be optimized or another hot gas cleaning technology has to be evaluated. Increasing the residence time or optimize the catalysator material could

be done to increase the separation efficiency of the decomposer. An alternative technology to the decomposition of ammonia is the controlled addition of an oxidizer like nitric oxide or oxygen to the product gas to selectively transform ammonia into nitrogen.

Beside the suggested methods to observe the specified limits of the methanation catalyst a guard reactor is installed at the end of the designed gas cleaning processes. This reactor can be equipped with different sorption materials depending on the product gas species which has to be further reduced.

Energy demand and temperature profile of both gas cleaning processes

According to the literature hot gas cleaning processes should offer significant efficiency gains in the conversion process from biomass to e.g. SNG because no cooling or reheating of the product gas should be needed [5,40,41]. In fact, especially cooling of the product gas has to be done since the water content needs to be reduced to meet the specified limit for water of the methanation catalyst. **Figure 40** shows the calculated temperature profile of the designed cold (1) and hot (2) gas cleaning process.

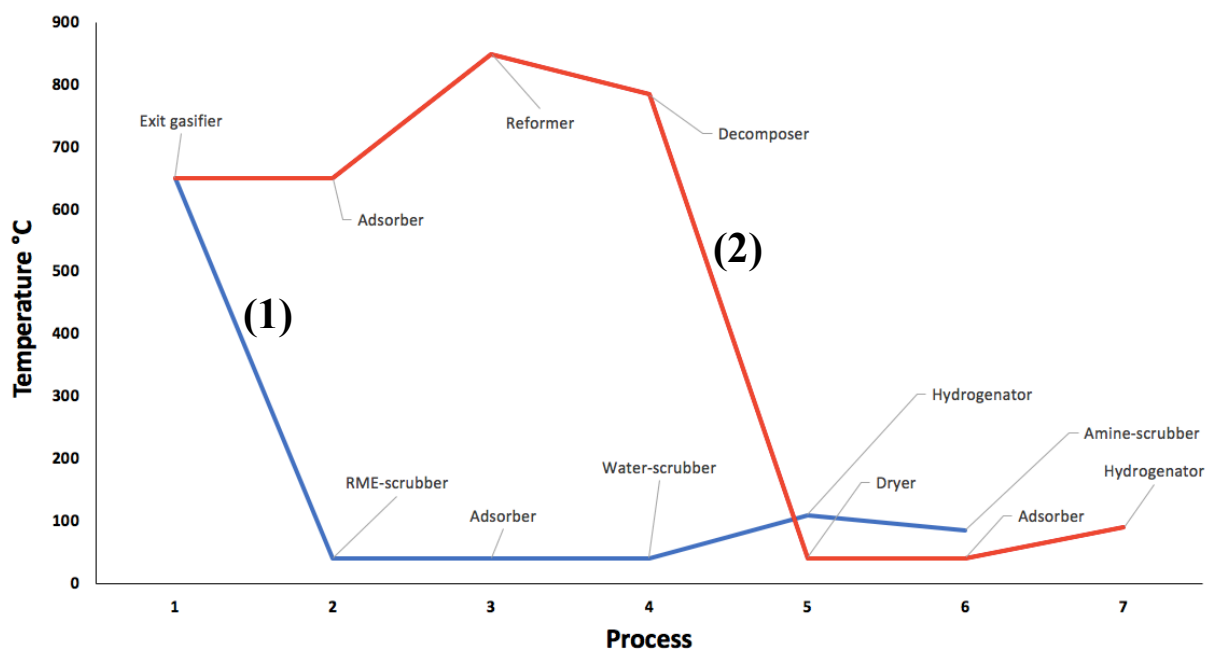


Figure 40: Temperature profile of the designed cold (1) and hot (2) gas cleaning process

It can be seen that most of the energy demand of the cold gas cleaning process (1) is related to the RME-scrubber. At this stage of the process most of the tar and water are condensed. The energy demand of the upcoming cold gas cleaning process is negligible compared to the RME-scrubber. To operate the designed hot gas cleaning process (2) the product gas has to be heated up to steam reform the tar and also cooled to condense the water. The energy demand of the hot gas cleaning process can be reduced by increasing the gasification temperature. By performing conventional gasification at around 800 °C for example, the product gas temperature at the exit of the gasifier is approximately in the operating

range of the hot gas steam reformer. The energy demand of the other hot gas cleaning reactors is negligible compared to the steam reformer and product gas dryer. To make detailed statements about the energy consumption of both gas cleaning processes the heat integration of the processes has to be investigated.

Solvent consumption of wet scrubbers

To calculate the amount of solvent two potential methods are presented in **Chapter 4. Table 30** compares the results from both methods. It can be seen that the differences are quite high between the calculation method and the use of the solubility diagram. The calculation method uses the Henry constant to describe the equilibrium between a gaseous compound and a liquid phase. To evaluate the effective amount of needed solvent more detailed research is needed and experiments should be conducted. An explanation for the relatively low amount of solvent according to the solubility diagram could be that it does not consider that the solvent is no continuous phase but dispersed into drops instead.

Table 30: Solvent consumption of wet scrubbers

Scrubber	Amount of solvent [kg/h]	
	Calculation (Eq. 4.13)	Diagram (Eq. 4.16)
RME	298	30
Water	4060	15
Amine	1155	N/A

Speaking to an expert, around 20 kg/h of RME were used at the 1MW_{SNG} demonstration plant in Güssing [67]. Further mentioned was that the RME-scrubber in Güssing was equipped with high efficiency packing to optimize the solvent distribution inside the column and enable the best possible gas/liquid contact. SULZER is a manufacturer which produces such high efficiency packings. Unfortunately, no information regarding specific data of their packings could be received by request. Due to this Raschig-rings were chosen for the adsorption columns. Data for that type of packing were received from [62].

Regeneration cycle of adsorption materials

Based on the assumption that the height of the adsorption material filling is 1 m the regeneration cycle is calculated. **Table 31** shows the regeneration cycle and amount of the respective adsorption material for the cold and hot gas cleaning process. It can be seen that the regeneration cycles of the material mixtures vary widely. To adapt the regeneration cycle of the mixture the amount of one bed material can be increased or decreased. Furthermore, the mixture could be separated when replaced and the partial loaded material could be used again in the next cycle.

Table 31: Calculated regeneration cycle of adsorption materials

Process	Species	Bed material	Regeneration cycle in days	Amount of bed material in kg
Cold gas cleaning	Tar, Hydrogen sulphide	Activated carbon,	39	270
		Activated carbon impregnated	10	270
Hot gas cleaning	Hydrochloric acid, hydrogen sulphide	Trona,	227	2209
		Zinc-titanium-oxide	15	2209
	Tar, Hydrogen sulphide	Activated carbon,	39	270
		Activated carbon impregnated	200	270

Used recourses per day to clean the gas

Table 32 compares the daily recourses of the cold and hot gas cleaning process to clean the gas so that a further methanation is possible.

Table 32: Comparison of daily recourses to clean the product gas for further methanation

Cold gas cleaning			Hot gas cleaning		
Solvent	Unit	Value	Solvent	Unit	Value
RME	kg/d	526	Trona + Zinc-titanium-oxide	kg/d	142
Activated carbon mixture	kg/d	35	Activated carbon mixture	kg/d	9
Water	kg/d	29000			
Amine	kg/d	7800			

As already mentioned, there is quite a big difference if the solvent stream of an absorption column is calculated using **Eq. 4.13** or the solubility diagram (**Eq. 4.16**). For the comparison of the daily recourses in **Table 32** the solvent stream calculated with **Eq. 4.13** was used. Hot gas cleaning in this configuration needs sorption materials in just two of five reactors due to mostly catalytic reactions. However, the assumption was made that just the catalytic reactions and no side reactions take place. These side reactions can lead, amongst other negative effects, to the formation of undesirable species on the catalysator surface [5,49,58]. Especially during hot gas cleaning where three reactors operate with catalysts the amount of catalytic material could raise. Additionally, the high heat in combination with vibrations, caused through e.g. blower, gasifier etc., is stress which lowers the durability of used material like ceramic [60,61]. In terms of the daily recourses needed for cold gas cleaning the assumption was made that 70 % of the spent solvent can be regenerated and fed back to the respective column. The other 30 % have to be removed. Water contaminated with chlorides for example could be send to an acid regeneration plant where hydrochloric acid can be recovered. Another possibility is to neutralize the

spent water. As mentioned in **Chapter 2** a partial amount of the spent RME can be fed back to the combustor acting as additional fuel or regenerated using a stripper.

Table 33 summarizes the calculated key parameters of both gas cleaning processes.

Table 33: Summary of the calculated key parameters from both gas cleaning processes

Cold gas cleaning process				Hot gas cleaning process			
Reactor	Parameter	Value	Unit	Reactor	Parameter	Value	Unit
RME-scrubber (Tar)	L_T (Eq. 4.13)	298	kg/h	Adsorber (HCl + H ₂ S)	z_{Ads}	1	m
	L_T (Eq. 4.16)	30	kg/h		A_{Column}	3.7	m ²
	z_{Abs}	9	m		t_{Trona}	227	days
	A_{Column}	1.8	m ²		t_{ZnTiO_3}	15	days
	$T_{PG,out}$	40	°C		$S_{ZnTiO_3+Trona}$	4417	kg
	\dot{Q}_{cool}	1.3	MW		$T_{PG,out}$	650	°C
Activated carbon filter (H ₂ S + Tar)	z_{Ads}	1	m	Steam reformer (Tar)	$\dot{Q}_{Reaction}$	- 0.2	kW
	A_{Column}	0.45	m ²		V_{Cat}	0.65	m ³
	$t_{AC,st}$	39	days		$\dot{m}_{H_2O,used}$	27	kg/h
	$t_{AC,impr}$	10	days		A_{Column}	4.5	m ²
	$S_{AC,st+impr}$	540	kg		$T_{PG,out}$	850	°C
	$T_{PG,out}$	40	°C		\dot{Q}_{in}	280	kW
	$\dot{Q}_{Reaction}$	74	W		$\dot{Q}_{Reactions}$	30	kW
Water-scrubber (NH ₃ + HCl)	L_T (Eq. 4.13)	4060	kg/h	Decomposer (NH ₃)	V_{Cat}	0.65	m ³
	L_T (Eq. 4.16)	15	kg/h		A_{Column}	4.2	m ²
	z_{Abs}	34	m		$T_{PG,out}$	785	°C
	A_{Column}	0.45	m ²	$\dot{Q}_{Reaction}$	16	kW	
	$T_{PG,out}$	40	°C	Dryer	$T_{PG,out}$	40	°C
Hydrogenator (C ₂ H ₄ + COS)	V_{Cat}	0.3	m ³		\dot{Q}_{cool}	1.4	MW
	$\dot{m}_{H_2,used}$	2.6	kg/h	Activated carbon filter (H ₂ S + Tar)	z_{Ads}	1	m
	A_{Column}	0.55	m ²		A_{Column}	0.45	m ²
	$T_{PG,out}$	111	°C		$t_{AC,st}$	39	days
	$\dot{Q}_{Reactions}$	- 46	kW		$t_{AC,impr}$	200	days
Amine-scrubber (H ₂ S + CO ₂)	L_T (Eq. 4.13)	1155	kg/h		$S_{AC,st+impr}$	540	kg
	L_T (Eq. 4.16)	N/A	kg/h	$T_{PG,out}$	40	°C	
	z_{Abs}	1.5	m	$\dot{Q}_{Reaction}$	- 10	W	
	A_{Column}	0.55	m ²	Hydrogenator (C ₂ H ₄ + COS)	V_{Cat}	0.3	m ³
	$T_{PG,out}$	66	°C		$\dot{m}_{H_2,used}$	2.6	kg/h
			A_{Column}		0.53	m ²	
			$T_{PG,out}$		94	°C	
			$\dot{Q}_{Reactions}$		- 46	kW	

8 Conclusion and Outlook

This work was developed with the aim of finding answers to the research question “can a process for the production of SNG from biogenic residues be designed that meets the requirements of the methanation catalyst?”

First a literature review was conducted to evaluate the state of the art of dual fluidized bed gasification including sorption enhanced reforming, gas cleaning and methanation, which are the three main parts of this process. The outcome of the literature review is as follows. With regard to the methanation step the generated product gas from biomass gasification should contain no nitrogen. Furthermore, the ideal ratio between hydrogen, carbon monoxide and carbon dioxide is 7:1:1. These product gas requirements can be reached with a dual fluidized bed gasifier and sorption enhanced reforming as operation mode. To meet the specified limits of the product gas impurities for the methanation catalyst several cold gas cleaning options are commonly used today e.g. tar absorption using an RME-scrubber or hydrogen sulphide removal with activated carbon. In contrast to cold gas cleaning hot gas cleaning processes are also under investigation because research is done to improve the durability of the used materials. Additionally, different methanation catalysts are also under investigation to improve activity and durability. Ruthenium and nickel have a high activity but are easily poisoned by sulphur. Molybdenum on the other hand is resistant against sulphur but high temperatures are needed for conversion at a moderate activity. To execute the methanation reaction a fluidized bed reactor type is suggested due to the favourable heat management and the fact that only one reactor is needed. Using fixed bed reactors for methanation several reactors are needed to manage the heat removal.

To gain a data basis, a gasification experiment with hazelnut shells as fuel was conducted at TU Wien’s dual fluidized bed gasifier. With the obtained data first a scale up to an 8 MW_{th} gasifier was conducted. Further on mathematical models were created to design reactors which are able to efficiently remove the product gas impurities. The major indicator was to provide a gas which suits the specified limits of the upcoming methanation catalyst. Then a potential design of a cold and hot gas cleaning process is described. The design is based on the mathematical models for the individual reactors. The cold gas cleaning process was slightly modified from a previous diploma thesis conducted at the TU Wien. The hot gas cleaning was designed using the literature. Data for the calculation were found in the literature and assumptions were made to determine the parameter of each gas cleaning reactor.

The calculation results show that neither the cold gas nor the hot gas cleaning process is capable of reaching the specified limits for all impurities which are harmful for the methanation catalyst. For cold gas cleaning the concentration of ammonia and especially hydrogen cyanide is too high. At the exit of the hot gas cleaning process the concentration of ammonia, hydrogen sulphide, hydrochloric acid and

hydrogen cyanide is too high. The calculated temperature profile of both gas cleaning processes shows that for the cold gas cleaning process most of the energy demand is related to the RME-scrubber where most of the tar and water are condensed. To operate the designed hot gas cleaning process most of the energy demand is related to steam reform nearly all tar and to condense most of the water. The energy demand of the hot gas cleaning process can be reduced by increasing the gasification temperature. Looking at the amount of solvent for the respective absorption columns high differences are obtained between the use of the solubility diagram and the calculation methods. The calculation method uses the Henry constant to describe the equilibrium between a gaseous compound and a liquid phase compared to the solubility diagram. To evaluate the effective amount of needed solvent more detailed research is needed and experiments should be conducted. For the adsorption processes the calculated regeneration cycles of the material mixtures vary widely. To adapt the regeneration cycle of the mixture the amount of one bed material can be increased or decreased. Furthermore, the mixture could be separated when replaced and the partial loaded material could be used again in the next cycle. In terms of used recourses per day to clean the gas the hot gas cleaning process needs less recourses. In the designed configuration the process needs sorption materials in just two of five reactors due to mostly catalytic reactions. However, the assumption was made that just the catalytic reactions and no side reactions take place. These side reactions can lead to the formation of undesirable species on the catalysator surface and therefore increase the amount of catalytic material. Furthermore, no cost analysis of the respective sorption materials was conducted. This could have an impact which materials will be used in industrial scale methanation plants.

Overall it can be said that, based on the used calculation models, an implementation of both designed gas cleaning facilities in the biomass to SNG process is possible. To meet the requirements of the methanation catalyst the designed gas cleaning processes have to be adapted.

Further research should be done:

- Evaluating the designed gas cleaning processes experimentally and with the use of simulations.
- Investigations in terms of long-term behaviour of the methanation catalyst.
- Refine the solvent stream and packing of absorption columns
- Considering a wider range of chemical reactions for catalytical gas cleaning
- Improvement in terms of sorption material for cold and hot gas cleaning. Especially when mixtures of different materials are used to increase the operation time till regeneration is necessary.
- Improvements on the methanation catalyst to higher the resistance against impurities and thereby lower the gas cleaning effort.

Abbreviations & Symbols

Table 34: Abbreviations

Abbreviation	Description
Abso	Absolute
Abs	Absorbed
Ads	Adsorbed
AC	Activated carbon
CaO	Calcium oxide
CO	Carbon oxide
CO ₂	Carbon dioxide
COS	Carbonyl sulphide
C ₂ H ₆	Ethane
CR	Combustion reactor
d	Days
daf	Dust and ash free
db	Dry basis
ECN	Energy Research Centre Netherlands
EU	European Union
FICFB	Fast internally circulating fluidized bed gasifier
GmbH	Gesellschaft mit bestimmter Haftung
GR	Gasification reactor
H ₂	Hydrogen
HS	Hazelnut shells
HSC 6	Software for process simulation, reactions equations and equilibrium calculations; Version 6
Impr	Impregnated
IPSE	Integrated Project Support Environment
W _{th}	Thermal power gasifier
lhv	Lower heating value
Nm ³	Norm cubic meter
NO _x	Nitrogen oxides

Ni/Al ₂ O ₃	Nickel/Aluminium oxide
n.m.	Not measured
N/A	Not applicable
O ₂	Oxygen
PG	Product gas
ppb	Part per billion
ppm	Part per million
RME	Rapeseed methyl ester
SNG	Synthetic natural gas
SER	Sorption enhanced reforming
St	Standard
TREMP	Topsøe Recycle Energy-efficient Methanation Process
vol.-%	Volume percental in wet basis
vol.-% _{db}	Volume percental in dry basis
waf	Water and ash free
ZnO	Zinc oxide

Table 35: Symbols

Symbol	Dimension	Description
A_c	m^2	Column surface
$B_{Y,X}$	kg/kg	Adsorption capacity of sorbent y of species x
c_{PG}	$kJ/kmol \cdot K$	Specific heat capacity of the product gas
$c_{PG,X}$	mg/Nm^3	Concentration of species x from the product gas
$c_{X,Y}$	g/l	Solubility of species X at temperature Y
$E_{Gasifier}$	MW_{th}	Thermal power of the gasifier
G_T	$kmol/h$	carrier gas stream
H_u	MJ/kg_{db}	Net calorific value
$H_{X,Y}$	$mbar$	Henry constant of species x at temperature y
HTU	m	Hight of transfer unit
$\Delta h_{H_2O,condense}$	kJ/kg	Condensation enthalpy of water
$\Delta h_{c,Naphtha.}$	kJ/mol	Condensation heat of tar represented by naphthalin

ΔH	kJ/mol	Heat of reaction
k_{Gy}	$\text{kmol}/\text{m}^3 * \text{h}$	Mass transfer coefficient
L_T	kmol/h	Solvent stream
$L_{T,min}$	kmol/h	Minimum solvent stream
\dot{m}_{HS}	t_{ab}/h	Mass flow rate of hazelnut shells
\bar{M}_{PG}	kg/kmol	Average molar mass of the product gas
\dot{m}_{H_2O}	t/h	Mass flow of water
$m_{x,PG}$	kg	Mass of species x from the product gas
M_X	kg/kmol	Molar mass of species x
M_Y	kg/kmol	Molar mass of species y
\dot{m}_{PG}	kg/h	Mass flow of product gas generated in the gasifier
$\dot{m}_{PG,X}$	kg/h	Mass flow of species x from the product gas
\dot{m}_{Ads}	kg/h	Adsorbed mass flow
$n_{x,PG}$	kmol	Mol number of species x from the product gas
\dot{n}_{PG}	kmol/h	Molar flow of product gas generated in the gasifier
$\dot{n}_{PG,X}$	kmol/h	Molar flow of species x from the product gas
NTU	-	Number of transfer units
\dot{n}_Y	kmol/h	Molar flow of species y
\dot{n}_X	kmol/h	Molar flow of species x
\dot{n}_{Abs}	kmol/h	Absorbed molar flow
p	bar	Pressure
\dot{Q}_{cool}	MJ/h	Cooling heat
\dot{Q}_{PG}	MJ/h	Thermal energy product gas
\dot{Q}_{H_2O}	MJ/h	Thermal energy water
\dot{Q}_{in}	MJ/h	Thermal heat input
$\dot{Q}_{Reaction}$	MJ/h	Heat of reaction
S_Y	kg	mass of sorbent y
t_y	h	Regeneration cycle of sorbent y
T_X	$^{\circ}\text{C}$	Temperature of the product gas at stage X of the respective gas cleaning process
$T_{PG,in}$	$^{\circ}\text{C}$	Temperature of the product gas at the inlet
$T_{PG,out}$	$^{\circ}\text{C}$	Temperature of the product gas at the outlet
T_{PG}	$^{\circ}\text{C}$	Temperature of the product gas

V_{cat}	m^3	Catalysator volume
$V_{m,SC}$	$m^3/kmol$	Molar volume at standard conditions (25 °C and 1 bar)
\dot{V}_X	Nm^3/s	Volume flow at stage X of the respective gas cleaning process
\dot{V}_{PG}	Nm_{db}^3/h	Volume flow of product gas generated in the gasifier
$\dot{V}_{PG,\eta}$	Nm_{db}^3/h	Adjusted volume flow of product gas generated in the gasifier
\dot{V}_{H_2O}	m^3/h	volume flow of water
$v_{1\ bar,642\ ^\circ C}$	m^3/kg	Specific volume of water at 1 bar and 642 °C
$v_{PG,X}$	Vol. %	Volume fraction of species x from the product gas
v_{min}	-	Minimum solvent ratio
v	-	Solvent ratio
w_g	m/s	Admissible gas velocity
X_X	-	Molar/mass fraction of species x in the liquid phase at a general point of the reactor
$X_{X,\alpha}$	-	Molar/mass fraction of species x in the liquid phase at the entry of the reactor
$X_{X,\omega}$	-	Molar/mass fraction of species x in the liquid phase at the exit of the reactor
$X_{X,\omega,max}$	-	Maximal molar/mass fraction of species x in the liquid phase at the exit of the reactor
Y_X	-	Molar/mass fraction of species x in the gas phase at a general point of the reactor
$Y_{X,\alpha}$	-	Molar/mass fraction of species x in the gas phase at the entry of the reactor
$Y_{X,\omega}$	-	Molar/mass fraction of species x in the gas phase at the exit of the reactor
Y_X^*	-	Molar/mass fraction of species x in the gas phase at equilibrium state
y_{HS}	Nm_{db}^3/kg_{HS}	Product gas yield of hazelnut shells
z_{Abs}	m	Hight of substance-exchanging layer
z_{Ads}	m	Hight of adsorption material
α	m^2/m^3	Specific surface Raschig-rings
β	%	Separation efficiency
ε	-	Adsorption coefficient of activated carbon
φ	-	Wetting factor
$\bar{\rho}_{PG}$	kg/m^3	Average density of the product gas
ρ_y	kg/m^3	Bulk density of sorbent y
τ	s	Residence time
η	-	Efficiency reference

References

- [1] European Commission (2017). COMMUNICATION FROM THE COMMISSION TO THE EUROPEAN PARLIAMENT, THE COUNCIL, THE EUROPEAN ECONOMIC AND SOCIAL COMMITTEE AND THE COMMITTEE OF THE REGIONS, Brussels
- [2] McKendry, P. (2002). Energy production from biomass (part 2): conversion technologies. *Bioresource Technology* 83, 47–54.
- [3] Bridgewater, A.V., Hofbauer, H., & van Loo, S. (2009) Thermal biomass conversion. Newbury, UK: Scientific Publishing Services Ltd.
- [4] Rehling, B. (2012). *Development of the 1MW Bio-SNG plant, evaluation on technological and economical aspects and upscaling considerations*. TU Wien.
- [5] Schildhauer, T. J., & Biollaz, S. M. A. (2016). *Synthetic natural gas from coal, dry biomass, and power-to-gas applications*. John Wiley & Sons, Inc., Villigen/Switzerland.
- [6] Benedikt, F., Fuchs, J., Schmid, J. C., Müller, S., & Hofbauer, H. (2017). Advanced dual fluidized bed steam gasification of wood and lignite with calcite as bed material. *Korean Journal of Chemical Engineering*, 34(9), 2548–2558. <https://doi.org/10.1007/s11814-017-0141-y>
- [7] Müller, S. (2013). *Hydrogen from Biomass for Industry - Industrial Application of Hydrogen Production Based on Dual Fluid Gasification*. TU Wien.
- [8] Pfeifer, C., Rauch, R., & Hofbauer, H. (2004). In-Bed Catalytic Tar Reduction in a Dual Fluidized Bed Biomass Steam Gasifier. *Industrial & Engineering Chemistry Research*, 43(7), 1634–1640. <https://doi.org/10.1021/ie030742b>
- [9] Diem, R. (2015). *Design, Construction and Startup of an Advanced 100 kW Dual Fluidized Bed System for Thermal Gasification*. TU Wien.
- [10] Kaltschmitt, M., Hartmann, H. & Hofbauer, H. (2009). *Energien aus Biomasse*. Springer., Berlin, Heidelberg.
- [11] Koppatz, S., Pfeifer, C., & Hofbauer, H. (2011). Comparison of the performance behaviour of silica sand and olivine in a dual fluidised bed reactor system for steam gasification of biomass at pilot plant scale. *Chemical Engineering Journal*, 175(1), 468–483. <https://doi.org/10.1016/j.cej.2011.09.071>
- [12] Müller, S., Fuchs, J., Schmid, J. C., Benedikt, F., & Hofbauer, H. (2017). Experimental development of sorption enhanced reforming by the use of an advanced gasification test plant. *International Journal of Hydrogen Energy*, 42(50), 1–14. <https://doi.org/10.1016/j.ijhydene.2017.10.119>
- [13] Ridha, F. N., Lu, D. Y., Symonds, R. T., & Champagne, S. (2016). Attrition of CaO-based pellets in a 0.1 MWth dual fluidized bed pilot plant for post-combustion CO₂ capture. *Powder Technology*, 291, 60–65. <https://doi.org/10.1016/j.powtec.2015.11.065>

- [14] Scala, F., & Salatino, P. (2010). Attrition of limestones by impact loading in fluidized beds: The influence of reaction conditions. *Fuel Processing Technology*, 91(9), 1022–1027. <https://doi.org/10.1016/j.fuproc.2010.03.003>
- [15] Stanmore, B. R., & Gilot, P. (2005). Review-calcination and carbonation of limestone during thermal cycling for CO₂ sequestration. *Fuel Processing Technology*, 86(16), 1707–1743. <https://doi.org/10.1016/j.fuproc.2005.01.023>
- [16] Bhatia, S., & Perlmutter, D. (1983). Effect of the product layer on the kinetics of the CO₂ lime reaction. *AIChE Journal*, 29(1), 79–86. <https://doi.org/10.1002/aic.690290111>
- [17] Abanades, J. C. (2002). The maximum capture efficiency of CO₂ using a carbonation/calcination cycle of CaO/CaCO₃. *Chemical Engineering Journal*, 90(3), 303–306. [https://doi.org/10.1016/S1385-8947\(02\)00126-2](https://doi.org/10.1016/S1385-8947(02)00126-2)
- [18] Poboß, N., Zieba, M., & Scheffknecht, G. (2010). Experimental investigation of affecting parameters on the gasification of biomass fuels in a 20kWth dual fluidized bed. 2nd Int. Conf. Polygeneration Strateg.
- [19] Hawthorne, C., Poboss, N., Dieter, H., Gredinger, A., Zieba, M., & Scheffknecht, G. (2012). Operation and results of a 200-kWth dual fluidized bed pilot plant gasifier with adsorption-enhanced reforming. *Biomass Conversion and Biorefinery*, 2, 217–227. <https://doi.org/10.1007/s13399-012-0053-3>
- [20] Soukup, G. (2009). *Der AER – Prozess, Weiterentwicklung in einer Technikumsanlage und Demonstration in einer Großanlage*. TU Wien.
- [21] Schmid, J.C., Fuchs, J., Benedikt, F., et al (2017). Sorption Enhanced Reforming with the Novel Dual Fluidized Bed Test Plant at TU Wien. *Eur. Biomass Conf. Eshib*. Stockholm, pp. 421-428.
- [22] Koppatz, S., Pfeifer, C., Rauch, R., Hofbauer, H., Marquard-Moellenstedt, T., & Specht, M. (2009). H₂rich product gas by steam gasification of biomass with in situ CO₂ absorption in a dual fluidized bed system of 8 MW fuel input. *Fuel Processing Technology*, 90(7–8), 914–921. <https://doi.org/10.1016/j.fuproc.2009.03.016>
- [23] Coppola, A., Montagnaro, F., Salatino, P., & Scala, F. (2012). Limestone Attrition During Fluidized Bed Calcium Looping Cycles for CO₂ Capture : the Effect of SO₂. *XXXV Meeting of the Italian Section of the Combustion Institute, Session V(1)*, 1–6.
- [24] Sun, P., Grace, J. R., Lim, C. J., & Anthony, E. J. (2007). Removal of CO₂ by calcium-based sorbents in the presence of SO₂. *Energy and Fuels*, 21(1), 163–170. <https://doi.org/10.1021/ef060329r>
- [25] Harrison, D.P., Silaban, A., Narcida, M., & Han, C. (1990). A Calcium Oxide Sorbent Process for Bulk Separation of Carbon Dioxide. United States: N. p.
- [26] Matsukata, M., Takeda, K., Miyatani, T., & Ueyama, K. (1996). Simultaneous chlorination and sulphation of calcined limestone. *Chemical Engineering Science*, 51(11), 2529–2534. [https://doi.org/10.1016/0009-2509\(96\)00106-6](https://doi.org/10.1016/0009-2509(96)00106-6)

- [27] Al-Jeboori, M. J., Fennell, P. S., Nguyen, M., & Feng, K. (2012). Effects of different dopants and doping procedures on the reactivity of CaO-based sorbents for CO₂ capture. *Energy and Fuels*, 26(11), 6584–6594. <https://doi.org/10.1021/ef301153b>
- [28] Fuchs, J., Müller, S., Schmid, J. C., Hofbauer, H., Stocker, H., Kieberger, N., & Bürgler, T. (2017). *Sorption Enhanced Reforming of Different Fuel Types for the Production of a Hydrogen-Rich Reduction Gas*. Proceedings of SEEP2017, 27-30 June 2017, Bled, Slovenia.
- [29] Mills, G. A., & Steffgen, F. W. (2006). Catalytic Methanation. *Catalysis Reviews: Science and Engineering*, 8(1), 159–210. <https://doi.org/10.1080/01614949308013910>
- [30] Bartholomew, C. (2001). Mechanisms of catalyst deactivation. *Applied Catalysis*, 212, 17–60. [https://doi.org/10.1016/S0926-860X\(00\)00843-7](https://doi.org/10.1016/S0926-860X(00)00843-7)
- [31] Gao, J., Wang, Y., Ping, Y., Hu, D., Xu, G., Gu, F., & Su, F. (2012). A thermodynamic analysis of methanation reactions of carbon oxides for the production of synthetic natural gas. *RSC Advances*, 2(6), 2358–2368. <https://doi.org/10.1039/c2ra00632d>
- [32] Rehmat, A., & Randhava, S. S. (1970). Selective Methanation of Carbon Monoxide. *Industrial and Engineering Chemistry Product Research and Development*, 9(4), 512–515. <https://doi.org/10.1021/i360036a009>
- [33] Kopyscinski, J., Schildhauer, T. J., & Biollaz, S. M. A. (2010). Production of synthetic natural gas (SNG) from coal and dry biomass - A technology review from 1950 to 2009. *Fuel*, 89(8), 1763–1783. <https://doi.org/10.1016/j.fuel.2010.01.027>
- [34] Ruggeri, F. (2012). The Novel VESTA Process for Substitute Natural Gas Production. *Amec Foster Wheeler*. Clarant.
- [35] Haldor-Topsoe (2009). From solid fuels to substitute natural gas (SNG) using TREMP.
- [36] Pedersen, K., Skov, A., & Rostrup-Nielsen, J. R. (1980). Catalytic Aspects of High Temperature Methanation. *ACS Division of Fuel Chemistry, Preprints*, 25(2), 89–100.
- [37] Kantarci, N., Borak, F., & Ulgen, K. O. (2005). Bubble column reactors. *Process Biochemistry*, 40(7), 2263–2283. <https://doi.org/10.1016/j.procbio.2004.10.004>
- [38] Kopyscinski, J., Schildhauer, T. J., & Biollaz, S. M. A. (2011). Fluidized-bed methanation: Interaction between kinetics and mass transfer. *Industrial and Engineering Chemistry Research*, 50(5), 2781–2790. <https://doi.org/10.1021/ie100629k>
- [39] Martin, R.A., Guan, X., Gardner, B., & Hendrix, H. (2002). Power systems development facility: high temperature, high pressure, filtration in gasification operation. *United states: N.p.*
- [40] Woolcock, P. J., & Brown, R. C. (2013). A review of cleaning technologies for biomass-derived syngas. *Biomass and Bioenergy*, 52, 54–84. <https://doi.org/10.1016/j.biombioe.2013.02.036>
- [41] Leibold, H., Hornung, A., & Seifert, H. (2008). HTHP syngas cleaning concept of two stage biomass gasification for FT synthesis. *Powder Technology*, 180(1–2), 265–270. <https://doi.org/10.1016/j.powtec.2007.05.012>

- [42] Houben, M. P., De Lange, H. C., & Van Steenhoven, A. A. (2005). Tar reduction through partial combustion of fuel gas. *Fuel*, 84(7–8), 817–824. <https://doi.org/10.1016/j.fuel.2004.12.013>
- [43] Rhyner, U., Edinger, P., Schildhauer, T. J., & Biollaz, S. M. A. (2014). Applied kinetics for modeling of reactive hot gas filters. *Applied Energy*, 113, 766–780. <https://doi.org/10.1016/j.apenergy.2013.07.063>
- [44] Ross, J. R. H. (1985). *Metal Catalysed Methanation and Steam Reforming. Catalysis Volume 7*. <https://doi.org/10.1039/9781847553195-00001>
- [45] Rönsch, S., Schneider, J., Matthischke, S., Schlüter, M., Götz, M., Lefebvre, J., ... Bajohr, S. (2016). Review on methanation – From fundamentals to current projects. *Fuel*, 166, 276–296. <https://doi.org/10.1016/j.fuel.2015.10.111>
- [46] Lefebvre, J., Götz, M., Bajohr, S., Reimert, R., & Kolb, T. (2015). Improvement of three-phase methanation reactor performance for steady-state and transient operation. *Fuel Processing Technology*, 132, 83–90. <https://doi.org/10.1016/j.fuproc.2014.10.040>
- [47] Kulik, A., & Saliger, R. (2006). *Heterogene Katalyse an Festkörperoberflächen*. TU Braunschweig.
- [48] Zwart, R. W. R., Drift, A. Van Der, Bos, A., Visser, H. J. M., Cieplik, M. K., & Ko, H. W. J. (2009). Oil-Based Gas Washing — Flexible Tar Removal for High-Efficient Production of Clean Heat and Power as Well as Sustainable Fuels and Chemicals. *Environmental Progress & Sustainable Energy*, 28(3), 324–335. <https://doi.org/10.1002/ep>
- [49] Torres, W., Pansare, S. S., & Goodwin, J. (2007). Hot Gas Removal of Tars, Ammonia, and Hydrogen Sulfide from Biomass Gasification Gas. *Catalysis Reviews: Science and Engineering*, (January 2014), 407–456. <https://doi.org/10.1080/01614940701375134>
- [50] Fuchs, M., Rauch, R., & Hofbauer, H. (2007). *Deliverable D5.4 - Report on the design of a suitable gas cleaning system for synthesis gas applications based on experimental and simulation results*.
- [51] Malicha, M. (2014). *Untersuchung der Adsorptionskapazitäten verschiedener Metalloxide für die Abtrennung von Schwefelwasserstoff aus Gasmischungen*. TU Wien.
- [52] Donau Carbon. (n.d.). Abscheidung von Schwefelwasserstoff und Mercaptanen.
- [53] Anis, S., & Zainal, Z. A. (2011). Tar reduction in biomass producer gas via mechanical, catalytic and thermal methods: A review. *Renewable and Sustainable Energy Reviews*, 15(5), 2355–2377. <https://doi.org/10.1016/j.rser.2011.02.018>
- [54] Kohl, H., & Siber, M. Prüflabor für Feuerungsanlagen, PL-18005-A, PL-15065-A. TU Wien.
- [55] Bardolf, R. (2017). *Optimierung eines Produktgaswäschers bei der Biomassedampfvergasung im Zweibettwirbelschichtverfahren*. TU Wien.
- [56] Friedl, A. (WS 2000/2001). Thermische Verfahrenstechnik 1. TU Wien.
- [57] Teles, M. B. (2017). *OPTIMIZATION OF SYNTHETIC NATURAL GAS PRODUCTION FROM BIOMASS GASIFICATION*. TU Wien.

- [58] Kaisalo, N. (2017). *Tar reforming in biomass gasification gas cleaning*. Aalto University.
- [59] Tabellensammlung Chemie / Löslichkeit einiger Gase und Ionensubstanzen, https://de.wikibooks.org/wiki/Tabellensammlung_Chemie/Löslichkeit_einiger_Gase_und_Ionensubstanzen. Accessed on: 10.05.18
- [60] Oakey, J. E., & Fantom, I. R. (1997). Hot gas cleaning - materials and performance. *Materials at High Temperatures*, 14(3), 337–345. <https://doi.org/10.1080/09603409.1997.11689559>
- [61] D’Orazio, A., Rapagna, S., Foscolo, P. U., Gallucci, K., Nacken, M., Heidenreich, S., ... Dell’Era, A. (2015). Gas conditioning in H₂ rich syngas production by biomass steam gasification: Experimental comparison between three innovative ceramic filter candles. *International Journal of Hydrogen Energy*, 40, 7282–7290. <https://doi.org/10.1016/j.ijhydene.2015.03.169>
- [62] Mihalyi, B. (SS 2013). Verfahrenstechnik Rechenübung. TU Wien.
- [63] VDI-Gesellschaft Verfahrenstechnik und Chemieingenieurwesen (GVC) (2013). *VDI Wärmeatlas*, Springer Berlin Heidelberg (Wiesbaden).
- [64] Schwister, K., & Leven, V. (2014). *Verfahrenstechnik für Ingenieure*, Carl Hanser Verlag, München.
- [65] Rosso, S. (2009). *Entwicklung einer speziellen Aktivkohle für den Einsatz zur Biogasentschwefelung und Untersuchung der Leistungsfähigkeit im Labor und im praktischen Einsatz*. Universität Rostock.
- [66] Slimane, R. B., Akpolat, O. M., Pandya, K., Lau, F. S., Brett E, W., & Leppin, D. (2001). *NOVEL GAS CLEANING/ CONDITIONING FOR INTEGRATED GASIFICATION COMBINED CYCLE*.
- [67] Interview with plant operator of experimental facility containing relevant gas cleaning steps: Dr. Gerald Weber, Wien am 03.06.18
- [68] Hofbauer, H. (WS 2001/2002). Chemische Verfahrenstechnik 1. TU Wien.
- [69] Everychina, <http://www.everychina.com/m-co-methanation-catalyst>, Accessed on: 10.05.18
- [70] Paul Scherrer Institut (n.d.). *The SNG Technology Platform in Güssing, A Status report of Bio-SNG project*.
- [71] Jou, F., Mather, A. E., & Otto, F. D. (1982). Solubility of H₂S and CO₂ in Aqueous Methyl-diethanolamine Solutions. *Ind. Eng. Chem. Process Des. Dev.*, 21, 539-544.

Annex

- General conversion equations
- Cold gas cleaning reactors
- Hot gas cleaning reactors

General conversion equations

The following conversions in between the units are used to represent the results in an illustrative way.

Nm³/h to kmol/h:

$$\dot{n}_{PG} = \frac{\dot{V}_{PG}}{V_{m,SC}}$$

vol.% to kmol/h:

$$\dot{n}_{PG,X} = \frac{\dot{V}_{PG} * \left(\frac{v_{PG,X}}{100}\right)}{V_{m,SC}}$$

mg/Nm² to kmol/h:

$$\dot{n}_{PG,X} = \frac{\left(\frac{c_{PG,X}}{1000}\right)}{M_X} * \dot{V}_{PG} * \frac{1}{1000}$$

kmol/h to kg/h:

$$\dot{m}_{PG} = \dot{n}_{PG} * \bar{M}_{PG}$$

$$\dot{m}_{PG,X} = \dot{n}_{PG,X} * M_X$$

Cold gas cleaning

Table 36 to Table 45 contain the characteristics, assumptions and calculation results of the individual reactors from the cold gas cleaning process.

- *Characteristics and assumptions*

Table 36: Characteristics and assumptions of the RME-scrubber

Characteristics		
Usage	tar removal	
Physical principle	absorption	
Solvent	rapeseed methyl ester (RME)	
Reactor type	packed spray column	
Packing	Raschig-rings	
Assumptions	Unit	Value
Physical properties		
$T_{PG,in}$	$^{\circ}C$	180
$X_{Tar,\alpha}$	–	0
$H_{Tar,40^{\circ}C}$	<i>mbar</i>	21.2 [62]
p	<i>bar</i>	1
k_{Gy}	$kmol/m^3 * h$	5.22 [62]
β	%	99
Packing		
φ	–	0.8 [62]
α	m^2/m^3	195 [62]
Thermal values		
$\Delta h_{H_2O,condense}$	kJ/kg	2262 [63]

Table 37: Characteristics and assumptions of the activated carbon filter

Characteristics		
Usage	Tar and sulphur removal	
Physical principle	adsorption	
Adsorbent	Activated carbon (standard and impregnated with sodium hydroxide at a ratio of 1 to 1)	
Reactor type	adiabatic fixed bed	
Assumptions	Unit	Value
Physical properties		
$X_{AC,st+im,\alpha}$	–	0
$B_{AC,st,Tar}$	g/g_{AC}	0.5 [64]
B_{AC,im,H_2S}	g/g_{AC}	0.5 [65]
ε	–	0.9 [64]
$\rho_{AC,st+im}$	kg/m^3	600 [64]
z_{Ads}	<i>m</i>	1
p	<i>bar</i>	1
β_{Tar}	%	99
β_{H_2S}	%	95

Table 38: Characteristics and assumptions of the water-scrubber

Characteristics		
Usage	HCl and NH ₃ removal	
Physical principle	absorption	
Solvent	water	
Reactor type	packed spray column	
Packing	Raschig-rings	
Assumptions	Unit	Value
Physical properties		
$X_{HCl+NH_3,\alpha}$	–	0
$H_{NH_3,40^\circ C}$	bar	2.8 [62]
$H_{HCl,40^\circ C}$	bar	2.0 [63]
p	bar	1
k_{Gy}	kmol/m ³ * h	5.22 [62]
β	%	99
Packing		
φ	–	0.8 [62]
α	m ² /m ³	195 [62]

Table 39: Characteristics and assumptions of the hydrogenator

Characteristics		
Usage	Olefin conversion	
Physical principle	Catalytic hydrogenation	
Catalyst material	Nickel-based	
Reactor type	Isothermal catalytic fixed bed	
Assumptions	Unit	Value
Physical properties		
$\tau_{Hydrogenation}$	s	0.5
$\beta_{C_2H_4}$	%	99
β_{CO_2}	%	99
p	bar	16

Table 40: Characteristics and assumptions of the amine-scrubber

Characteristics		
Usage	H ₂ S and CO ₂ removal	
Physical principle	absorption	
Solvent	amine	
Reactor type	packed spray column	
Packing	Raschig-rings	
Assumptions	Unit	Value
Physical properties		
$X_{H_2S+CO_2,\alpha}$	–	0
$H_{H_2S,70^\circ C}$	bar	1.7 [71]
$H_{CO_2,70^\circ C}$	bar	3.4 [71]
p	bar	16
k_{Gy}	kmol/m ³ * h	5.22 [62]
β_{CO_2}	%	50
β_{H_2S}	%	99
Packing		
φ	–	0.8 [62]
α	m ² /m ³	195 [62]
General		
Temperature drop of around 40 %		

- **Calculation results**

Table 41: Calculated parameters of the RME-scrubber

Calculation of gas, solvent and column parameters					
Product gas	Unit	Value	Solvent	Unit	Value
$\dot{m}_{PG,in}$	kg/h	1063	\dot{m}_{Abs}	kg/h	12.9
$\dot{m}_{Tar,in}$	kg/h	13.1	$X_{Tar,\omega}$	–	0.04
$Y_{Tar,\alpha}$	–	0.012	L_T (Eq. 4.13)	kg/h	298
$Y_{Tar,\omega}$	–	0.00012	L_T (Eq. 4.16)	kg/h	30
$\dot{m}_{Tar,out}$	kg/h	0.13	Column design		
$\dot{m}_{PG,out}$	kg/h	1050	HTU	m	0.72
$\dot{m}_{H_2O,in}$	kg/h	1500	NTU	–	12
$\dot{m}_{H_2O,out}$	kg/h	90	Z_{Abs}	m	8.9
$T_{PG,out}$	°C	40			
\dot{Q}_{cool}	MW	1.2			

Table 42: Calculated parameters for the activated carbon filter

Calculation of gas and solid parameters					
Product gas	Unit	Value	Sorbent	Unit	Value
$\dot{m}_{PG,in}$	kg/h	1050	\dot{m}_{Ads}	kg/h	0.6
$\dot{m}_{Tar,in}$	kg/h	0.13	Z_{Ads}	m	1
$\dot{m}_{H_2S,in}$	kg/h	0.5	$t_{AC,st}$	days	39
$Y_{Tar,\alpha}$	–	0.00012	$t_{AC,imp}$	days	10
$Y_{H_2S,\alpha}$	–	0.00048	$S_{AC,st+imp}$	kg	540
$Y_{Tar,\omega}$	–	$1 \cdot 10^{-6}$			
$Y_{H_2S,\omega}$	–	$2 \cdot 10^{-5}$			
$\dot{m}_{H_2S,out}$	g/h	25			
$\dot{m}_{Tar,out}$	g/h	1			
$\dot{m}_{PG,out}$	kg/h	1049			
$T_{PG,out}$	°C	40			
$\dot{Q}_{reaction}$	W	74			

Table 43: Calculated parameters of the water-scrubber

Calculation of gas, solvent and column parameters					
Product gas	Unit	Value	Solvent	Unit	Value
$\dot{m}_{PG,in}$	kg/h	1049	\dot{m}_{Abs}	kg/h	9
$\dot{m}_{HCl,in}$	kg/h	0.14	$X_{HCl+NH_3,\omega}$	–	0.002
$\dot{m}_{NH_3,in}$	kg/h	9	L_T (Eq. 4.13)	kg/h	4060
$Y_{HCl+NH_3,\alpha}$	–	0.01	L_T (Eq. 4.16)	kg/h	15
$Y_{HCl+NH_3,\omega}$	–	0.0001	Column design		
$\dot{m}_{HCl,out}$	g/h	1.3	HTU	m	2.8
$\dot{m}_{NH_3,out}$	g/h	89	NTU	–	12
$\dot{m}_{PG,out}$	kg/h	1040	z_{Abs}	m	34
$T_{PG,out}$	°C	40			

Table 44: Calculated parameters of the hydrogenator

Calculation of gas parameters					
Product gas	Unit	Value	Product gas	Unit	Value
V_{cat}	m ³	0.2	$\dot{m}_{C_2H_6,out}$	kg/h	38
$\dot{m}_{PG,in}$	kg/h	1040	$\dot{m}_{H_2S,out}$	kg/h	0.15
$\dot{m}_{C_2H_4,in}$	kg/h	36	$\dot{m}_{H_2,used}$	kg/h	2.6
$\dot{m}_{COS,in}$	kg/h	0.2	$\dot{m}_{PG,out}$	kg/h	1040
$\dot{m}_{C_2H_4,out}$	kg/h	0.36	$T_{PG,out}$	°C	111
$\dot{m}_{COS,out}$	g/h	2	$\dot{Q}_{reactions}$	kW	- 46

Table 45: Calculated parameters of the amine-scrubber

Calculation of gas, solvent and column parameters					
Product gas	Unit	Value	Solvent	Unit	Value
$\dot{m}_{PG,in}$	kg/h	1040	\dot{m}_{Abs}	kg/h	264
$\dot{m}_{CO_2,in}$	kg/h	528	$X_{CO_2+H_2S,\omega}$	–	0.2
$\dot{m}_{H_2S,in}$	kg/h	0.15	L_T (Eq. 4.13)	kg/h	1086
$Y_{CO_2+H_2S,\alpha}$	–	1	L_T (Eq. 4.16)	kg/h	N/A
$Y_{CO_2+H_2S,\omega}$	–	0.5	Column design	Unit	Value
$\dot{m}_{CO_2,out}$	kg/h	264	HTU	m	1.3
$\dot{m}_{H_2S,out}$	g/h	1.5	NTU	–	1.2
$\dot{m}_{PG,out}$	kg/h	776	z_{Abs}	m	1.5
$T_{PG,out}$	$^{\circ}C$	66			

Hot gas cleaning

Table 46 to Table 56 contain the characteristics, assumptions and calculation results of the individual reactors from the hot gas cleaning section.

- *Characteristics and assumptions*

Table 46: Characteristics and assumptions of the trona and zinc-titanium-oxide filter

Characteristics		
Usage	Sulphur and halide removal	
Physical principle	adsorption	
Adsorbent	Trona and zinc titanium oxide at a ratio of 2 to 1 respectively	
Reactor type	Adiabatic fixed bed	
Assumptions	Unit	Value
Physical properties		
$X_{ZnTiO_3+Trona,\alpha}$	–	0
$B_{Na_2CO_3,HCl}$	g/g_{Trona}	0.32 [66]
B_{ZnTiO_3,H_2S}	g/g_{ZnTiO_3}	0.08 [66]
ε	–	0.9 [64]
$\rho_{Na_2CO_3+ZnTiO_3}$	kg/m^3	600 [64]
z_{Ads}	m	1
p	bar	1
β_{H_2S}	%	95
β_{HCl}	%	95

Table 47: Characteristics and assumptions of the steam reformer

Characteristics		
Usage	tar removal	
Physical principle	Steam reforming	
Catalyst material	precious metal	
Reactor type	Catalytic fixed bed	
Assumptions	Unit	Value
Physical properties		
τ_{SR}	s	0.5
p	bar	1
β_{Tars}	%	99
General		
Only steam reforming reactions (Eq. 4.32 and Eq. 4.33) take place		
Benzene represent tar for calculation		

Table 48: Characteristics and assumptions of the decomposer

Characteristics		
Usage	ammonia removal	
Physical principle	decomposing	
Catalyst material	iron	
Reactor type	Adiabatic catalytic fixed bed	
Assumptions	Unit	Value
Physical properties		
$\tau_{Decomposer}$	<i>s</i>	0.5
p	<i>bar</i>	1
β_{NH_3}	%	99
General		
Only decomposition reaction (Eq. 4.34) takes place		

Table 50: Characteristics and assumptions of the hydrogenator

Characteristics		
Usage	Olefin conversion	
Physical principle	Catalytic hydrogenation	
Catalyst material	Nickel-based	
Reactor type	Isothermal catalytic fixed bed	
Assumptions	Unit	Value
Physical properties		
$\tau_{Hydrogenation}$	<i>s</i>	0.5
$\beta_{C_2H_4}$	%	99
β_{COS}	%	99
p	<i>bar</i>	16

Table 49: Characteristics and assumptions of the activated carbon filter

Characteristics		
Usage	Tar and sulphur removal	
Physical principle	adsorption	
Adsorbent	Activated carbon (standard and impregnated with sodium hydroxide at a ratio of 1 to 1)	
Reactor type	adiabatic fixed bed	
Assumptions	Unit	Value
Physical properties		
$X_{AC,st+im,\alpha}$	–	0
$B_{AC,st,Tar}$	<i>g/g_{AC}</i>	0.5 [64]
B_{AC,im,H_2S}	<i>g/g_{AC}</i>	0.5 [65]
ϵ	–	0.9 [64]
$\rho_{AC,st+im}$	<i>kg/m³</i>	600 [64]
z_{Ads}	<i>m</i>	1
p	<i>bar</i>	1
β_{Tar}	%	99
β_{H_2S}	%	99

- **Calculation results**

Table 51: Calculated parameters for trona and zinc-titanium-oxide filter.

Calculation of gas and solid parameters					
Product gas	Unit	Value	Activated carbon	Unit	Value
$\dot{m}_{PG,in}$	kg/h	1063	\dot{m}_{Ads}	kg/h	0.6
$\dot{m}_{HCl,in}$	kg/h	0.14	z_{Ads}	m	1
$\dot{m}_{H_2S,in}$	kg/h	0.5	$t_{Na_2CO_3}$	days	227
$Y_{HCl,\alpha}$	—	0.0001	t_{ZnTiO_3}	days	15
$Y_{H_2S,\alpha}$	—	0.0005	$S_{ZnTiO_3+Na_2CO_3}$	kg	4417
$Y_{HCl,\omega}$	—	$6 \cdot 10^{-6}$			
$Y_{H_2S,\omega}$	—	$2 \cdot 10^{-5}$			
$\dot{m}_{H_2S,out}$	g/h	26			
$\dot{m}_{HCl,out}$	g/h	7			
$\dot{m}_{PG,out}$	kg/h	1062			
$T_{PG,out}$	°C	650			
$\dot{Q}_{reaction}$	kW	-0.2			

Table 52: Calculated parameters of the steam reformer

Calculation of gas parameters					
Product gas	Unit	Value	Product gas	Unit	Value
V_{cat}	m^3	0.65	$\dot{m}_{CO,out}$	kg/h	224
$\dot{m}_{PG,in}$	kg/h	1062	$\dot{m}_{CO_2,out}$	kg/h	550
$\dot{m}_{Tar,in}$	kg/h	13	$\dot{m}_{H_2,out}$	kg/h	90
$\dot{m}_{H_2O,in}$	kg/h	1500	$T_{PG,out}$	°C	850
$\dot{m}_{PG,out}$	kg/h	1089	\dot{Q}_{in}	kW	280
$\dot{m}_{H_2O,out}$	kg/h	1473	$\dot{Q}_{reactions}$	kW	30
$\dot{m}_{Tar,out}$	kg/h	0.13			

Table 53: Calculated parameters of the decomposer

Calculation of gas parameters					
Product gas	Unit	Value	Product gas	Unit	Value
V_{cat}	m^3	0.65	$\dot{m}_{H_2,out}$	kg/h	92
$\dot{m}_{PG,in}$	kg/h	1089	$\dot{m}_{N_2,out}$	kg/h	7
$\dot{m}_{NH_3,in}$	kg/h	9	$T_{PG,out}$	$^{\circ}C$	785
$\dot{m}_{PG,out}$	kg/h	1089	$\dot{Q}_{reaction}$	kW	16

Table 54: Calculated parameters of the product gas dryer

Calculation of gas parameters		
Product gas	Unit	Value
$\dot{m}_{PG,in=out}$	kg/h	1089
$\dot{m}_{H_2O,in}$	kg/h	1473
$\dot{m}_{H_2O,out}$	kg/h	88
$T_{PG,out}$	$^{\circ}C$	40
\dot{Q}_{cool}	MW	1.4

Table 55: Calculated parameters for the activated carbon filter

Calculation of gas and solid parameters					
Product gas	Unit	Value	Sorbent	Unit	Value
$\dot{m}_{PG,in}$	kg/h	1089	\dot{m}_{Ads}	kg/h	0.2
$\dot{m}_{Tar,in}$	kg/h	0.13	z_{Ads}	m	1
$\dot{m}_{H_2S,in}$	g/h	26	$t_{AC,st}$	$days$	39
$Y_{Tar,\alpha}$	—	0.0001	$t_{AC,impr}$	$days$	200
$Y_{H_2S,\alpha}$	—	$2*10^{-5}$	$S_{AC,st+impr}$	kg	540
$Y_{Tar,\omega}$	—	$1*10^{-6}$			
$Y_{H_2S,\omega}$	—	$2*10^{-7}$			
$\dot{m}_{H_2S,out}$	g/h	0.3			
$\dot{m}_{Tar,out}$	g/h	1.3			
$\dot{m}_{PG,out}$	kg/h	1089			
$T_{PG,out}$	$^{\circ}C$	40			
$\dot{Q}_{reaction}$	W	-10			

Table 56: Calculated parameters of the hydrogenator

Calculation of gas parameters					
Product gas	Unit	Value	Product gas	Unit	Value
V_{cat}	m^3	0.3	$\dot{m}_{COS,out}$	g/h	2
$\dot{m}_{PG,in}$	kg/h	1089	$\dot{m}_{H_2S,out}$	kg/h	0.15
$\dot{m}_{C_2H_4,in}$	kg/h	36	$\dot{m}_{H_2,used}$	kg/h	2.6
$\dot{m}_{COS,in}$	kg/h	0.2	$\dot{m}_{PG,out}$	kg/h	1089
$\dot{m}_{C_2H_6,out}$	kg/h	38	$T_{PG,out}$	$^{\circ}C$	94
$\dot{m}_{C_2H_4,out}$	kg/h	0.36	$\dot{Q}_{reactions}$	kW	- 46